POWER LINE COMMUNICATION CHANNEL MODELLING

by

Fulatsa Zwane

Dissertation submitted in fulfilment of the requirements for the degree

Master of Science in Engineering: Electronic Engineering

in the

College of Agriculture, Engineering and Science

UNIVERSITY OF KWAZULU-NATAL

2014

Supervisor: **Prof. Thomas Joachim Odhiambo Afullo**

As the candidate's Supervisor I agree to the submission of this thesis.

Signed …… Date……

Name: Prof. Thomas J. O. Afullo

DECLARATION 1 - PLAGIARISM

I, **Fulatsa Zwane**, declare that

1. The research reported in this thesis, except where otherwise indicated, is my original research.

2. This thesis has not been submitted for any degree or examination at any other university.

3. This thesis does not contain other persons' data, pictures, graphs or other information, unless specifically acknowledged as being sourced from other persons.

4. This thesis does not contain other persons' writing, unless specifically acknowledged as being sourced from other researchers. Where other written sources have been quoted, then:

a. Their words have been re-written but the general information attributed to them has been referenced

b. Where their exact words have been used, then their writing has been placed in italics and inside quotation marks, and referenced.

5. This thesis does not contain text, graphics or tables copied and pasted from the Internet, unless specifically acknowledged, and the source being detailed in the thesis and in the References sections.

Signed …… Date……

DECLARATION 2 - PUBLICATIONS

DETAILS OF CONTRIBUTION TO PUBLICATIONS

1. F. Zwane and T.J.O. Afullo, "Power Line Communication Channel Modelling: Establishing The Channel Characteristics," *South African Universities Power Engineering Conference, Durban, South Africa, Presented 30-31 January 2014*.

2. F. Zwane and T.J.O. Afullo, "An Alternative Approach in Power Line Communication Channel Modelling," Progress in Electromagnetics Research C (PIERC), vol. 47, pp. 85-93, 2014.

In the first paper, the attenuation coefficients are derived from both the calculations and measurements and then the prediction bounds for the same are determined. An analysis of measurement results for a single phase low voltage Power Line Communication network is done, from which a correlation of network constituent elements and topology to the channel characteristics is inferred. The transfer function of a single branch channel is found to follow an average path loss determined by the attenuation constant coefficients. Expressions of the position of the notches are established from the correlation of the signal frequency to the propagation velocity and length of the branch in a single branch network.

In the second paper, we present the measurement methodology and results for a low voltage Power Line Communications network under different configurations. Based on the measurements, a correlation of the channel transfer characteristics to the network topology is established and a deterministic model based on two-wire transmission line theory for transverse electromagnetic (TEM) wave propagation is proposed. The channel frequency response in frequency range of 1-30 MHz is determined, where the model results agree well with the measurements and another deterministic model.

Signed ……

ACKNOWLEGEMENTS

I would like to especially acknowledge Professor T.J.O. Afullo who supervised the research and provided invaluable insights and support. The opportunity to develop this work has been greatly rewarding, but I also believe that its findings will make a meaningful contribution to the study and application of power line communication. I acknowledge the institutional support in this regard. I would also like to thank the Swaziland Posts and Telecommunications Corporation for affording me the opportunity to study as well as for providing financial assistance in the past two years.

I further acknowledge my colleagues; Abraham Nyete, M. Asiyo, M. Sefuba, B. Awoyemi and J. Musumba for their moral support. M. Mosalaosi and D. Moodley for technical assistance with setting up the test bed as well as the measurement process. I extend my appreciation also to my family, which has provided support in ways too many to mention; my husband Nsika, son Hlelo, my parents, Mr and Mrs Zwane and my siblings. Lastly, to God, whose grace made it possible for effort to culminate to success.

ABSTRACT

Powerline communication technology capitalises on the existing power networks for communication purposes which offer fewer expenses in new connection set ups. This technology has evolved through the years, shifting focus from narrowband to broadband and different techniques being employed so as to achieve higher bit-rates and more reliable communication over the power lines. Considerable research on this important area is therefore ongoing. The power line's inherent problems are largely due to its novel design which is primarily devised for the transmission of electric power and not communication signals, moreover, in the broadband range. This possibly explains why a universally accepted model for the powerline communication channel has not yet been established.

The work presented here seeks to contribute to the ongoing research of developing a better understanding of the presently unpredictable and harsh communication medium. Transmission line theory is studied, and then different analytical models selected from different techniques classified as parametric and deterministic in frequency and time domain are explored. In addition, low voltage distribution network measurements are conducted to ascertain the performance of the powerline as a communication channel.

Detailed PLC channel measurements are done, ranging from primary cable parameters to frequency and phase responses for different cable lengths and configurations, which are all pivotal in the modeling of the powerline communication channel. The coupling and decoupling circuits used for this research are also presented. Measurements to outline the effects of cable specifications, length, number of branches, and configuration of a powerline network to the performance of the channel are also done. This is done over the frequency range of 1-30 MHz following the recommended ETSI standards for first generation PLC systems. Results obtained are then compared and validated against existing models.

CONTENTS

LIST OF FIGURES

Chapter 1

Chapter 2

Chapter 3

Chapter 4

Chapter 5

LIST OF TABLES

CHAPTER 1

INTRODUCTION

1.1. Power Line Communication Overview

Power line communication (PLC) is the transfer of data and voice signals from one communication system to another over the electric power delivery network. After generation, electrical power is transmitted over the high voltage (44-132kV) transmission lines. It is then distributed over medium voltage lines (1-44kV) and then converted for consumer premises in the distribution transformers to the low voltage (0-1000V)[1]. PLC is applicable in all the three distribution stages.

The establishment of PLC focused on the delivery of low speed communication on power lines with the pioneering efforts put in place in the early 1920s [2], seeing to the operation of the first carrier frequency systems for telemetry applications over the high voltage lines in the frequency range of 15-500 kHz [3]. Ripple carrier signals were later introduced on the medium voltage and low voltage networks. The principal drive for PLC was to cater for future load control and to facilitate, from a distance, automatic meter reading [4]. The prevalence of the infrastructure for the supply network meant that the need for alternative cable links to customer premises was covered, further reducing roll out expenses. The increase in the electrical supply networks informed the rapid evolution of the PLC technology and the ever increasing demands in the area of communications instigated the power supply system to migrate from a pure energy distribution network to a multi service data transmission medium, supplying energy, voice and some data services.

Of the many applications, some are explained below:

i. Automatic Meter Reading: this is the technology of acquiring data from energy metering devices automatically and transferring the same data to a database for analysing and billing [5].
ii. Smart grid: this is an intelligent electricity network that makes use of an integrated control, information and communications technology on the power line supply networks, providing a communication path between the generation plants and consumer premises to improve the reliability, efficiency and safety of power delivery [6].
iii. Transportation systems: The direct current battery power line is used to enable in-vehicle communication. Applications comprise of mechatronics-based climate control, door modules and immobilizers [7].
iv. Home Networking: home entertainment devices having an ethernet port are interconnected by the use of PLC to computers and peripherals to share data. PLC adapters are plugged on to sockets establishing the ethernet connection through the network wiring.

v. Building automation: this is an electric device control system which includes controlling lights, heating and fire alarming systems.

PLC is also known as mains communications, Power line Technology (PLT) and Power Line Networking. Broadband PLC enables the implementation of Local Area Networks (LANs) and fast internet amongst other applications. The broadband PLT operates in frequencies from 150 kHz to 34 MHz having a theoretical maximum speed of 200Mbps [8]. Falling within the broadband PLT frequency range, the range of interest in this work is 1.6-30 MHz on the low voltage supply network following the ETSI standard for 1st generation PLT requirements [9], which propositioned a split at 10 MHz, where the lower range is for the access domain and the upper range for in-house use. The separation in frequency is essential for the coexistence of various indoor systems and PLC access systems. Due to the channel response's low pass characteristic of the access domain, frequencies above 10 MHz have not been seen to be feasible. The high speed applications for indoor use have sufficient bandwidth above 10 MHz as the indoor channel lengths are shorter.

In physical properties and structure, the low voltage power line network topology diverges extensively from conventional media such as coaxial, twisted pair and fiber-optic cables. True to its original purpose, the low voltage power line network within a typical in-building structure as in Figure 1.1 is optimized for the transmission of high voltages at low frequencies contrary to data transmission which necessitates the transmission of low voltage at high frequencies. The communication signals therefore suffer some hostile channel parameters. The three most important parameters are noise, impedance mismatch, and attenuation which are frequency, time and location variant, this in turn makes PLC modelling and characterization a non trivial task.

A minimal PLC system is illustrated in Figure1.2 where the signal traverses from the transmitter to receiver through couplers. The power line channel is mainly characterized in terms of the attenuation parameter and the impedance parameter which arises from mismatches in the power line network. The noise parameter, which is added to the signal, originates from several sources. Couplers are used to block the 230 V, 50 Hz frequency currents so as to protect the connected systems from the mains.

The development of accurate PLC channel transfer characteristics models is very important as it forms the basis for computer simulations which are useful in appropriate system design, and further enabling the analysis of the performance of different schemes as well as recognising probable difficulties in the development of communication systems in different network configurations and loads [10].

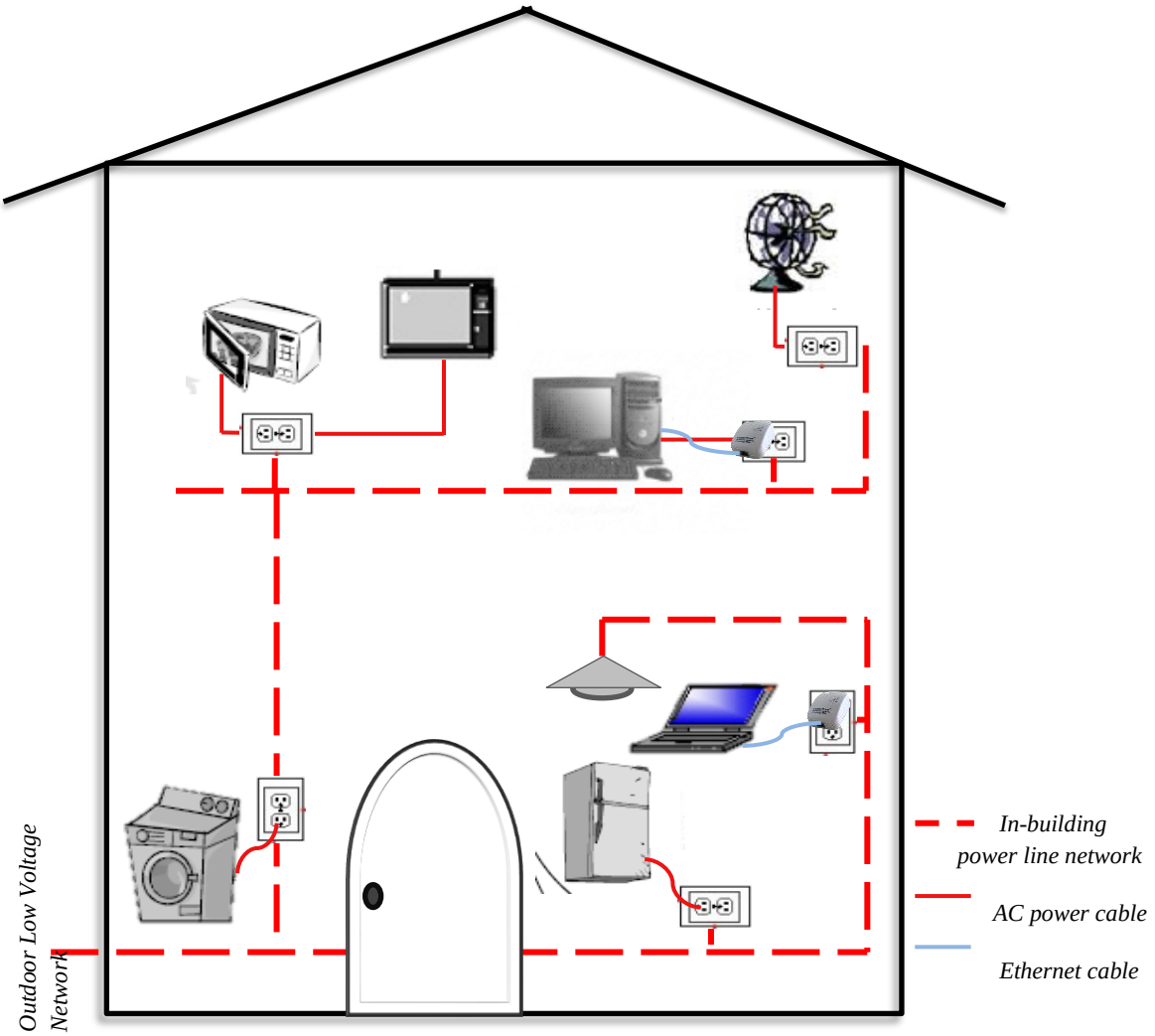

Figure 1.1: Typical structure of a PLC in-building network

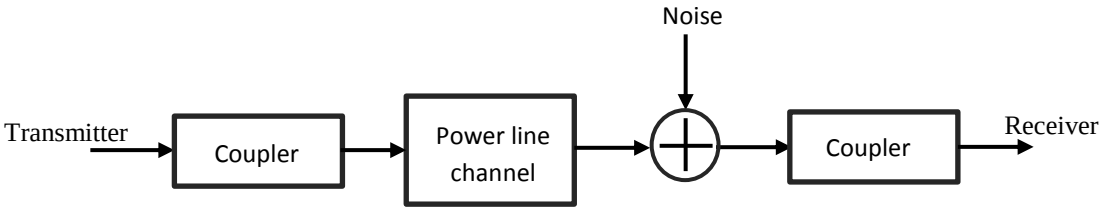

Figure 1.2: Simplified Power Line Communication System

There is therefore continued research in the characterization of the power line as a communication medium. Different techniques which are based on either measurements or theoretical derivations from physical parameters, denoted as top-down or empirical models, and bottom-up or deterministic models, respectively, are employed. They are either in the frequency domain or time domain which relates to the popular multipath environment concept of the power line.

The on-going intensive study in broadband power line communications modelling has had researchers [11-15] obtaining good results as far as the closeness of their models is to the actual behavior of a power line in this usage. In the initial stages of the work, most researchers used empirical models to study the behavior of this channel. However, in the recent studies, this communication channel has also been treated as a black box employing statistical approaches [16] or from the explicit knowledge of the channel [15] deterministically modelled offering a description of its transfer characteristics studied up to 30 MHz. A significant contribution to this study is evident in [11] [13] and [15] and all the contributing factors towards the characterisation of the power line channel are studied separately therein. The model proposed in [12] and refined in [13], has a fair agreement with practical measurements and hence most researchers adopt it to facilitate their work.

Meticulous measurements are required in the investigation of each of the channel parameters and subsequent modelling of the same. The behaviour of the channel is better understood by varying different components, which in the case of PLC, are: the topology; the cable types; the cable length and number of branches; as well as the loads terminating at each end of the network. Once relations of the variations of these are obtained, any given network can therefore be sufficiently modelled. The current study however does not model noise in the PLC channel but is rather focussed on the other PLC components highlighted earlier in this paragraph.

1.2. Research Objectives

The objectives of this work entail the following;

1. To study the power line cables of low voltage supply networks and compare the theoretical models to measurements, determining the influence of their properties on the characteristics of the PLC channel.
2. To characterize and model the channel through extensive measurements coupled with theoretical derivations for different network topologies and load components, as well as drawing relations for the variation in channel properties.
3. To compare different existing models to the measured channel transfer functions as applicable for different configurations.

1.3. Methodological Approach

1. Literature Review – establishing existing theoretical bases of the study, further establishing the existing techniques to characterise the medium.
2. Power line network measurements- by setting up a test bed to measure the channel characteristics of the power line under different network topologies and conditions.

3. Data analysis – to characterise the data obtained from the measurements, with a view to determining the cable coefficients and establishing the relations of different network topologies and load conditions.
4. Comparison and validation of the results obtained with existing models.

1.4. Significance of the Study

Accurate approximation of the line parameters, the characteristic impedance, and propagation constant, which in turn are used to determine the PLC channel constants, is essential in the channel transfer function calculations. Meticulous measurements are required in the investigation of the channel parameters and consequent modelling of the same where the behaviour of the channel is better understood by varying different components. Once relations of the variations of these are obtained, any given network can then be sufficiently modelled. The identification of the notches which prevent the use of the correspondent carriers discussed is an important tool which can be used in the prediction of the bandwidth of the communication channel. Due to the complexity of models found in literature effort is required to provide a model that serves as a general reference channel model for a network of the same cable parameters, helping in the design and development of PLC communication systems.

1.5. Thesis Organization

The rest of the dissertation is organized as follows;
Chapter two entails the study of the indoor power cables, their characteristics and influence on the PLC channel characteristic. Further entailed is the study on the PLC channel characteristics determining factors in terms of the impedance mismatches which account for the reflection and transmission coefficients, attenuation and noise.

In Chapter three, different techniques employed in the characterisation and modelling of the PLC channel, as well as their advantages and disadvantages are reviewed, a proposed model is presented. The investigation of channel parameters calls for exhaustive tests and measurements. The accuracy of the measurements is imperative if reliable PLC characterisation and models are to be established. Chapter four discusses the measurement methodology used for the extraction of intrinsic line parameters for the power line and presents measurement results.

In Chapter five, the methodology used for obtaining the channel frequency response is discussed. The results obtained from the measurements are presented. The relationships between the different network topologies and the transfer functions obtained are drawn. These results to an extent demystify the unpredictability of the power line network for communication purposes.

In Chapter six, concluding remarks for the work carried out in this dissertation are presented. Recommendations for future work are also presented in the same chapter.

CHAPTER TWO

LITERATURE REVIEW

2.1 Introduction

The accuracy of a power line communications channel model is predominantly reliant on the primary parameters and algorithm [11]. In this chapter therefore, we study the characteristics of the channel, in terms of the primary parameters of the power cables, and how they impede a signal passing through, to the factors dictating the power line channel behaviour, that is, the different channel parameters accounting for the time, frequency and location variant nature of the PLC channel.

2.2 Transmission Line Theory

2.2.1 Primary Transmission Line Parameters

The typical low voltage power line for single phase distribution consists of three conducting cores; phase, neutral and ground. The cross sectional view of such a power line is shown in Figure 2.1. The three conducting cores are the live, neutral and earth conductors. Each is encapsulated in a homogenous dielectric jacket and all are further enclosed in an insulating sheath, also made of the same dielectric material. The thermoplastic, poly vinyl chloride (PVC), as the dielectric material forming the insulating sheath, is the one that is of interest of in this study.

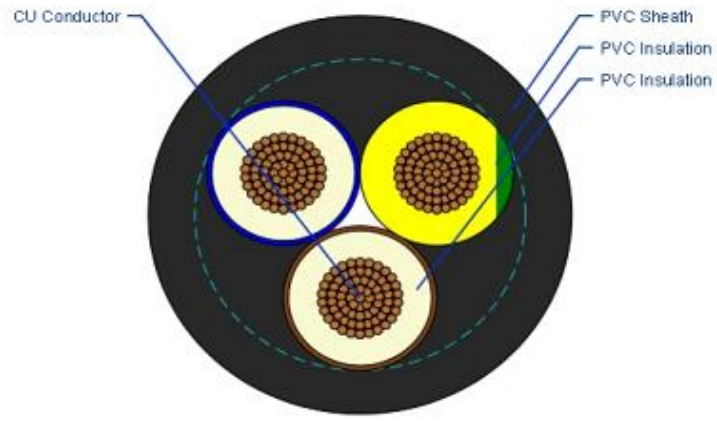

Figure 2.1: Cross sectional view of the typical indoor power line cable

There are different closed current paths which may be applied in PLC applications with the use of three core power cables. When the live wire is considered as one terminal and the neutral as the other, it is regarded as differential mode coupling. When the neutral and live wires are used simultaneously to form one terminal and the other terminal formed by the ground conductor, it is regarded as

common mode coupling which has a disadvantage of posing a potential danger to customers [17]. In this study, differential mode coupling is considered.

The two conductors are approximated as a two wire transmission line. The line is modelled by distributed elements as the high frequency wavelengths are comparable to the distances within an indoor power line network. The fundamental transverse electro-magnetic (TEM) wave propagation principles based on the distributed elements analysis are assumed. When the length of the cable is short, that is, its electrical length is less than λ/16 [18] or is less than λ/8[19] where λ is the wavelength of the signal, the transmission line analysis becomes unnecessary as at this length the voltage and current distribution is considered constant. As a result, determined by the signal frequency, the same line may be regarded as either electrically short or long. The signal frequency f and the propagation velocity v_p determine the electrical length as given in Equation 2.1 [20]:

$$\lambda = \frac{v_p}{f} \tag{2.1}$$

The phase velocity in (2.1) is given as [20]:

$$v_p = \frac{c_0}{\sqrt{\varepsilon_r \mu_r}} \tag{2.2}$$

Where;

ε_r = the dielectric constant

μ_r = relative magnetic permeability of the dielectric

Evaluation of the symmetrical three core indoor cables for high frequency signalling, qualifying the assumption of the two wire transmission model is provided by [21]. With the TEM wave consideration, the magnetic and electric fields are transversal to the propagating direction and orthogonal to each other [22]. As illustrated in Figure 2.2a and 2.2b the differential length Δx of the transmission line is described by distributed line parameters which are theoretically derived by electromagnetic field analysis of the transmission line. The electrical characteristics and cross-sectional dimensions of the transmission line influence these parameters. These differential length elements are:

i. *R'*, which is the resistance per unit length *(Ω/m)*
ii. *L'*, which is the inductance per unit length *(H/m)*
iii. *G'*, which is the conductance per unit length *(S/m)*
iv. *C'*, which is the capacitance per unit length *(F/m)*

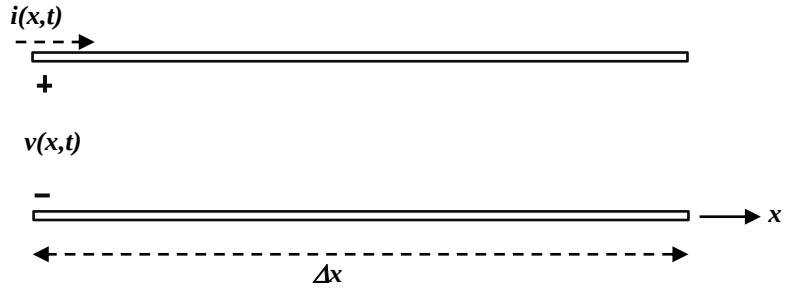

Figure 2.2a: Current and voltage definitions in a transmission line

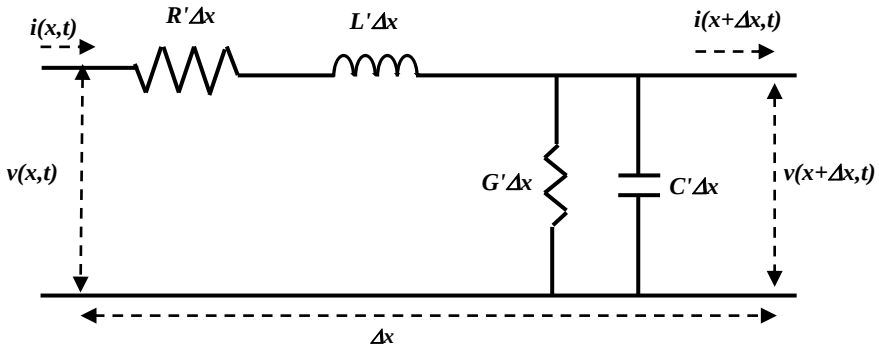

Figure 2.2b: The distributed lumped elements equivalent circuit of the transmission line

At the locations x and $x+\Delta x$, the instantaneous voltages, are designated as $v(x,t)$ and $v(x+\Delta x,t)$ and the instantaneous currents as $i(x,t)$ and $i(x+\Delta x,t)$, respectively. By applying Kirchhoff's voltage and current law, the differential equations describing these voltages and currents, also known as the telegraphers equations, are given as[23]:

$$\frac{\partial v(x,t)}{\partial x} + R' \cdot i(x,t) + L' \frac{\partial i(x,t)}{\partial t} = 0 \tag{2.3}$$

$$\frac{\partial i(x,t)}{\partial x} + G' \cdot v(x,t) + C' \frac{\partial v(x,t)}{\partial x} = 0 \tag{2.4}$$

The distributed lumped elements parameters are determined by giving consideration to the conducting material, dielectrics characteristics and cross sectional dimensions of the cable as shown in Figure 2.3 as follows:

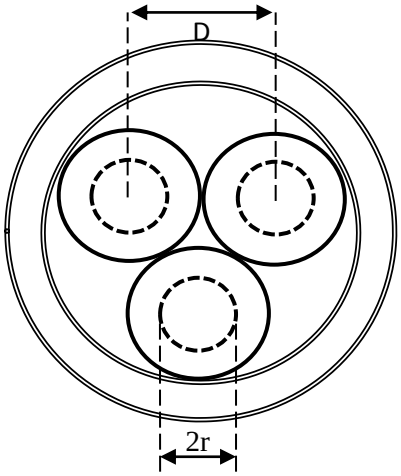

Figure 2.3: Cable cross section illustrating cable dimensions

Resistance:

The skin effect phenomenon, whereby the self-inductance within the conductor causes more current to flow near the outer surfaces of the wire causes an increase in the resistance of the cable, which heightens with increase in frequency accounting for the cable resistance as [21]:

$$R' = \sqrt{\frac{2f\mu_r\mu_o}{\pi r^2\sigma_c}}\left[\frac{\frac{D}{2r}}{\sqrt{\left(\frac{D}{2r}\right)^2 - 1}}\right] \tag{2.5}$$

Where;

f = the wave frequency

ε_r = the dielectric constant

μ_r = relative magnetic permeability of the dielectric

$\mu_0 = \pi \cdot 4 \times 10^{-7}$ H/m

σ_c = the electric conductivity of conducting material equal to 5.58×10^7S/m.

r = the radius of the conductor

D = the separation between conductors

Inductance:

When considering the two-wire transmission, the inductance L' is as a result of an internal inductance (L_{in}), the skin-effect's internal impedance's imaginary part and external (L_{ex}) inductance formed from the fields outside the conductor. The inductance per unit length is therefore proportional to the magnetic field induced by current flowing on the line and given as [16]:

$$L' = L_{in} + L_{ex} = \frac{R'}{2\pi f} + \frac{\mu_r \mu_o}{\pi}\ cosh^{-1}\left(\frac{D}{2r}\right) \quad (2.6)$$

Where;

f = the wave frequency

μ_r = relative magnetic permeability of the dielectric

$\mu_0 = \pi \cdot 4 \times 10^{-7}$ H/m

r = the radius of the conductor

D = the separation between conductors.

Capacitance:

Through the cable's dielectric occurs a leakage between the conductors and so the capacitance per unit length is proportional to the electric field established by a potential difference between the two conductors and is determined as [24]:

$$C' = \frac{\pi \varepsilon_r \varepsilon_o}{cosh^{-1}\left(\frac{D}{2r}\right)} \quad (2.7)$$

Where;

f = the wave frequency

ε_r = the relative dielectric constant

$\varepsilon_0 = 8.85 \times 10^{-12}$ F/m

r = the radius of the conductor

D = the separation between conductors

Conductance:

The conductance per unit length is mainly determined by dielectric losses of the insulating material between the live and the neutral wires. The following expression holds when the medium is considered homogenous [25]:

$$G' = 2\pi f C' \tan\delta \quad (2.8)$$

Where;

tan δ = the dissipation factor

f = the wave frequency

The skin depth describes the distribution of current on the cross sectional area of the conductor, and is given by[26]:

$$\delta = \frac{1}{\sqrt{2\pi f \sigma_c \mu_c}} \tag{2.9}$$

Where;

σ_c = the conductivity of conducting material equal to 5.58×10^7S/m

μ_c = the conductors relative permeability

2.2.2 Transmission Line Wave Propagation

From the lumped element circuit model as illustrated in Figure 2.2a and 2.2b, Equations (2.3) and (2.4) can be simplified to (2.10) and (2.11) when considering the steady state condition, with cosine-based phasors [22] as:

$$\frac{dV(z)}{dz} = -(R + jwL)I(z) \tag{2.10}$$

$$\frac{dI(z)}{dz} = -(G + jwC)V(z) \tag{2.11}$$

When further solved simultaneously, (2.10) and (2.11) give the wave equations for V(z) and I(z) as:

$$\frac{d^2V(z)}{dz^2} - \gamma^2 V(z) = 0 \tag{2.12}$$

$$\frac{d^2I(z)}{dz^2} - \gamma^2 I(z) = 0 \tag{2.13}$$

Where;

γ = the frequency variant complex propagation constant given as[27]:

$$\gamma = \sqrt{(R' + j\omega L')(G' + j\omega C')} \tag{2.14a}$$

$$= \alpha + j\beta \tag{2.14b}$$

Where;

α = the attenuation coefficient (Np/m)

β = the phase coefficient (rad/m)

ω = the angular frequency.

At any position z along the transmission line, the reverse and forward waves are summed and the total voltage and total current are found as [28]:

$$V(z) = V_0^+ e^{-\gamma z} + V_0^- e^{\gamma z} \tag{2.15}$$

$$I(z) = I_0^+ e^{-\gamma z} + I_0^- e^{\gamma z} \tag{2.16}$$

where the wave propagation in the $+z$ direction is represented by the $e^{-\gamma z}$ term, and in the –z direction represented by the $e^{\gamma z}$ term.

2.3 Representation by matrices

The transmission line is also represented by defining it as a two port circuit describing the outputs and inputs by the use of matrices, forming a suitable tool for the channel transfer function calculations [29]. These include the scattering and ABCD matrices which are represented by Figures 2.4a and 2.4b respectively.

The scattering matrix presents the relation of the terminals incident and reflected waves. The incident

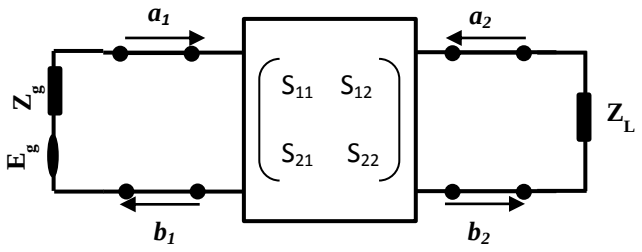

Figure 2.4a: The scattering matrix of a 2-port network

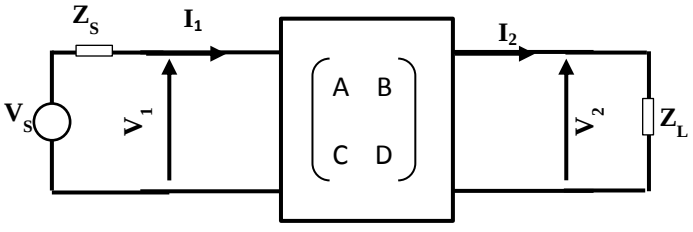

Figure 2.4b: The ABCD matrix of a 2 port network

wave is represented by a_i and the reflected wave by b_i at the *i*th port. Mathematically,

$$b_1 = S_{11}a_1 + S_{12}a_2 \tag{2.17}$$

$$b_2 = S_{21}a_1 + S_{22}a_2 \tag{2.18}$$

If transmission is considered to be from the source of voltage V_S and impedance Z_S to the load impedance Z_L, the transfer function is expressed by [30]:

$$H = \frac{V_L}{V_S} = \frac{S_{21}(1+\Gamma_L)(1-\Gamma_S)}{2(1-S_{22}\Gamma_L)(1-\Gamma_{in}\Gamma_S)} \tag{2.19}$$

Where:

$$\Gamma_{in} = S_{11} + \frac{S_{12}S_{21}\Gamma_L}{1-S_{22}\Gamma_L} \tag{2.20}$$

$$\Gamma_S = \frac{Z_S - Z_0}{Z_S + Z_0} \tag{2.21a}$$

$$\Gamma_L = \frac{Z_L - Z_0}{Z_L + Z_0} \tag{2.21b}$$

The ABCD matrix gives the relation of the input current and voltage and the output current and voltage of the two port network. It is represented by **[**31**]:**

$$\begin{bmatrix} V_2 \\ I_2 \end{bmatrix} = \begin{bmatrix} cosh(\gamma l) & Z_c sinh(\gamma l) \\ \frac{1}{Z_c} sinh(\gamma l) & cosh(\gamma l) \end{bmatrix} \begin{bmatrix} V_1 \\ I_1 \end{bmatrix} \tag{2.22}$$

Where:

γ = the propagation constant of the cable

l = the length of the cable

Z_c = the characteristic impedance of the cable

The transfer function of the two port circuit is [28]:

$$H = \frac{Z_L}{AZ_L + B + CZ_LZ_S + DZ_S} \tag{2.23}$$

The input impedance of the two port circuit is calculated as [32]:

$$Z_c = \frac{V_1}{I_1} = \frac{AZ_c + B}{CZ_L + D} \tag{2.24}$$

2.4 Transmission over Power-Line Communication Channel

2.4.1 Impedance

Impedance is a measure of the opposition to current flow in alternating current circuits. The power line channel impedance is frequency dependent and varies between several ohms to a few kilo-ohms [30]. Since loads with different impedances connected to the network are constantly varying, that is being switched on and off, with some being frequency dependent, the PLC channel impedance fluctuates according to the combination of all network and load impedances which therefore significantly affect the channel characteristics. The different impedance factors to consider in PLC channel characterization are sectioned as follows.

2.4.1.1 The Characteristic Impedance

The transmission line exhibits an intrinsic characteristic impedance Z_0, this impedance determines the reflection and transmission coefficients at points of discontinuity. From the transmission line theory, at any point on an infinite length line as illustrated in Figure 2.5, the ratio of the voltage to the corresponding current in a power line cable is a constant (2.25a) which is referred to as the characteristic impedance Z_0. This is determined from intrinsic line parameters based on the distributed element circuit model in Figure 2.2, and is defined in (2.25(b)) [27].

$$Z_0 = \frac{V_1}{I_1} = \frac{V_2}{I_2} = \cdots = \frac{V_n}{I_n} \tag{2.25a}$$

$$Z_0 = \sqrt{\frac{R' + j\omega L'}{G' + j\omega C'}} \tag{2.25b}$$

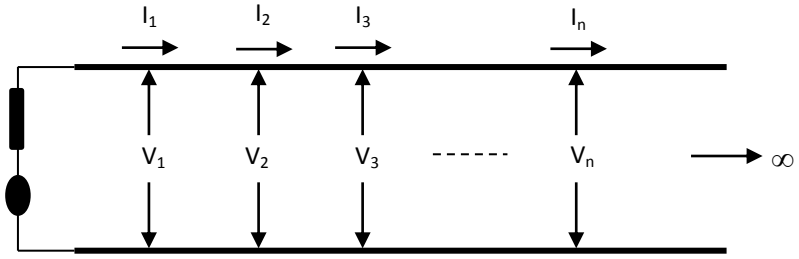

Figure 2.5: A voltage source and an infinitely long transmission line

Loads connected to the PLC network that are not properly matched to the characteristic impedance of the given network cable present points of mismatch which in turn cause reflections.

Reflection forms a significant contributor of path loss in the transmission line and is caused by discontinuities and impedance mismatch. The standing voltage and current waves produced by reflection account for the power losses and the frequency variant nature of the input impedance. This is because it dictates the power levels the transmitter is able to deliver to the PLC channel as well as the power received by the receiver device.

Change in the type of transmission line, branches connected to transmission line and load impedances not equal to the characteristic impedance of the transmission line are examples of points of mismatch. The application of the reflection coefficient characteristics are seen in a number of power line communication channel models in literature and in the formation of the multipath concept [34]. It is therefore imperative that proper calculation of the reflection coefficient is done.

2.4.1.2 Impedance at a termination load

The characteristic impedance is defined as the ratio of voltage to current, it is given as[28]:

$$Z_0 = \frac{V_0^+}{I_0^+} = -\frac{V_0^-}{I_0^-} \tag{2.26}$$

For the transmission-line circuit in Figure 2.6, the reflection coefficient of the load is the amplitude of reflected voltage to incident voltage, and is expressed as[28]:

$$\Gamma_L = \frac{V_0^-}{V_0^+} = \frac{Z_L - Z_0}{Z_L + Z_0} \tag{2.27}$$

The transmission coefficient T is given by[20]:

$$T = 1 + \Gamma_L \tag{2.28a}$$

$$T = \frac{2 \cdot Z_L}{Z_L + Z_0} \tag{2.28b}$$

Where:

Z_L = the termination load

Z_0 = the characteristic impedance of the transmission line

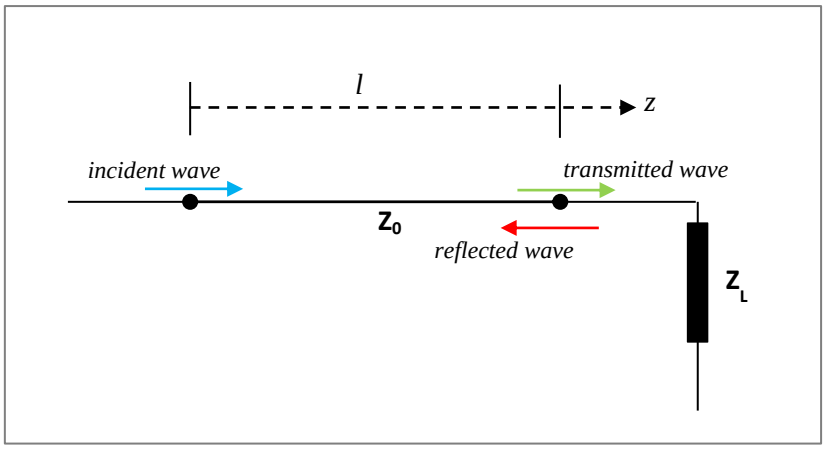

Figure 2.6: Illustration of the reflection at a termination load

Using the load reflection coefficient, the following expressions hold [28]:

$$V(z) = V_0^+(e^{-\gamma z} + \Gamma_L e^{\gamma z}) \tag{2.29}$$

$$I(z) = \frac{V_0^+}{Z_0}(e^{-\gamma z} - \Gamma_L e^{\gamma z}) \tag{2.30}$$

Where;

V_0^+ = the incident voltage

γ = the propagation constant of power line

z = the distance travelled by the signal.

2.4.1.3 Impedance at a node

An illustration of the reflection at the point of discontinuity formed by a branching node is given in Figure 2.7. At a branching node, the reflection coefficient is derived by considering the branches as forming a parallel connection. Therefore, the total impedance of n branches on the node is [16]:

$$Ztotal = Z_1//Z_2//..//Z_{n-1} \tag{2.31a}$$

Where;

n = the total number of branches extending from the branch, all inclusive.

If the network is formed by the same cable (all cables have the same characteristic impedance), the impedance seen by the incident wave is given by [35]:

$$Ztotal = \frac{Z_0}{n-1} \tag{2.31b}$$

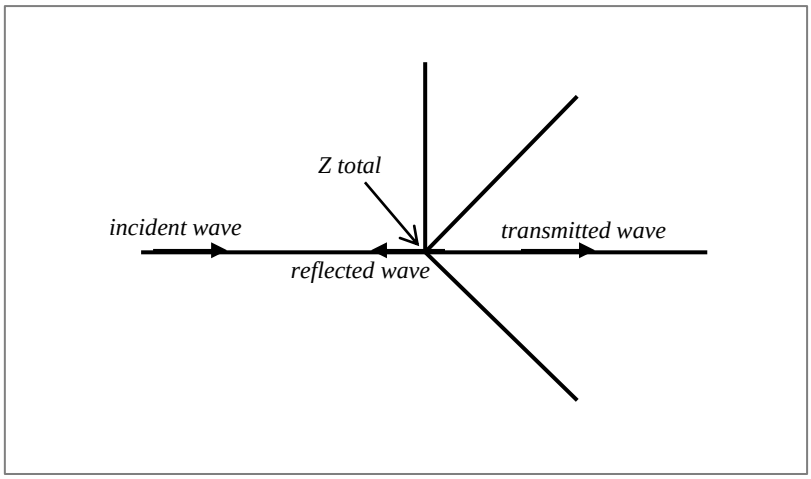

Figure 2.7: Reflection at a branching node

Where;

n = the total number of branches extending from the branch, all inclusive.

Z_0 = the characteristic impedance of the cables.

From Equations (2.27a, 2.27b and 2.28a), the reflection and transmission coefficient at the branching node are expressed as:

$$\Gamma = \frac{Ztotal - Z_0}{Ztotal + Z_0} = \frac{2 - n}{n} \tag{2.32a}$$

$$T = \frac{2}{n} \tag{2.32b}$$

2.4.1.4 Input Impedance

The input impedance is also a key characteristic of the PLC channel. The input impedance seen by a device connected to a PLC network varies due to the fact that devices are continuously connected or disconnected from the network. It changes with different topologies [36]. It therefore dictates the power the transmitting device is able to inject to the PLC channel as well as the power that gets to the receiver.

When considering impedance in a power line channel therefore, parameters such as the characteristic impedance of the line, the network topology and the impedance of loads connected to the PLC network affect the overall impedance. This is seen by the resultant reflections caused at points of discontinuity. The reflections are significant as they can limit the distance traversed by the signal through the transmission line.

2.4.2 Signal Attenuation

Extensive study of the attenuation characteristics of power line cables is found in literature[4, 13, 37]. The increase in signal attenuation as frequency and distance increase is one of the principal impairments of PLC channels. For the frequency band of interest in the current study, the signal attenuation in the channel is mainly due to three factors; resistive losses of conductors, dielectric losses of insulation and coupling losses [38]. Radiation losses are not considered a factor. This is because they are insignificant within the frequency range of interest (1.6 – 30 MHz), as the conductor separation is not a considerable fraction of the wavelength [18].

The resistive losses in power lines are caused by the finite conductivity of conductors as it has been mentioned earlier. Due to skin effect, the current flows on the surface of the conductor causing an increase in resistive losses with increase in frequency.

The propagation constant (Equation 2.12) can be determined using the condensed expression [39];

$$\gamma = k_1 \sqrt{f} + k_2 f + j k_3 f = \alpha + j\beta \tag{2.33}$$

Where;

k_1, k_2, and k_3 summarise the geometry and material parameters.

The real part of the propagation constant is the attenuation coefficient. R is proportional to $\sqrt{f}$ and G is proportional to f as seen in Equations (2.5) and (2.8) respectively. G is mainly affected by the dissipation factor of the insulating material, which points to dielectric losses.

Dielectric losses occur in the insulation material, and these are expressed by the dissipation factor or loss tangent $\tan\delta$. Though it is not the only option, Poly Vinyl Chloride (PVC) is normally used in insulating low voltage cables. The impediment however is that general dielectric characteristics of PVC cannot be defined. This is because it is dependent on temperature, frequency and composition of the insulation material. Figure 2.8a and 2.8b show the relationship between the relative dielectric constant, frequency and temperature from measurements obtained in [40] for PVC.

By employing the two conductor transmission line theory, attenuation coefficients are calculated using equation 2.14, for different cable cross sections and the different dielectric characteristics given in Table 2.1. These are taken from measurements given in [21] and [41]. Figure 2.9 illustrates that the dependence of attenuation is rather more on the dielectric and conductor properties than it is to the cross sectional area. The colours in the graph are correspondent to Table 2.1. The attenuation coefficients relative to frequency are nonlinear; this is due to the dielectric characteristics of the insulating material and skin effect.

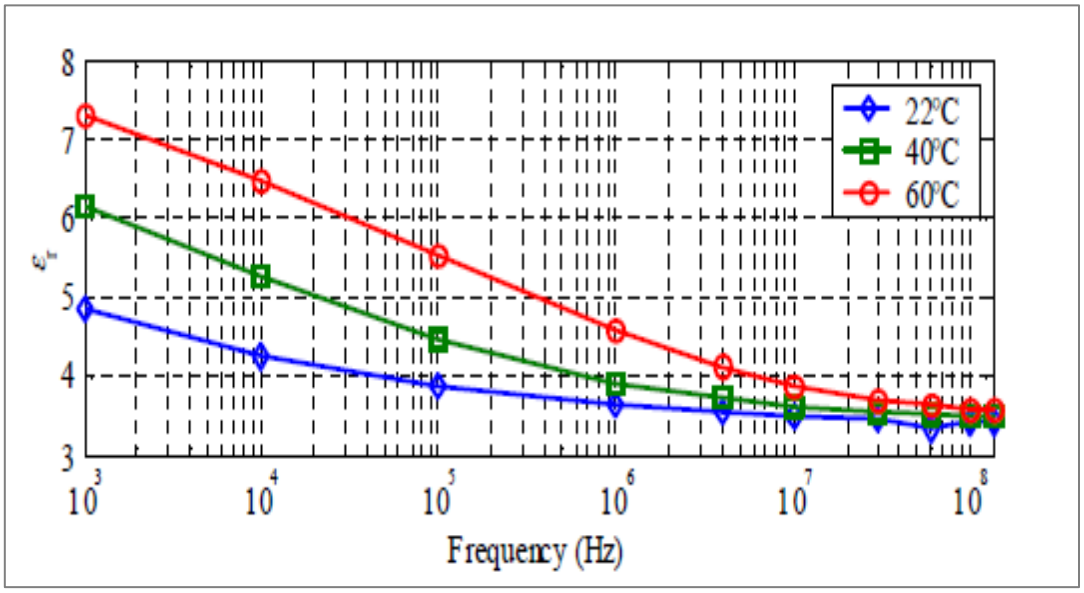

(a)

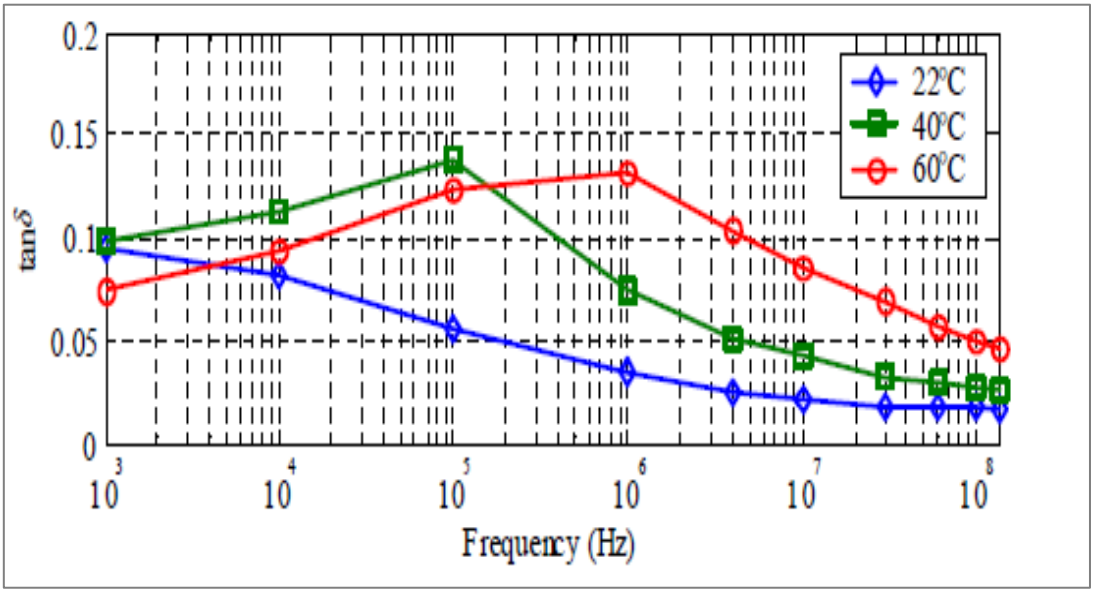

(b)

Figure 2.8(a) and (b): Measured dielectric characteristics of PVC [40]

Coupling losses are caused by discontinuities. Since the impedances at points of discontinuity are frequency dependent, attenuation caused by mismatch is therefore dependent on frequency, topology, characteristics of the transmission line and connected loads.

Cable type	*Dimensions*	*Relative dielectric permittivity*	*Dissipation factor*
VVF	**2.5mm²**	$-0.8802 \log10(f) + 8.9964$ 70k ≤ f ≤ 5MHz	$-5.7257 \times 10^{-10} f + 0.06$,
	4mm²	$-3.3333 \times 10^{-9} f + 3.116$ 5 ≤ f ≤ 35MHz	for 70k ≤ f ≤ 35MHz
NYM	**2.5mm²**	-0.88 log(f) + 9.60 1.6 MHz <f < 5MHz	$-5.7257 \times 10^{-10} f + 0.075$,
	4mm²	$-3.3333 \times 10^{-9} f + 3.71$ 5MHz< f <30MHz	for 1.6MHz≤ f ≤ 30MHz

Table 2.1 Dielectric constant for different cable types

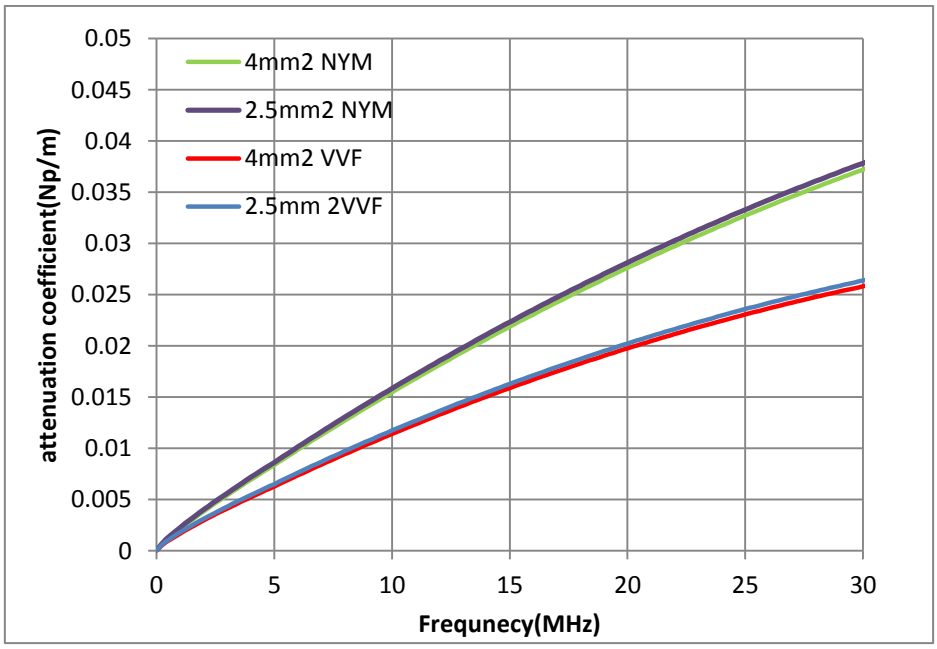

Figure 2.9: Attenuation constant for different geometry and dielectric composition

2.4.3 Noise

The performance and reliability of the PLC system as stated earlier is affected by noise. Just as the transfer function models it is necessary that noise is also accurately characterised. Unlike conventional systems, it is not modelled by Additive White Gaussian Noise (AWGN). [42] provides a classification of the noise types present in PLC network as:

1. Impulsive noise which is considered as the most significant, and is mostly generated by electrical appliances connected to the network. It is further classified as;

    a. Periodic Impulsive Synchronous to the mains, which is generated by power supplies with silicon controlled rectifiers.

b. Periodic Impulsive Synchronous to the mains, which is mostly caused by switched-mode power supplies.
c. Asynchronous Impulsive noise which is generated by switching transients.

2. Narrow-band noise which is mostly in sinusoidal form or modulated signal with various origins, and generated by the existence of broadcast waves and spurious instabilities caused by appliance with a transmitter or receiver.
3. Coloured Background noise which is mostly generated by noise sources of low intensity and not of the nature of those included above. They are characterised by a power spectral density that decreases with frequency.

2.5 Chapter Summary

In this chapter, factors necessary for the modelling of the power line communication channel were studied. We theoretically examined the characteristics of the three core power cables used in low voltage networks. The cables are studied with respect to the two conductor transmission line model where the distributed elements modelling the power line are defined. Also, the two port circuit model of the power line by the use of matrices is studied. The effect of the dielectric material on the attenuation coefficients of the power line is considered. The parameters determining the characteristics and transfer function of a typical PLC channel were reviewed, showing their dependence on the network constituents and the power cable used in forming the PLC channel.

CHAPTER THREE

MODELLING TECHNIQUES FOR THE PLC CHANNEL

3.1 Introduction

In the development of new communication systems, the technique chosen for transmission and other design parameters is informed by the properties of the channel transfer characteristics and capacity offered by the channel [43]. This calls for accurate models that can describe the transmission behaviour over the PLC channel with sufficient precision. Several techniques to model transfer characteristics of power line channels have been offered in the literature. For these models, essentially, the two factors which determine the reliability and accuracy of the model are the modelling algorithms and the model parameters. The modelling techniques can be classified into two approaches depending on the way the model parameters are obtained; the top-down approach and the bottom-up approach [11].

In the top-down approach, which is also termed as the empirical approach, the model parameters are obtained from measurements [12, 34]. Little computation is necessary in this approach and it is easy to implement. In contrast, the bottom-up approach computed with a priori methodology begins with theoretical derivation of the parameters [11, 14, 15, 44], clearly describing the relationship between network performance and the parameters.

The empirical and deterministic modelling approaches both have their advantages and disadvantages; the top-down modelling approach is easy to use as it calls for little computation and is easy to implement. The transfer function parameters are extracted from actual measurements of the given PLC channel or network. Its main setback however is that it is susceptible to measurement errors and cannot be used to reproduce the channel characteristics of a different PLC network.

The bottom-up modelling approach derives all parameters of transfer function from a theoretical basis. For a given channel, it necessitates detailed knowledge of all components and their respective characteristics. These details are the topology, lengths of the links, cable properties, and impedance values at every given branch termination. The network behaviour in relation to the model parameters is therefore clearly defined. Changes in the transfer function are predictable given the changes in the network configuration. The characterisation is however affected significantly if the values of some of the parameters are not known. Realistically, this approach is time consuming and requires more computational efforts.

The modelling techniques for the PLC channel transfer function are achieved in either time or frequency domain depending on the algorithms used. With the time domain, the channel is defined by a multipath model where the channel is viewed as a multipath environment. With the frequency

domain algorithms, the network is often fragmented and regarded as elements in cascade, defined with either transmission or scattering matrices [45].

In the following Sections of the Chapter, a number of models derived from the two modelling approaches are reviewed.

3.2 Top-Down PLC channel modelling

3.2.1 Echo Model

In the pioneering work by Phillips [12], the power line channel is considered as a multipath environment. The existence of several branches and impedance mismatches that cause multiple reflections bring about the multipath nature of the power line channel. When the powerline is characterized, each transmitted signal reaches the receiver on a direct path as well as on various other paths, which are delayed and mostly attenuated as a result of the reflections at impedance discontinuities. The receiver therefore obtains the transmitted signal via N different paths. Figure 3.1 depicts the implementation of Philipp's echo model with N paths.

The transfer function for N paths is described by a set of three parameters, given by [12]:

$$H(f) = \sum_{i=1}^{N} \rho_i \cdot e^{-j2\pi f \tau_i} \tag{3.1}$$

Where;

N = the number of signal flow paths

i = each flow path

τ_i = the time delay

ρ_i = the complex factor which is the product of transmission and reflection factors.

This complex attenuation factor is given by [12]:

$$\rho_i = |\rho_i| \cdot e^{-j\varphi_i} \tag{3.2}$$

Where:

$$\varphi_i = tan^{-1}\left(\frac{Im(\rho_i)}{Re(\rho_i)}\right) \tag{3.3}$$

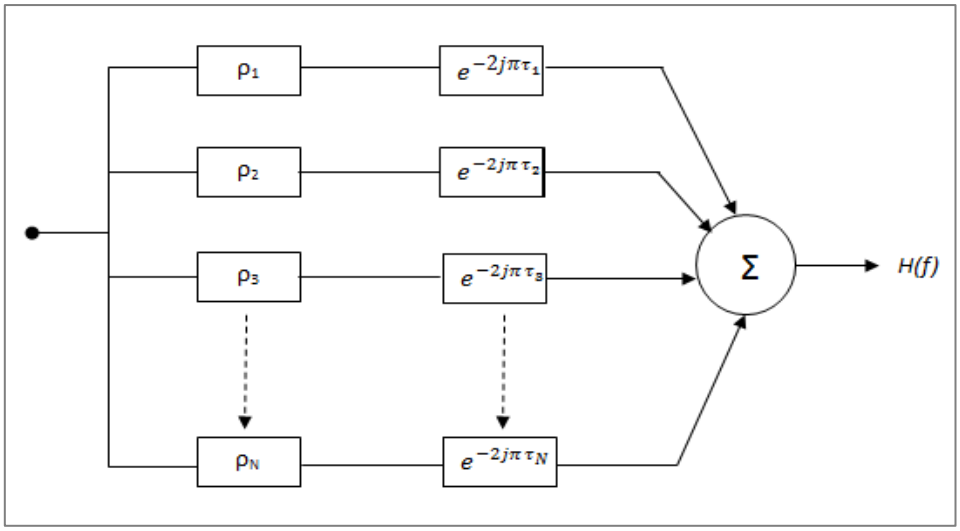

Figure 3.1 Conceptual sketch of Philipp's echo model

The transfer function is obtained by a Fourier transformation of the measured impulse response, this impulse response is represented as a sum of N Dirac pulses delayed by τ_i and multiplied by ρ_i, and is expressed as [46]:

$$h(t) = \sum_{i=1}^{N} |\rho_i| \cdot e^{-j\varphi_i} \cdot \delta(t - \tau_i) \tag{3.4}$$

3.2.2 Multipath Model

Zimmermann and Dostert [13] adapted the echo model in [12,46], and extend it by factoring the attenuation of signal as it traverses the network and consider the communication channel, by very few relevant parameters as a black box in the frequency range of 500kHz to 20MHz. The multipath propagation scenario with frequency selectivity is adopted considering that the signal is not transmitted to receiver along a quasi 'line of sight' path, but rather encounters reflections at points of discontinuities. These points of discontinuity are presented by, for example, cable joints, different cable characteristic impedance, series joints and connection boxes. They define the channel transfer characteristics by a frequency response [13] given as:

$$H(f) = \sum_{i=1}^{N} g_i \cdot e^{-(a_0 + a_1 f^k) \cdot d_i} \cdot e^{-j2\pi f \tau_i} \tag{3.5}$$

Where;

N =the number of paths of propagation

g_i = the weighting factor

a_0 , a_1 and exponent k = the attenuation coefficients

d_i = the path length,

τ_i = the path delay given by the following [13]:

$$\tau_i = \frac{d_i}{v_p} = \frac{d_i\sqrt{\varepsilon_r}}{c_0} \tag{3.6}$$

Where;

ε_r =the insulating material's dielectric constant

c_0 =the speed of light

d_i = the length of a path and

v_p =the propagation speed

To describe the multipath scenario a T node as in Fig 3.2 which is merely a link with one branch consisting of elements (1), (2) and (3) which have lengths L_1, L_2 and L_3 and the characteristic impedances Z_{L1}, Z_{L2} and Z_{L3} respectively, is considered. When points A and C are assumed to be matched, $Z_A = Z_{L1}$ and $Z_C = Z_{L2}$, the reflection points are reduced to be at points B and D, with reflection coefficients r_{1B}, r_{3B}, r_{3D} and the transmission coefficients denoted as t_{1B}, t_{3B}.

With these assumptions, the link may have an infinite number of propagation paths. Each path *i*, representing the product of the reflection and transmission coefficients along the path, has the weighting factor g_i. Therefore, after a reasonable number of paths, typically between 5-50 paths [47] the weight factor becomes negligible and the model is computed with a finite number of paths.

From the complex transfer function measurements of the channel, the parameters of equation (3.5) are obtained. The factor $e^{-(a_0+a_1 f^k)\cdot d_i}$ is considered the attenuation factor, forming the scaling operation describing linear path loss. Its parameters are determined therefore from the average magnitude of the

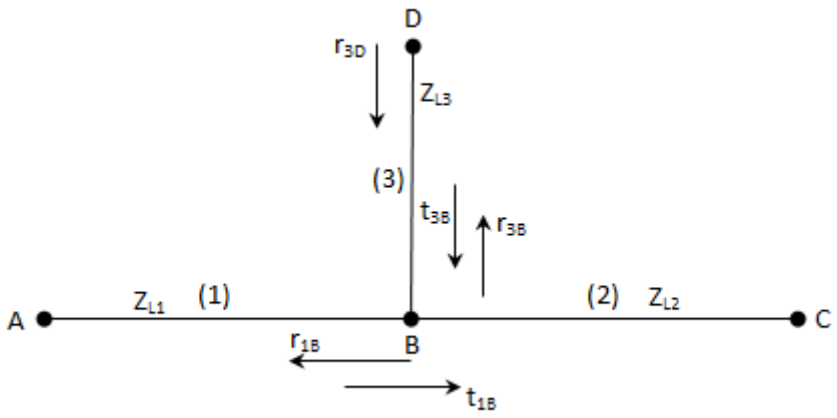

Figure 3.2: Single multipath signal propagation

frequency response where k is predictably between 0.5 and 1[34]. The factor $e^{-j2\pi f\tau_i}$ is considered the delay portion. The parameters τ_i, d_i as well as the weighting factor g_i are obtained from the channel's impulse response. The summary of the parameters is given in Table 3.1.

The amplitude of the weighting factor and the delay factors are illustrated in Figure 3.3. These are obtained when the frequency response acquired from measurements is converted to time domain. The amplitude decreases with increase in delay. This is due to the reduction in signal power as it traverses through points of discontinuity as well as the line attenuation.

Parameter	***Description***
i	The path number. The shortest delay being the first path, $i=1$
a_o, a_1	Attenuation coeffients
k	Exponent of the attenuation factor
g_i	The ith paths complex weighting factor which is a combination of the reflection and transmission coefficients in the related path
d_i	The length of path i
τ_i	The delay of path i

Table 3.1 Multipath transfer function model parameters

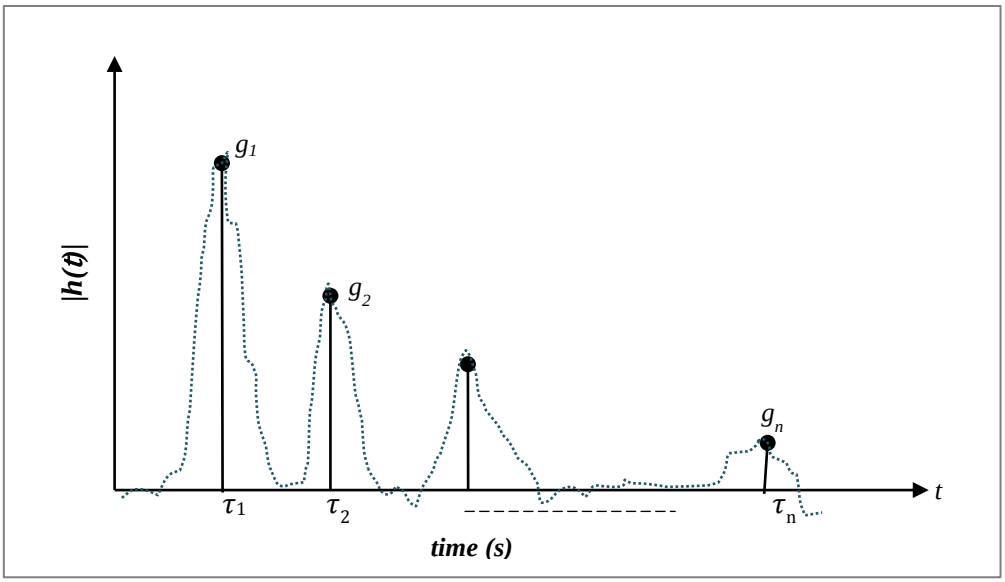

Figure 3.3: Graphical representation of a typical Impulse Response for a T-network topology.

3.3 Bottom-Up PLC channel modelling

3.3.1 Multipath Model

The analytical model by [34] [13] of the PLC Channel transfer function can be reconstructed into a deterministic approach. Models proposed by [44] and [48] and several others use this approach. For a given number of paths, an estimate of the path attenuation, weighting and delay factor are determined. The intrinsic line parameters (the characteristic impedance and propagation constant) are derived prior to the calculation of the transfer function shown in (3.7).

$$H(f) = \sum_{i=1}^{N} g_i \cdot e^{-\alpha \cdot d_i} \cdot e^{-j2\pi f \frac{d_i}{v_p}} \tag{3.7}$$

With the Zimmerman and Dostert analogy, the T node network (Figure 3.2), the reflection and transmission coefficients are computed as [48]:

$$r_{1b} = \frac{Z_{L2}||Z_{L3} - Z_{L1}}{Z_{L2}||Z_{L3} + Z_{L1}}, \quad t_{1b} = 1 - |r_{1b}| \tag{3.8}$$

$$r_{3d} = \frac{Z_0 - Z_{L3}}{Z_0 + Z_{L3}} \tag{3.9}$$

$$r_{3b} = \frac{Z_{L2}||Z_{L1} - Z_{L3}}{Z_{L2}||Z_{L1} + Z_{L3}}, \quad t_{3b} = 1 - |r_{3b}| \tag{3.10}$$

The backward reflections that occur at points of discontinuity are however assumed to be negligible [48]. A disadvantage with this modelling approach is that presenting the paths when the node has more than one branch becomes pretty complex. The possible paths and weighting factors for the T node are obtained as suggested in Table 3.2.

path no	**signal direction**	**path length (d_i)**	**weighting factor (g_i)**
1	$A \rightarrow B \rightarrow C$	l_1+l_2	t_{1b}
2	$A \rightarrow B \rightarrow D \rightarrow B \rightarrow C$	$l_1+2l_3+l_2$	$t_{1b} \times r_{3d} \times t_{3b}$
3	…	…	…
N	$A \rightarrow B \rightarrow (D \rightarrow B)^{N-1} \rightarrow C$	$l_1+2(N-1)\cdot l_3+l_2$	$t_{1b} \times r_{3d} \times (r_{3d} \times r_{3d})^{N-2} t_{3b}$

Table 3.2 Signal Propagation parameters

3.3.2 Anatory *et al.* Model

This model presents developed transfer characteristics of power line channels based on reflection and transmission factors, while taking into consideration loads, distances and interconnection nodes [49].

For a transmission line with multiple branches at a single node as in Fig. 3.4 where Z_S is the source impedance, Z_n is the characteristic impedance of any terminal with source while V_S and Z_L are source voltage and load impedance respectively, Anatory *et al.* formulated a generalized transfer function denoted by [15]:

$$H_m(f) = \sum_{M=1}^{L} \sum_{n=1}^{N_T} T_{LM} \alpha_{mn} H_{mn}(f) \qquad n \neq m \tag{3.11}$$

Where;

$N_{T,}$ = the total number of branches connected at node B and terminated in any arbitrary load

N = any branch number, m= any referenced (terminated) load

M= number of reflections (with total L number of reflections)

$H_{mn}(f)$ = transfer function between line n and a referenced load m

T_{LM}= transmission factor at the referenced load m, respectively

With these the signal contribution factor α_{mn} is given by:

$$\alpha_{mn} = P_{Ln}^{M-1} \rho_{nm}^{M-1} e^{-\gamma_n (2(M-1) l_n)} \tag{3.12}$$

Where;

ρ_{mn} = the reflection factor at node B between line n and the referenced load m

γ_n = the propagation constant of line n that has line length L_n.

With the exception at source where $\rho_{L1} = \rho_S$ is the source reflection factor, all terminal reflection factors P_{Ln} in general are given by:

$$P_{Ln} = \begin{cases} \rho_S & n = 1(source) \\ \rho_{Ln}, & otherwise \end{cases} \tag{3.13}$$

A further comprehensive case relevant to any line formation of a power line network with a range of branches was considered as shown in Fig. 3.5. The transfer function of such a network is denoted by (3.14) [50].

$$H_{mM_T}(f) = \sum_{d=1}^{M_T} \sum_{M=1}^{L} \sum_{n=1}^{N_T} T_{LM} \alpha_{mnd} H_{mnd}(f) \qquad n \neq m \tag{3.14}$$

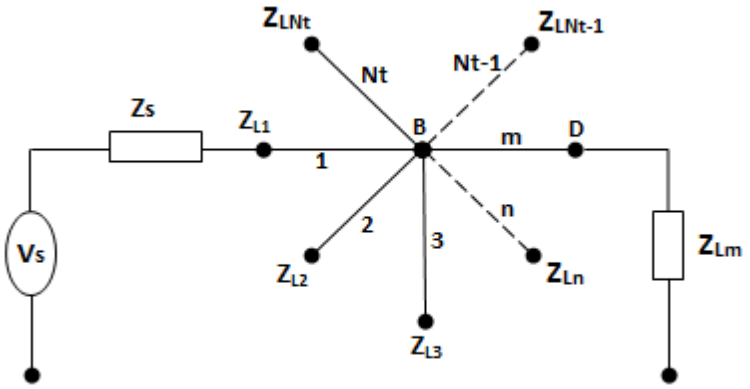

Figure 3.4: Power line network with multiple branches at a single node

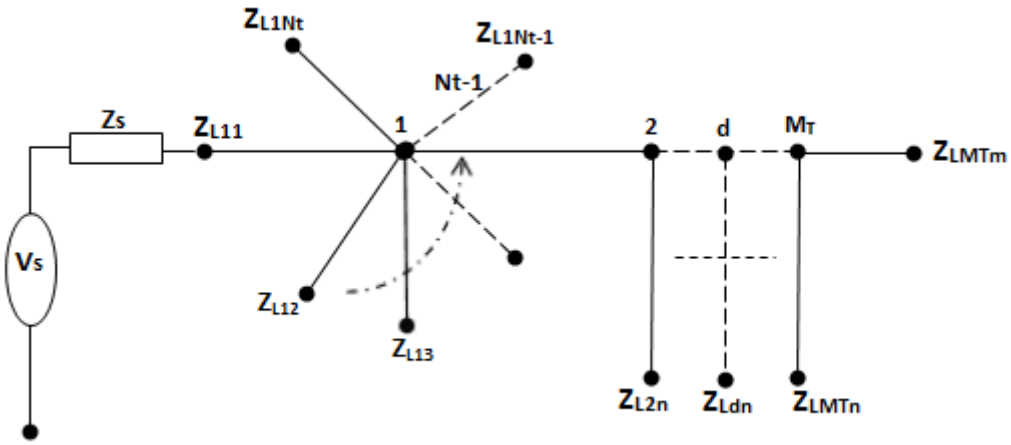

Figure 3.5: Power-line network with distributed branches

Where;

$$\alpha_{mnd} = P_{Lnd}^{M-1} \rho_{nmd}^{M-1} e^{-\gamma_{nd}(2(M-1)l_{nd})} \tag{3.15}$$

$$P_{Lnd} = \begin{cases} \rho_s & d = n = 1(source) \\ \rho_{Lnd} & otherwise \end{cases} \tag{3.16}$$

In (3.14) the parameters used have the same significance as mentioned above , that is, all parameters used in (3.11-3.13) are similar to (3.14-3.16), respectively, but with reference node *d* [49] and:

M_T = the total number of distributed nodes

d = any referenced node (1… MT),

$H_{mnd}(f)$ = the transfer function from line *n* to a referenced load *m* at a referenced node *d*.

3.3.3 Meng *et al*. Model

This frequency-domain modelling approach mainly focuses on the type of cable used and the impedances at terminations. The low voltage single phase power cable is modelled as a two conductor transmission line to compute the two intrinsic line parameters, the characteristic impedance, Z_0 and the propagation constant, γ [11]. The low voltage power network is considered as an *N*-branch network as in Figure 3.6, which is subdivided into several cascades of single branch channels. The channel transfer function is determined by deriving first the scattering matrix for each single-branch network and then the scattering matrix of the whole channel by using the chain-scattering matrix method.

The topology shown in Fig. 3.7 is used to evaluate the s-parameters of a single-branch network. In this derivation, the power line on the direct signal path (excluding the branches) is defined as the path line. Line 1 is the path power line with line parameter Zo, γ, Line 2 is the branch power line with line parameter Zo, γ, Line 3 is the transmission line with 50Ω characteristic impedance.

Where:

E_g = the source voltage

Z_s = the source impedance,

Z_L =the load impedance,

Z_b =the load impedance at the branch end.

Z_{in1} =the input impedance of the network on the right of the tap,

Z_{in2}= the input impedance of the branch network,

Z_{in} =the input impedance of the single branch network.

$\Gamma_{2=}$ the reflection coefficient from path end,

Γ_1 =the reflection coefficient from tap point calculated as:

$$\Gamma_1 = \frac{Z_L - Z_0}{Z_L + Z_0} \tag{3.17}$$

$$\Gamma_2 = \frac{Z_{in1}||Z_{in2} - Z_0}{Z_{in1}||Z_{in2} + Z_0} \tag{3.18}$$

The parameters S_{11} and S_{21} are computed as according to [51]:

$$S_{11} = \frac{Z_{in} - 50}{Z_{in} + 50} \tag{3.19}$$

$$S_{21} = 2\,\frac{V_3}{E_g} \tag{3.20}$$

The S_{21} parameter is indirectly calculated from:

$$S_{21} = 2\,\frac{V_3}{V_2}\,.\,\frac{V_2}{V_1}.\,\frac{V_1}{E_g} \tag{3.21}$$

$$\frac{V_1}{E_{g_1}} = \frac{Z_{in}}{Z_{in} + Z_g} \tag{3.22}$$

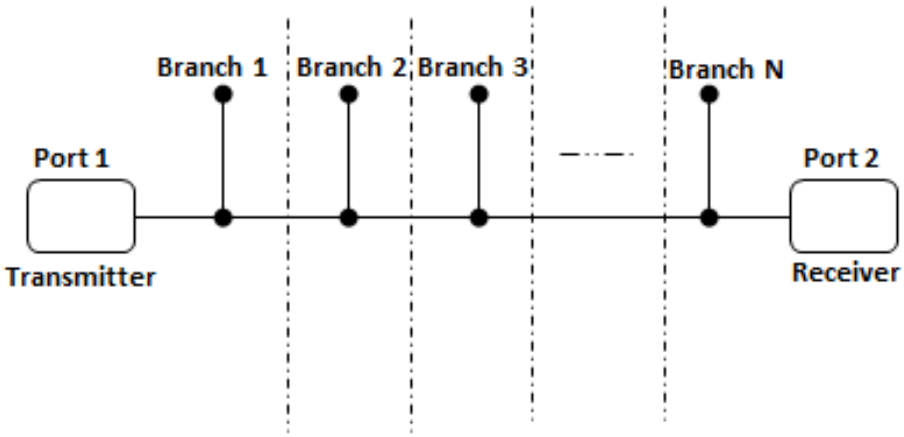

Figure 3.6: The simplified in house power line channel

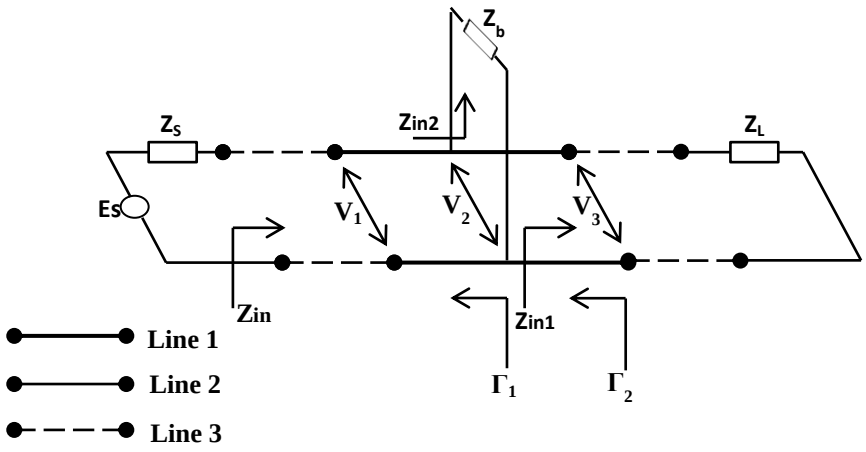

Figure 3.7: Single-branch network

Shifting in reference planes is applied as according to [28] to obtain the ratios:

$$\frac{V_3}{V_2} = \frac{(1+\Gamma_1)\, e^{-\gamma l_3}}{1+\Gamma_1 e^{-\gamma l_3}} \tag{3.23}$$

$$\frac{V_2}{V_1} = \frac{(1+\Gamma_2)\, e^{-\gamma l_1}}{1+\Gamma_2 e^{-\gamma l_1}} \tag{3.24}$$

Having calculated the S paramenters for a single branch, calculation for the whole network is done by cascading the T-matrices of each branch. Another possible method is the use of flow graphs which is not employed here due to its complexity. The T-matrix is given as [48, 51]:

$$[T] = \begin{bmatrix} \frac{1}{S_{21}} & -\frac{S_{22}}{S_{21}} \\ \frac{S_{11}}{S_{21}} & S_{12} - \frac{S_{11}S_{22}}{S_{21}} \end{bmatrix} \tag{3.25}$$

The N branch network will have a total T-matrix given by:

$$[T] = \prod_{k=1}^{N} [T_k] \tag{3.26}$$

Where:

T_k = the T-matrix of the k^{th} cascaded element in network.

Conversion of the total T-matrix is done to obtain the S-matrix of the whole network using the following equation:

$$[S] = \begin{bmatrix} \frac{T_{21}}{T_{11}} & T_{22} - \frac{T_{21}T_{12}}{T_{11}} \\ \frac{1}{T_{11}} & -\frac{T_{12}}{T_{11}} \end{bmatrix} \tag{3.27}$$

3.3.4 Esmailian *et al* Model

In this model, the transfer function of a sample power line channel with a single node is obtained using the ABCD matrix. The channel transfer function of multiple networks with a single tap is computed first and multiplication of the ABCD matrices is then done. The transfer function for a two port circuit is given by Equation 2.23. In the case of the network section consisting of a branch, an equivalent impedance Z_{eq} is given by[14]:

$$Z_{eq} = Z_c \frac{Z_b + Z_c \tanh(\gamma_b l_b)}{Z_c + Z_b \tanh(\gamma_b l_b)} \tag{3.28}$$

Where;

γ_b = the propagation constant of the branch cable

l_b = the length of the branch cable

Z_b = the characteristic impedance of the branch cable

Z_c = the characteristic impedance of the cable

The resulting simplified circuit is given by Figure 3.9, where the ABCD matrices for each section are formed (Equations 3.29b - 3.29e) and the total circuit ABCD matrix determined by:

$$\Phi = \prod_{i=0}^{3} \Phi_i \tag{3.29a}$$

$$\Phi_0 = \begin{bmatrix} 1 & Z_s \\ 0 & 1 \end{bmatrix} \tag{3.29b}$$

$$\Phi_1 = \begin{bmatrix} cosh(\gamma_1 d_1) & Z_1 sinh(\gamma_1 d_1) \\ \frac{1}{Z_1} sinh(\gamma_1 d_1) & cosh(\gamma_1 d_1) \end{bmatrix} \tag{3.29c}$$

$$\Phi_2 = \begin{bmatrix} 1 & 0 \\ Z_{eq} & 1 \end{bmatrix} \tag{3.29d}$$

$$\Phi_3 = \begin{bmatrix} cosh(\gamma_2 d_2) & Z_2 sinh(\gamma_2 d_2) \\ \frac{1}{Z_2} sinh(\gamma_2 d_2) & cosh(\gamma_2 d_2) \end{bmatrix} \tag{3.29e}$$

Where;

Z_1= characteristic impedance for the second sub-circuit

γ_1= propagation constants for the second sub-circuit

Z_2 = characteristic impedance for the fourth sub circuit

γ_2 = propagation constants for the fourth sub circuit.

Z_s = source impedance

Z_{eq} = equivalent branch impedance

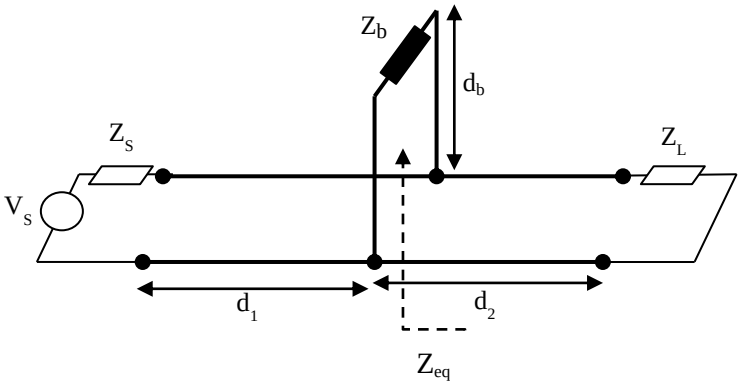

Figure 3.8: Transmission line with a single tap representation

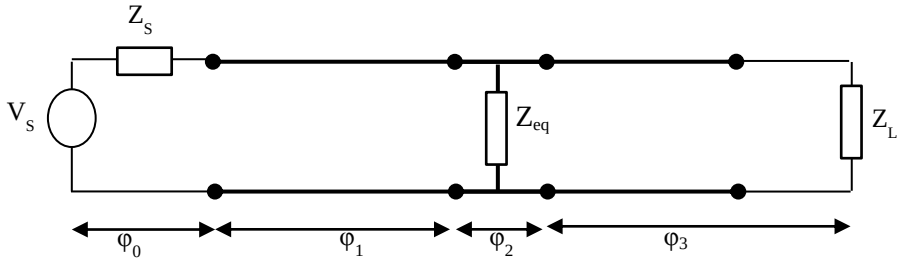

Figure 3.9: The circuit equivalent to Figure 3.8

3.4 Proposed Model

As discussed in the previous chapter, the PLC channel is time and frequency variant and therefore tracking the load impedances at multiple branch terminals is cumbersome. To serve as a general reference channel model for a network of the same cable parameters, this proposed model will help in the design and development of PLC communication systems by considering the extreme cases, that is, the short circuit and open circuit branch termination impedances. The characteristic impedance of the cable is assumed to be uniform and the source and load impedances at transmitter and receiver respectively are known.

The power line is described as a cascade of series resonant circuits (SRC) by [12], where one series resonant circuit connected to a line with impedance Z is represented as in Figure 3.10. The resulting amplitude and phase response of each resonant circuit is depicted in Figure 3.11.

The impedance of the frequency dependent resonant circuit Z_S is described by:

$$Z_S = R + j \cdot 2\pi f \cdot L + \frac{1}{j \cdot 2\pi f \cdot C} \tag{3.30}$$

Where:

R = the series resistance

L= the series inductance

C = the series capacitance.

The transfer function for each resonant circuit is given by:

$$Hr(f) = \frac{Z_S(f)}{Z_S(f) + Z} \tag{3.31}$$

Where:

Z = the line impedance.

An evolutionary strategy is employed by [12] to determine the optimized component parameters of the SRC. The model by [52] uses the two conductor transmission line theory unit length parameters as given in Equations (2.5 – 2.8). When considering measurement results shown by various literature and as shown in the following chapters, the transfer function can be viewed as a cascade of the amplitude response for a single SRC, with different resonant frequencies following a certain gradient.

From measurements in the Section 5, a correlation of the notches to the branch properties was obtained. The transmission line theory for short circuited and open circuited ends is employed. By analysing the input impedance characteristics around a resonant wavelength λr, circuits in Figure 3.12a and Figure 3.12b behave like a series RLC circuit [53]. We take Figure 3.10 therefore to represent our equivalent circuit for the branch line as in Figure 3.9.

For the open circuited end, the length of the cable is in odd multiples of λr/4 and for the short circuited end, the length of the cable is in even multiples of λr/2. Table 3.3 summarizes the determination of the series RLC parameters [53].

Each resonant circuit is described by a transfer function $Hr_i(f)$ and the overall transfer function is given as:

$$H(f) = A\prod_{i=1}^{n} Hr_i(f) \tag{3.32}$$

Where:

n =the number of series resonant circuits forming the total transfer function

A = the average path loss factor from transmitter to receiver distance determined by $e^{-\gamma d}$

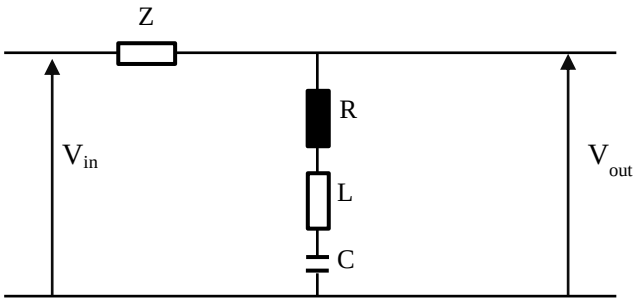

Figure 3.10: The series resonant circuit

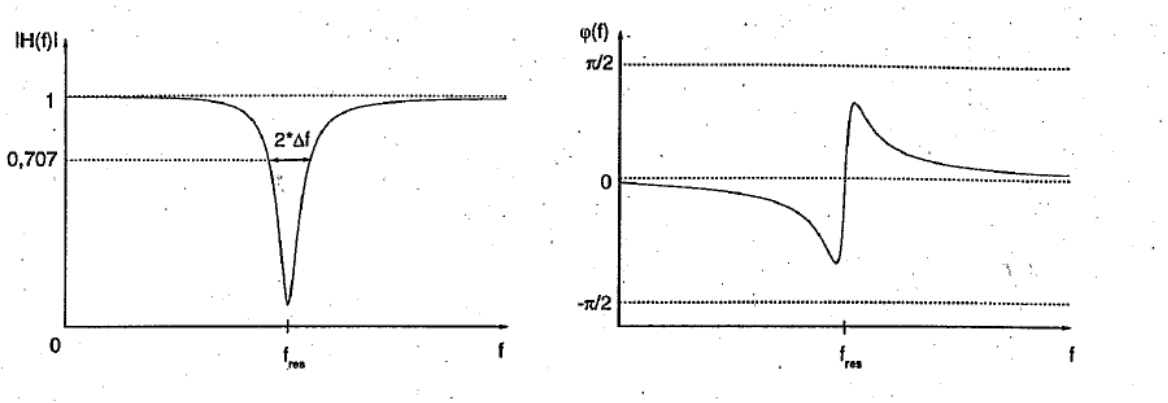

Figure 3.11: The amplitude and phase response of a series resonant circuit [12]

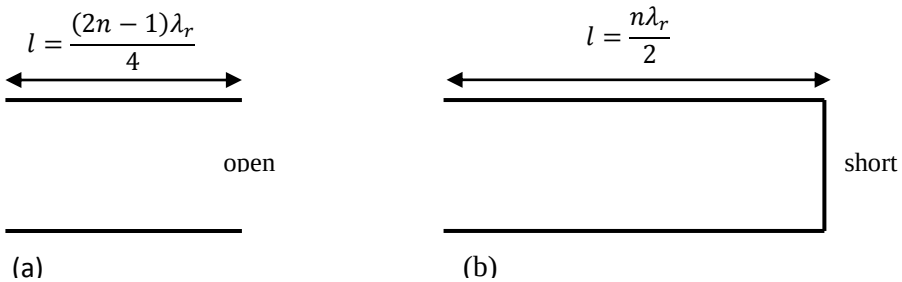

Figure 3.12a and 3.12b: Types of transmission line series resonant circuits

Resonance	Quarter wavelength ($\lambda_r/4$)	Half wavelength ($\lambda_r/2$)
	Open circuit	Short circuit
R	$\frac{1}{4}Z_0\alpha\lambda_r$	$\frac{1}{2}Z_0\alpha\lambda_r$
L	$\frac{\pi Z_0}{4\cdot\omega_0}$	$\frac{\pi Z_0}{2\cdot\omega_0}$
C	$\frac{4}{\pi\omega_0 Z_0}$	$\frac{2}{\pi\omega_0 Z_0}$
Q	$\frac{\beta_r}{2\alpha}$	$\frac{\beta_r}{2\alpha}$

Table 3.3 Series resonance RLC parameters

Where;

Z_0 = the characteristic impedance of the line

ω_0 = the resonant angular frequency

α = the attenuation constant of the line

λ_r = the wavelength at resonance

$\beta_r = \pi/l$

3.5 Chapter Summary

Presented in this chapter are different techniques and tools used to model the PLC channel. The demand for accuracy in the derivation of intrinsic line parameters is identified. Bottom-up and Top-down modelling approaches are studied and their complexities examined. A model based on the transmission line theory on series resonance circuit equivalence at quarter and have wavelength is proposed and its formulation is explained.

CHAPTER FOUR

INTRINSIC POWER LINE PARAMETER EXTRACTION

4.1 Introduction

Having discussed the modelling techniques, algorithms and parameters used to formulate the power line communication channel transfer functions, the calculation of accurate distribution parameters of the cables forming the PLC networks is seen to be an important aspect in PLC research. The following sections outline the techniques and measurement setups used to obtain the parameters of low voltage cables commonly used in building power networks. . The cables used in the carrying out of measurements were the Cu $3 \times 4mm^2$ and $3 \times 2.5mm^2$Cabtyre flexible PVC cables.

4.2 Line Parameter Extraction Technique

To obtain the primary line distributed parameters, that is, the unit length resistance, inductance, conductance and capacitance, the vector network analyser S_{11} parameter measurements for a defined length are taken. The measured normalized parameter gives the reflection coefficient from which we calculate the input impedance.

Considering Figure 4.1, from transmission line theory, the input impedance Z_{in} looking into the transmission line terminated by a load Z_L at a distance l from the generator end, the input impedance Z_{in} of the transmission line is determined by [54]:

$$Z_{in} = Z_0 \frac{Z_L + Z_0 tanh\, \gamma l}{Z_0 + Z_L tanh\, \gamma l} \tag{4.1}$$

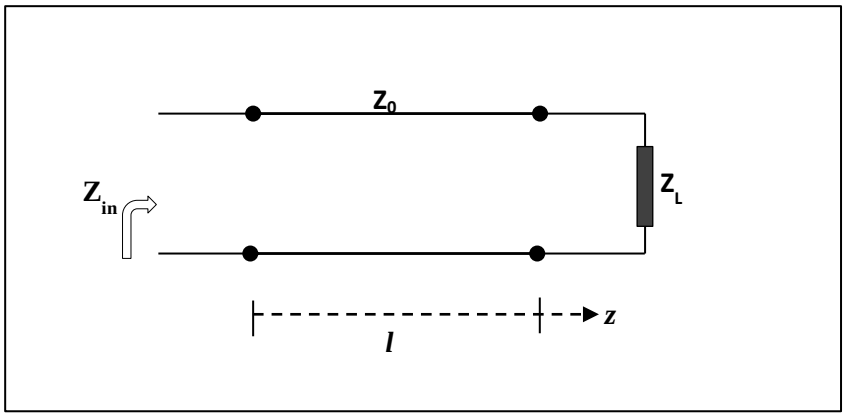

Figure 4.1: The reflection coefficient consideration

If the terminal is short circuited, making Z_L equal zero, (4.1) the input impedance Z_{sc} is given by :

$$Z_{sc} = Z_0 \tanh \gamma l \tag{4.2}$$

If the terminal is open circuited making Z_L equal to infinity (4.1), then:

$$Z_{oc} = Z_0 coth\, \gamma l \tag{4.3}$$

From (4.2) and (4.3), the characteristic impedance is therefore given by [55]:

$$Z_0 = \sqrt{Z_{sc} Z_{oc}} \tag{4.4}$$

And, the propagation constant is determined from [55]:

$$\gamma = {}^{1}/_{l} \tanh^{-1} \sqrt{Z_{sc}/Z_{oc}} \tag{4.5}$$

.

For each cable, the network analyzer gives an estimate of the reflection coefficient versus the measured frequency, f. From the complex S_{11} parameter measurements we derive from Equation (4.6) the input impedance for series component and input admittance for shunt component as shown in (4.7):

$$\Gamma_{in} = \frac{Z_{in} - Z_0}{Z_{in} + Z_0} \tag{4.6}$$

$$Z_{in} = Z_0 \frac{1 + \Gamma_{in}}{1 - \Gamma_{in}}, \quad Y_{in} = 1/Z_{in} \tag{4.7}$$

$$\Gamma_{in} = S_{11} \angle \phi \tag{4.8}$$

Where;

Z_0 =the reference impedance of the network analyzer port

Γ_{in}= the measured reflection coefficient

4.3 Measurement Setup

The aim of the measurements is to obtain the distributed elements unit length values for our cables so as to compare them to theoretical results. The ZVL Rohde & Shwarz Vector Network Analyzer was used for the measurements after one port calibration. This calibration procedure included three standardized loads implementing a 50Ω load, a short and an open circuit, ensuring high precision measurements to minimize measurement errors.

A. Resistance and Inductance

To measure these parameters, we short circuit the end of the cable, effectively establishing a connection through the series elements R' and L' as illustrated in Figure 4.2a and then the complex input impedance is measured.

B. Conductance and Capacitance

To measure these parameters, we open circuit the end of the cable, which effectively establishes a connection through the shunt elements, G and C as illustrated in Figure 4.2b, and then measure the complex input impedance.

Apart from obtaining elements R and L from the short circuit ended input impedance and elements G and C from the open ended circuit input admittance, from the characteristic impedance and propagation constant the elements may be obtained as follows [56]:

$$R' = \Re(\gamma \cdot Z_0) \tag{4.9}$$

$$G' = \Re(\gamma / Z_0) \tag{4.10}$$

$$L' = \Im(\gamma \cdot Z_0)/\omega \tag{4.11}$$

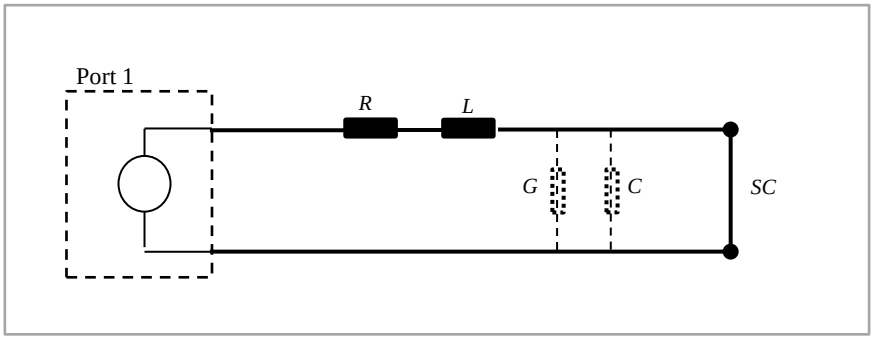

Figure 4.2a: Illustration of the short circuit ended measurement

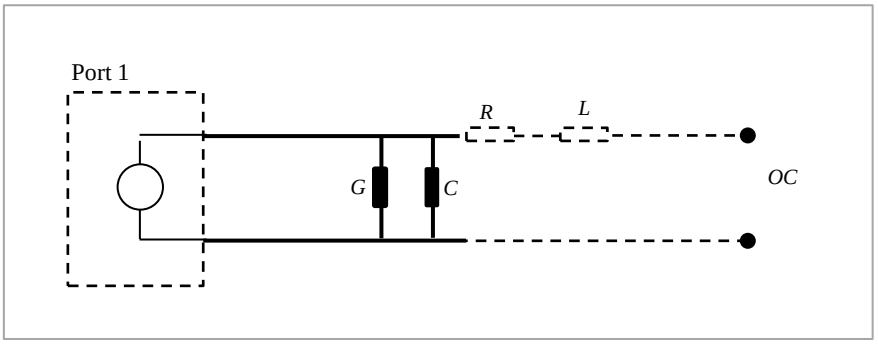

Figure 4.2b: Illustration of the open circuit ended measurement

$$C' = \Im(\gamma/Z_0)/\omega \qquad (4.12)$$

Where;

ω = the angular frequency

$\Re$ and $\Im$ denote the real and imaginary parts respectively

4.4 Line Parameter Measurements Results

The S parameters measured are used to obtain the cable input impedances for short circuited and open circuited ends so as to obtain primary line parameters as discussed in Section 4.2. Presented in Figure 4.3a and 4.3b for both open circuit and short circuit ended measurements is the input impedance for the 4mm^2 cable used.

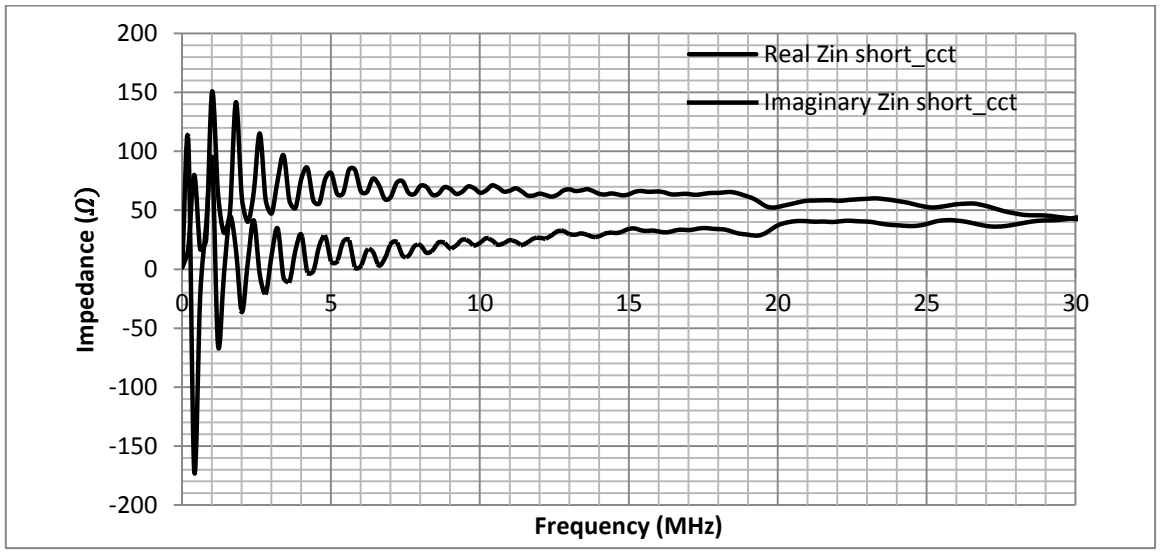

(a)

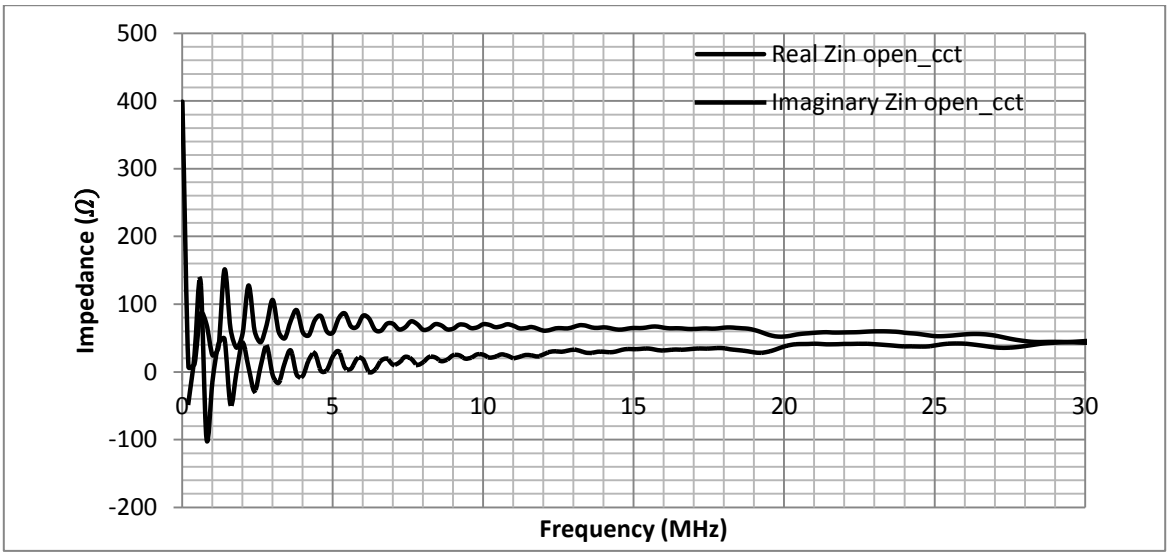

(b)

Figure 4.3: Input impedance of (a) short and (b) open circuit cable end

These measurements were obtained using a 99m cable. It can be seen that there are peaks in the lower frequencies, but these diminish with increase in frequency. The cable length is comparable to the wavelength within the frequency range, and the peaks are due to the cable resonance at the particular frequencies. With the cable losses increasing with frequency, at high frequencies, the wave reflected back from the point of mismatch is attenuated nearly completely. The primary cable parameters were measured from this cable length but followed the measured input impedance trend, that is, oscillations in lower frequencies, which die down at higher frequencies. The line under test therefore needs to be electrically short.

In order for a line to be electrically short, at the highest frequency it is required that the length of the line to be [26]:

$$l = \frac{1}{10}\lambda = \frac{1}{10}\frac{v_p}{f_{max}} \tag{4.13}$$

Where;

λ = the wavelength

v_p= the propagation velocity

f_{max}= the highest frequency to be measured

The parameter measurements that follow were obtained from a line length following the criterion in Equation (4.13).

Directly obtained from the vector network analyzer, for the 3x2.5mm^2 cabtyre PVC cable, the normalized complex S_{11} parameters for short circuited and open circuited cable ends are shown in Figures 4.4a and 4.4b respectively. For the 3x4mm^2 cabtyre PVC cable, the normalized complex S_{11} parameters for short circuited and open circuited ends are as shown in Figures 4.4c and 4.4d respectively.

Figure 4.5a and 4.5b show the capacitance per unit length for the CU 3x4mm^{2}and 3x2.5mm^2 cabtyre PVC cables compared to the theoretical model calculation as given in (2.7). Figures 4.6a and 4.6b show the inductance per unit length for the 4mm^{2}and 2.5mm^2 cabtyre three core cables compared to the theoretical model calculation as given in (2.6). Figures 4.7a and 4.7b show the resistance per unit length for the 2.5mm^2 and 4mm^2 cabtyre three core cables compared to the theoretical model calculation as given in (2.5). Figures 4.8a and 4.8b show the conductance per unit length for the 2.5mm^2 and 4mm^2 cabtyre three core cables compared to the theoretical model calculation as given in

(2.8). Figure 4.9a and 4.9b show the characteristic impedance for the 4mm^{2}and 2.5mm^2 cabtyre three core cables compared to the theoretical model calculation as given in (2.25b).

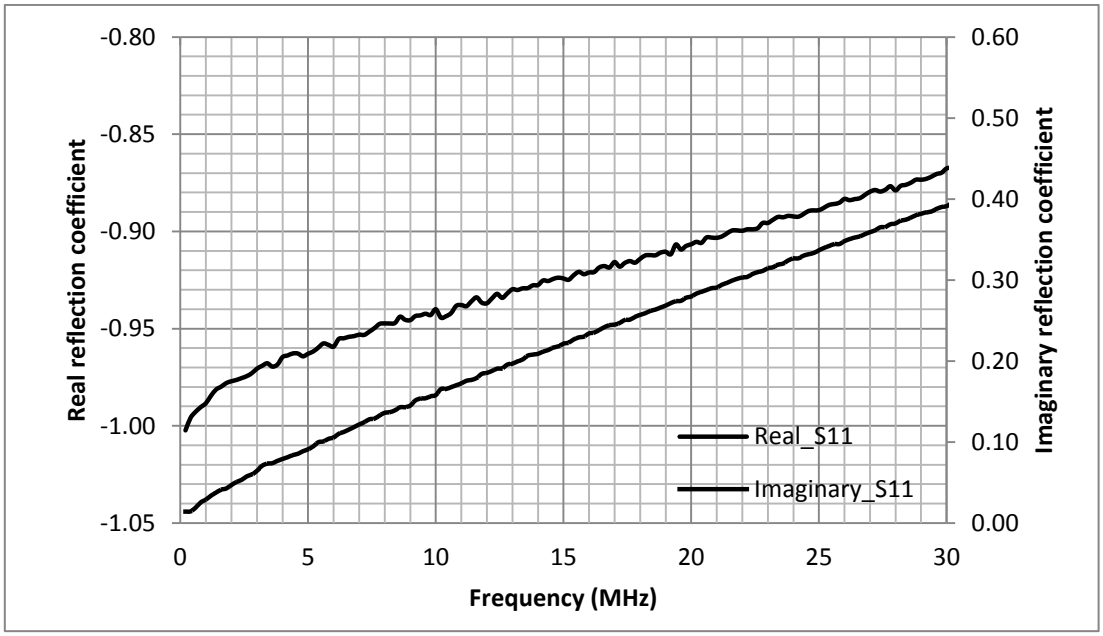

(a)

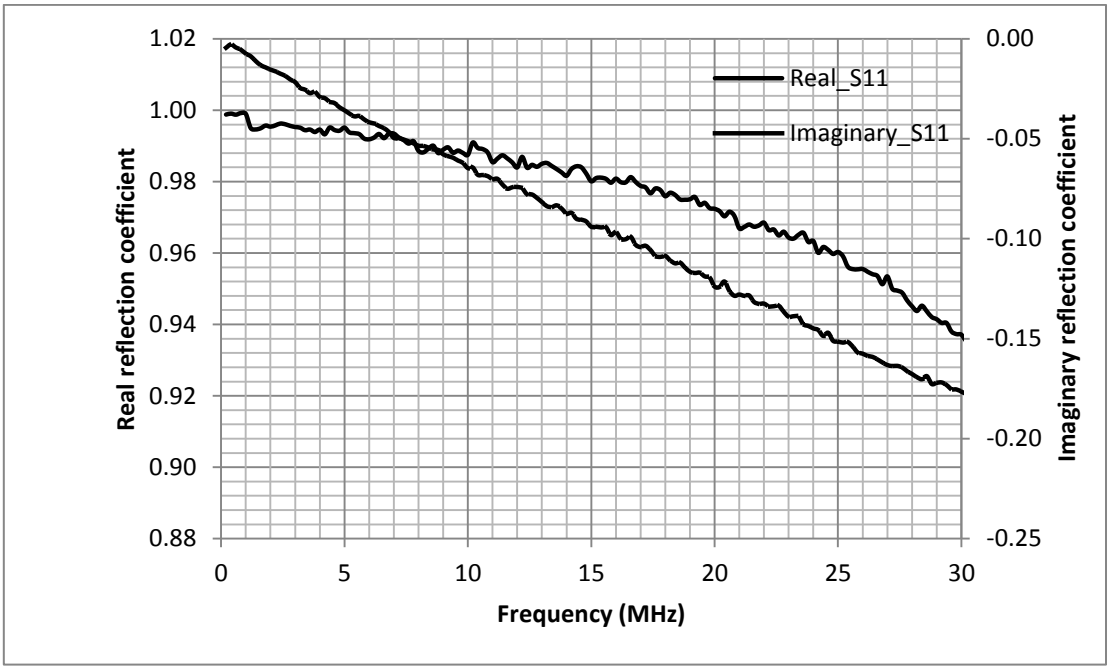

(b)

Figure 4.4: The 2.5mm^2 (a) short circuited and (b) open circuited ended cable normalized S_{11} parameters

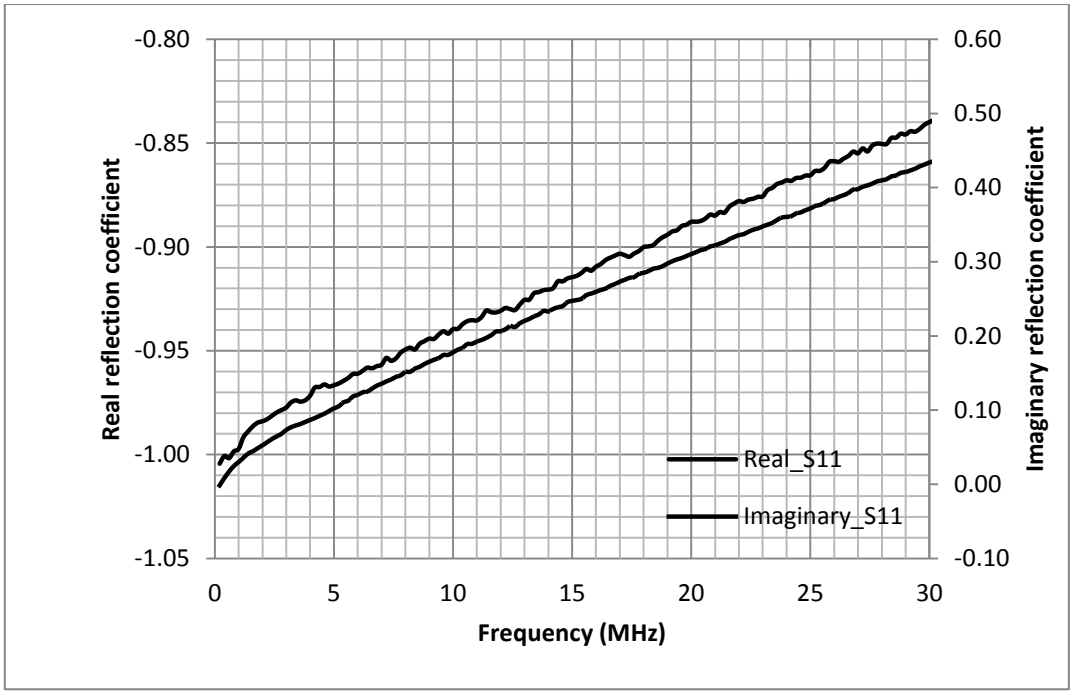

(c)

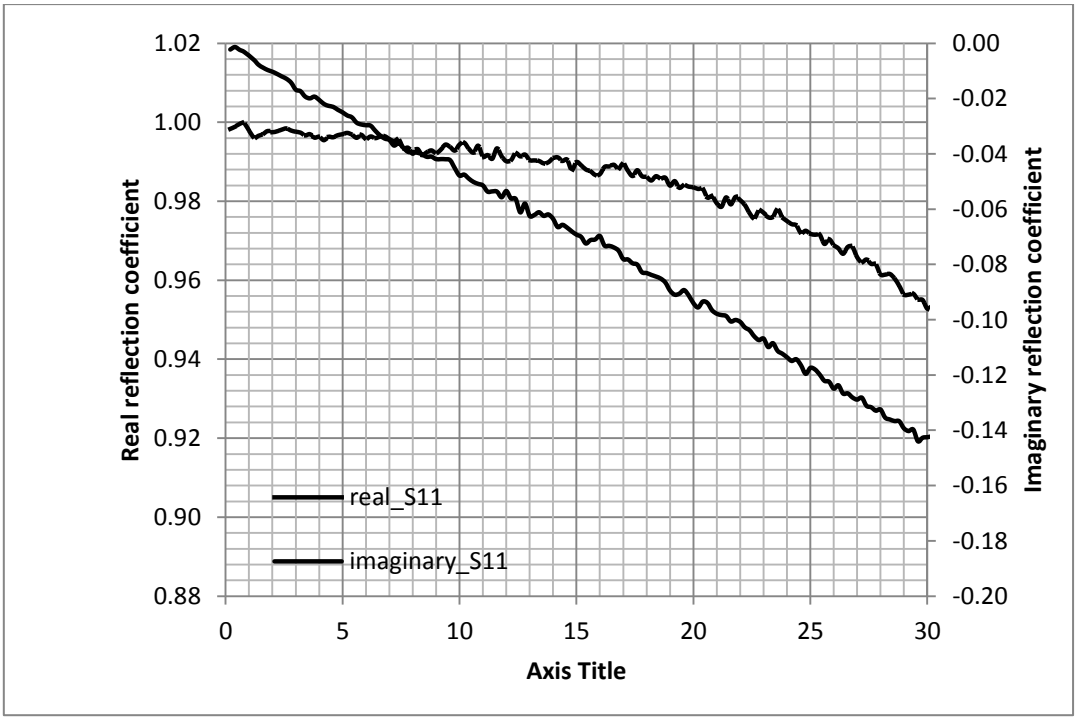

(d)

Figure 4.4: The 4mm^2 (c) short circuited and (d) open circuited ended cable normalized S_{11} parameters

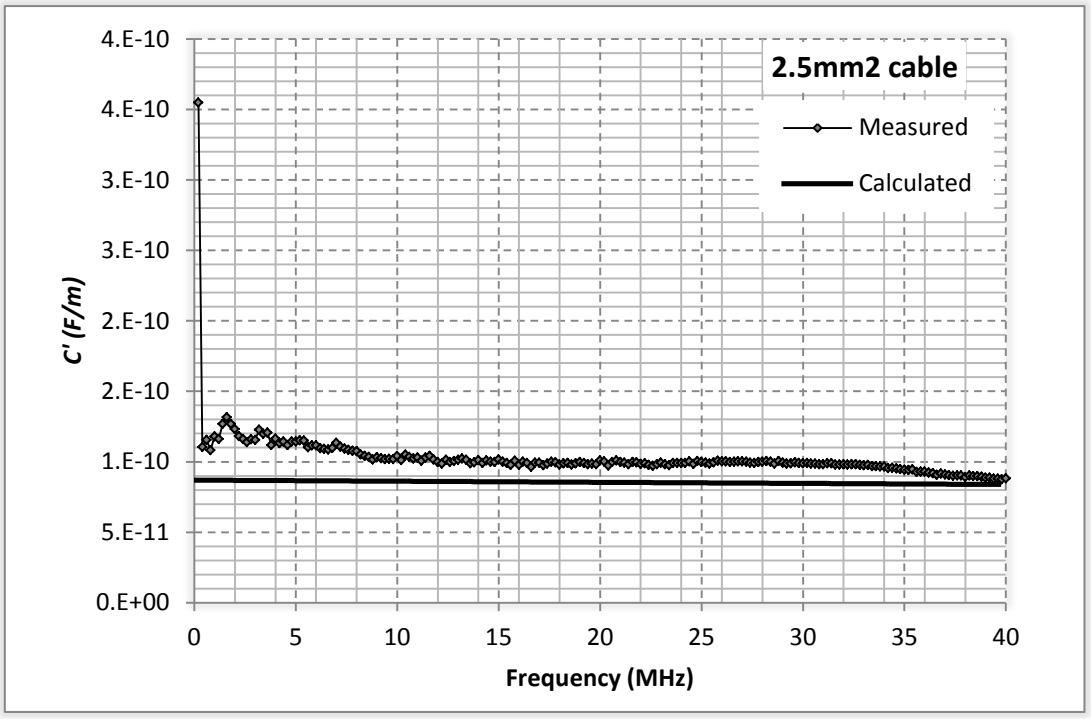

Figure 4.5a: The capacitance per unit length for the 2.5mm ^{2} transmission line

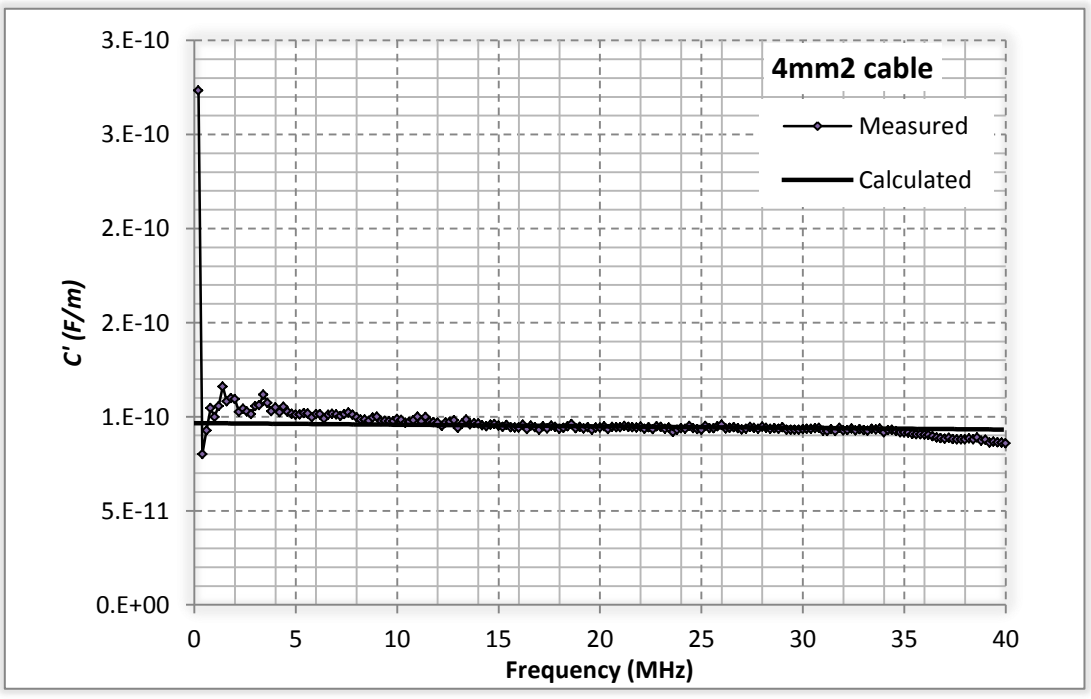

Figure 4.5b: The capacitance per unit length for the 4mm ^{2} transmission line

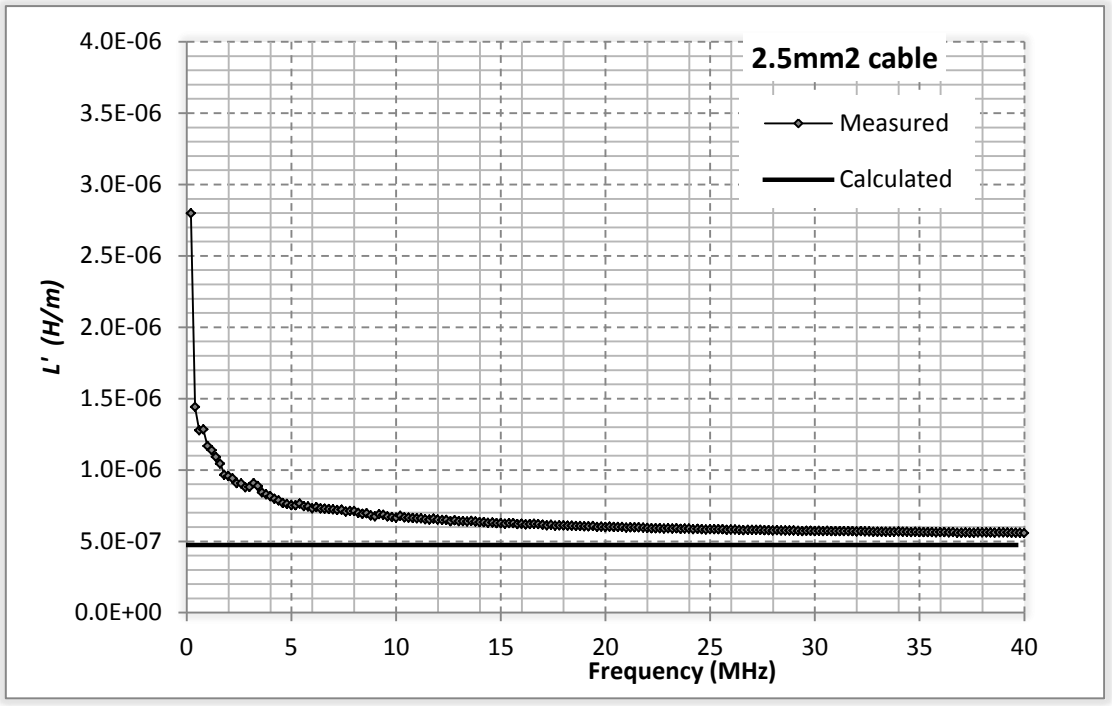

Figure 4.6a: The inductance per unit length for the 2.5mm ^{2} transmission line

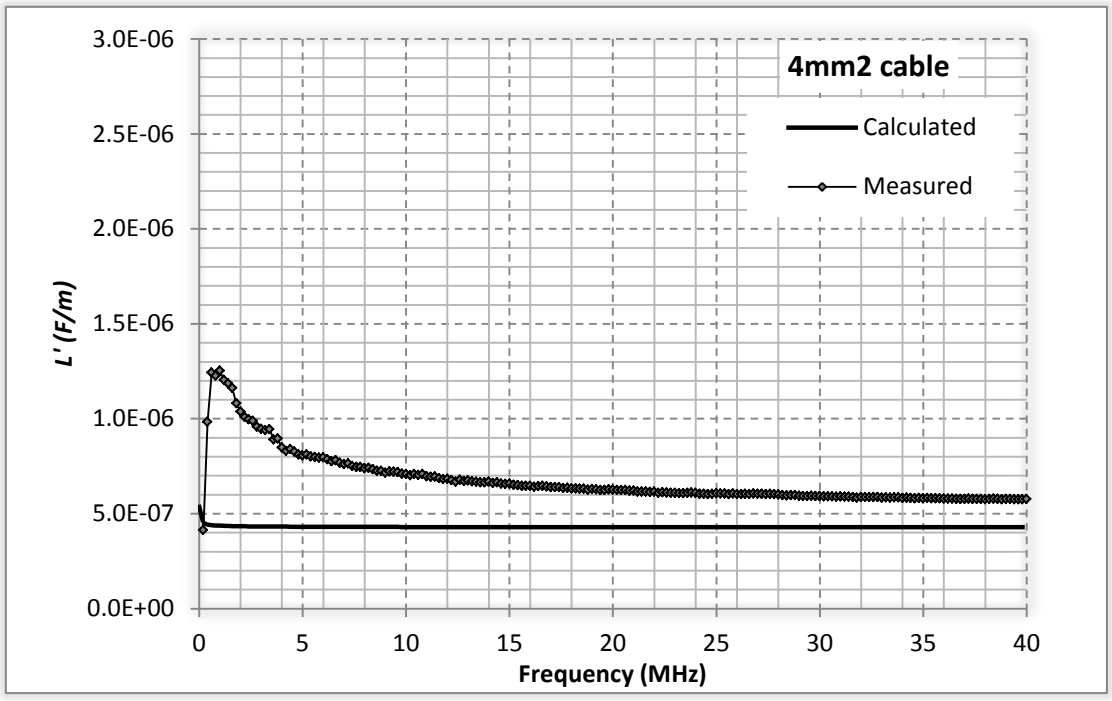

Figure 4.6b: The inductance per unit length for the 4mm ^{2} transmission line

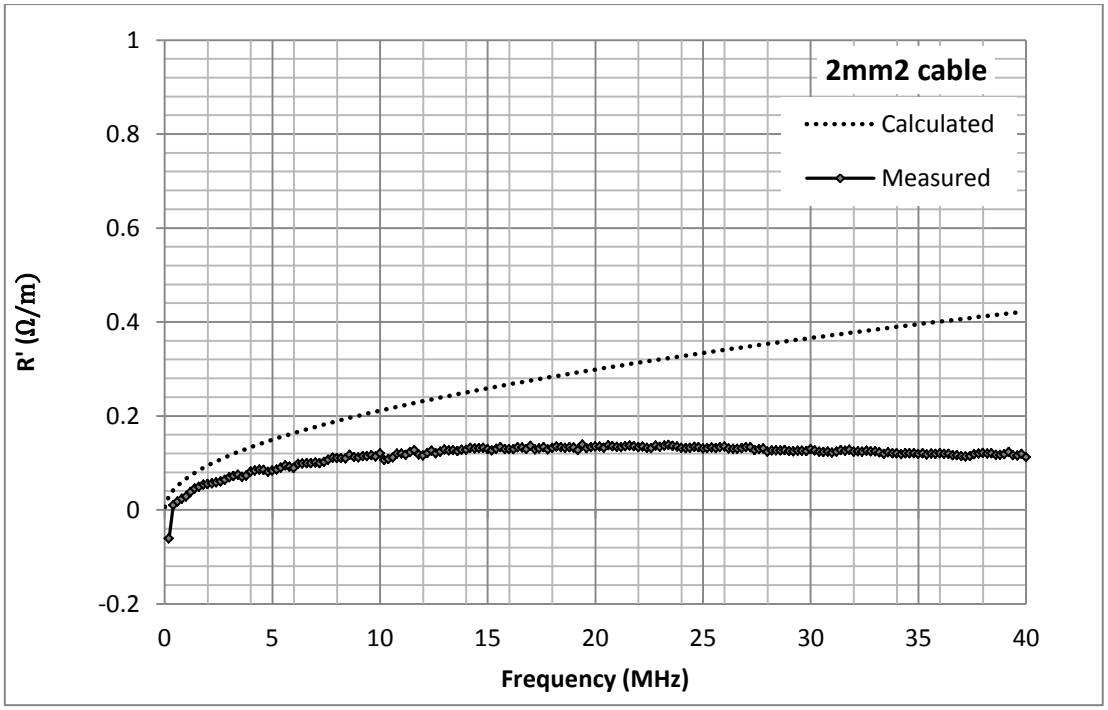

Figure 4.7a: The resistance per unit length for the 2.5mm ^{2} transmission line

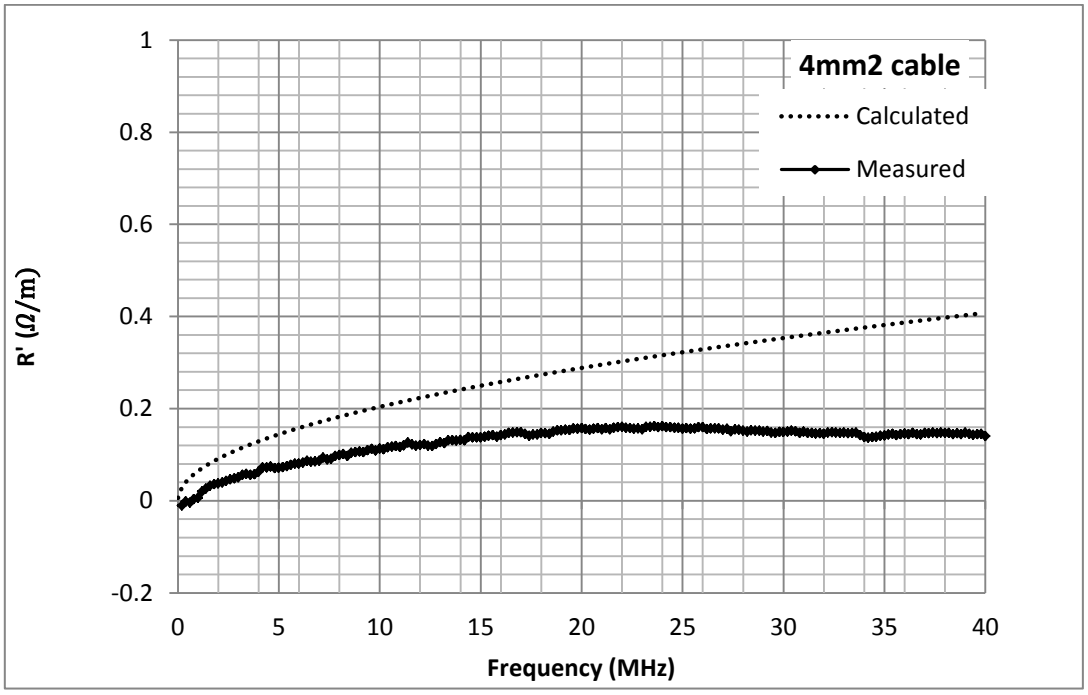

Figure 4.7b: The resistance per unit length for the 4mm ^{2} transmission line

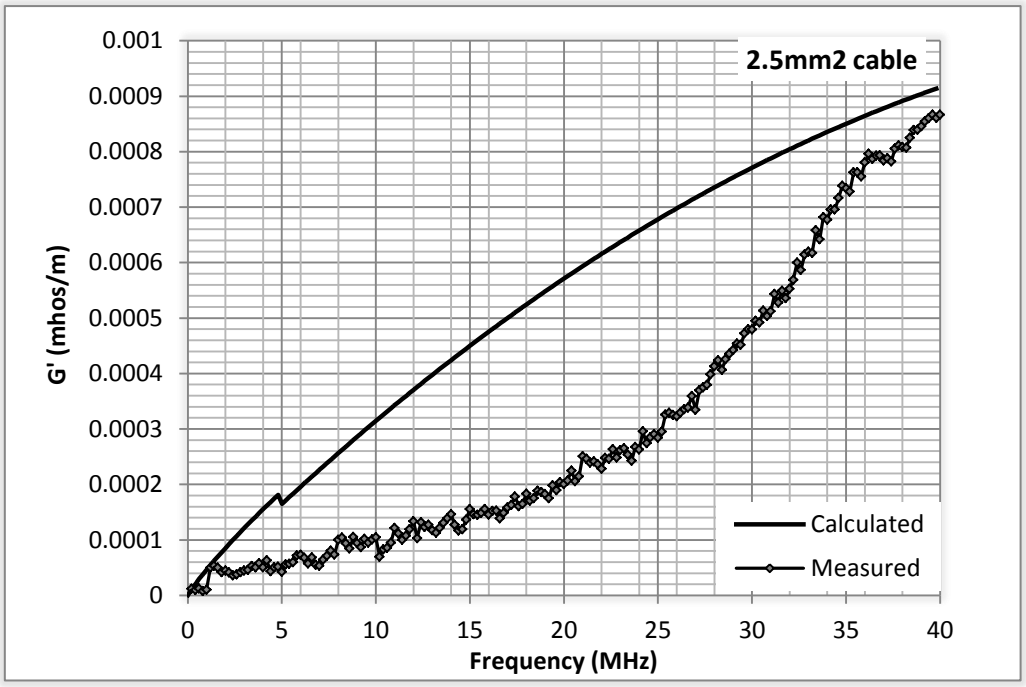

Figure 4.8a: The conductance per unit length for the 2.5mm ^{2} transmission line

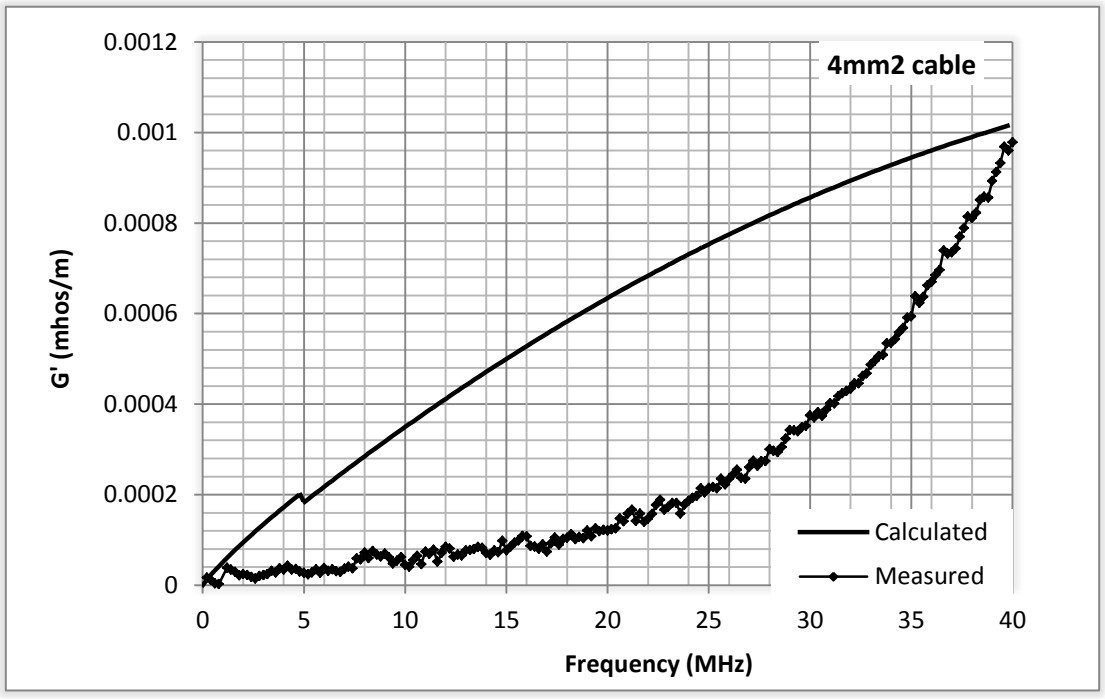

Figure 4.8b: The resistance per unit length for the 4mm ^{2} transmission line

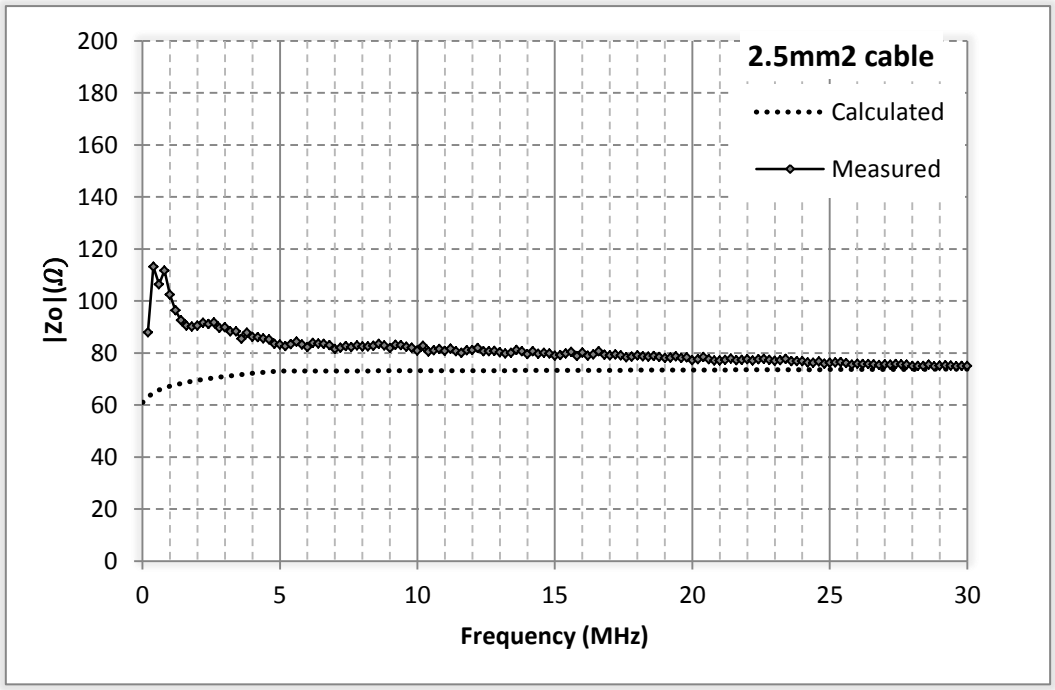

Figure 4.9a: The characteristic impedance for the 2.5mm ^{2} transmission line

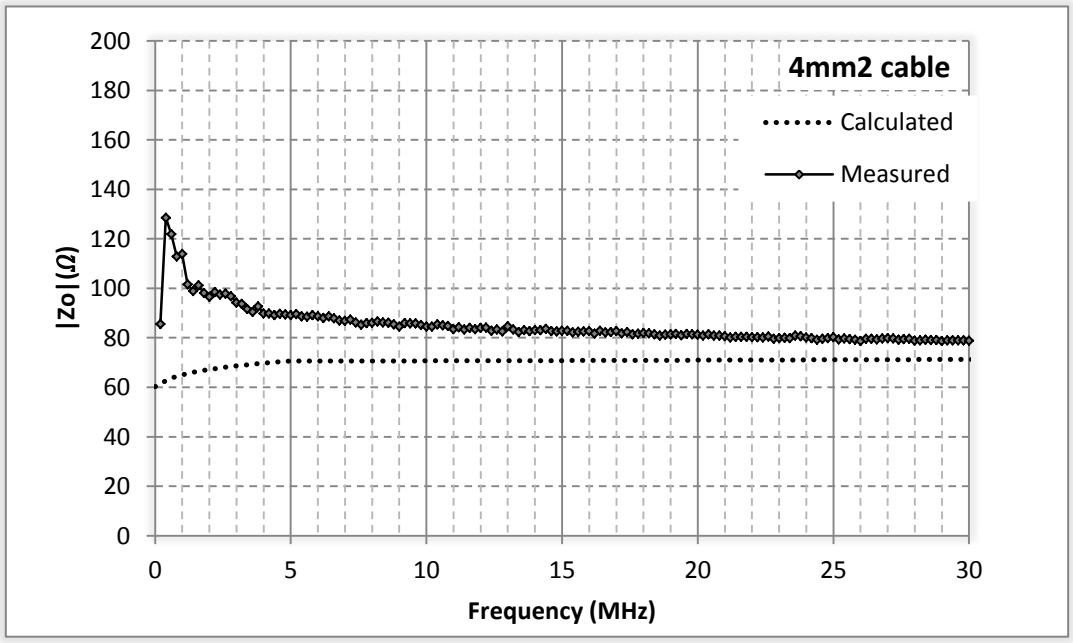

Figure 4.9b: The characteristic impedance for the 4mm ^{2} transmission line

The root mean square error (RMSE) between the measured and calculated characteristic impedance values for the 3x2.5mm^2 cable is 2.809 and for the 3x4mm^2 is 3.58.

The measurements show good agreement with the theoretical models. However deviations are noted with the resistance and conductance which are dependent on the dielectric material characteristics.

This shows that the characteristic impedance is mainly dependent on the distributed inductance and capacitance parameters of the cable. For the calculations dielectric characteristics estimates obtained by [41] from experiments were used. However the composition of the PVC varies with manufacturers and therefore the results vary for the two cases.

4.5 Propagation velocity

From the measurements an estimate of the proper propagation velocity was obtained and is shown in Figure 4.10 compared to the calculated propagation velocity [38] discovered that propagation velocities of the electromagnetic wave in measured PVC cables are in the range of $0.57c_o$ to $0.66c_o$, However, [57] determined that the approximate value of $0.5c_o$ is sufficient and our measurements agree with his results.

The dielectric constant has much significance on propagation velocity values. The dielectric constant is given as [58]:

$$\varepsilon_{\mathrm{r}} = \left(\frac{c_0}{v_{\mathrm{p}}}\right)^2 \tag{4.14}$$

The relative dielectric constant of the PVC material of the cable is deduced from measurements and its fit is presented in Figure 4.11.

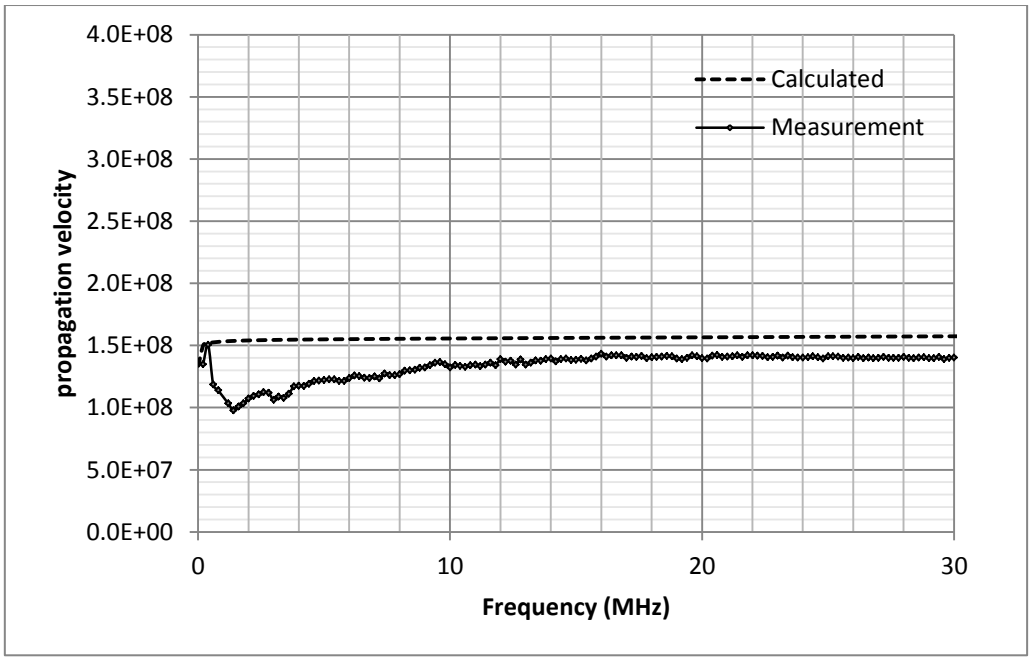

Figure 4.10: Propagation velocity

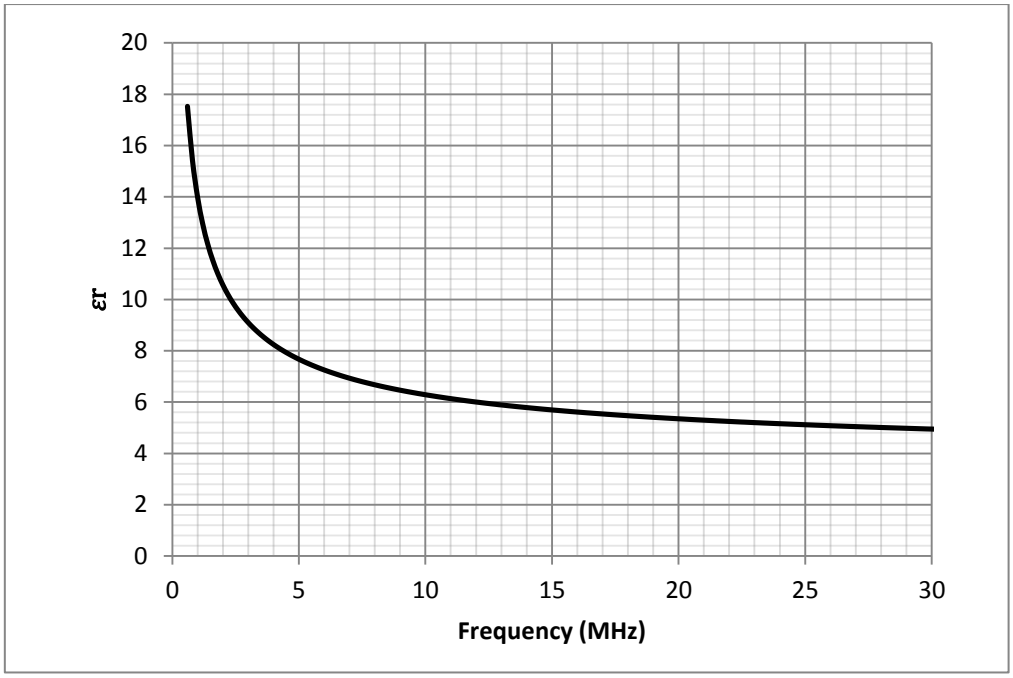

Figure 4.11: Dielectric constant fit

4.5 The Attenuation Constant Analysis

Each transmission line is characterized by the characteristic impedance and its propagation constant, which are complex, see (2.12)**.** The real part of the propagation constant is the attenuation constant which determines the path loss. From the measurements, the attenuation coefficient was deduced and the values obtained plotted in Figure 4.12 against the theoretically calculated attenuation coefficient.

The attenuation constant is often expressed as [34]:

$$\alpha = a_0 + a_1 f^k \tag{4.15}$$

From the measured attenuation constant, a fit is generated using the Least Absolute Residual (LAR) robust method. The maximum and minimum bounds are then determined. The coefficients obtained are given in Table 4.1. The calculated and measured average attenuation constant regression fit show a good agreement, with the RMSE between the two being 0.000702. The attained maximum and minimum attenuation constant coefficients are used to determine the average path loss bounds for the transfer function of the channel of a given length. It is seen that the attenuation coefficient increases as a function of frequency. To ascertain on the nonlinearity at frequencies above 8MHz, multiple measurements at different cable lengths may be considered and an average obtained in future work.

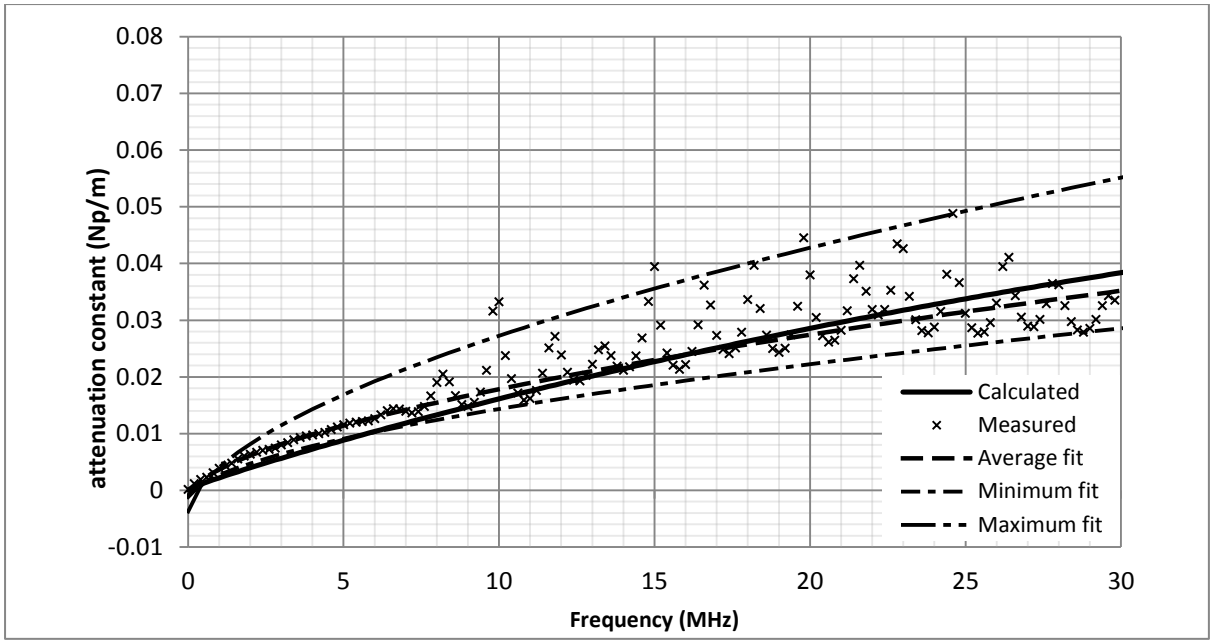

Figure 4.12: The measured and calculated attenuation coefficient for the 2.5mm^2 cable

		Measured		
Coefficient	Calculated	Average	Maximum	Minimum
a_0	-0.00316	-0.001247	-0.004296	-0.00145
a_1	5.43E-6	1.438E-6	2.884E-6	1.294E-6
k	0.517	0.5893	0.577	0.5838

Table 4.1 Attenuation constant coefficients

4.6 Chapter Summary

This chapter entails the line parameter extraction techniques, the measurement setup and results obtained for low voltage power cables. From the line parameter results, we conclude that the characteristic impedance of the cables under consideration can be modelled with the parameters R' ,L', G' and C' given the closeness of the measured values to the theoretically calculated values. To cater for the divergences noted at frequencies less than 400 kHz, several measurements may be done and results averaged for future work. The insulation materials and conductor materials are seen to play a significant role in the high frequency characteristics of the power cables and therefore need to be specified for the PVC material used so as to ensure accurate calculations. The propagation velocity and dielectric characteristics for the particular cables are further deduced from the measurements. From the measurements, the attenuation constant coefficients are attained as well as the confidence bounds.

CHAPTER FIVE

CHARACTERISING AND MODELLING OF THE PLC CHANNEL

5.1 Introduction

In Chapter Three, different top-down and bottom up modelling techniques and their theoretical basis were discussed. Subsequently, accurate approximation of the line parameters which in turn are used to determine the PLC channel constants, the characteristic impedance $Z_{0,}$ and propagation constant γ were determined in Chapter Four. These constants are essential in the channel transfer function calculations. The test bed set up, extraction techniques and measurement results of the channel frequency response for different configurations are discussed in the following subsections.

5.2 Channel Frequency Response Extraction Technique

5.2.1 Coupling Method and Circuit

Measuring equipment, in our case, the Vector Network Analyzer, are sensitive and rather expensive. What acts as a protection interface between the communications equipment and the power line is a power line coupler. When there are either faults or switching transients or there are surges on the power line when lightning strikes or even when at nominal operating voltage, the power lines carry high levels of energy. Therefore, to minimize risks associated with isolation installation, properly designed and tested couplers are imperative [60]. Explicated below is how this was achieved. Figure 5.1 shows the circuit diagram of the designed coupler to be used for interfacing the measuring equipment to the power lines.

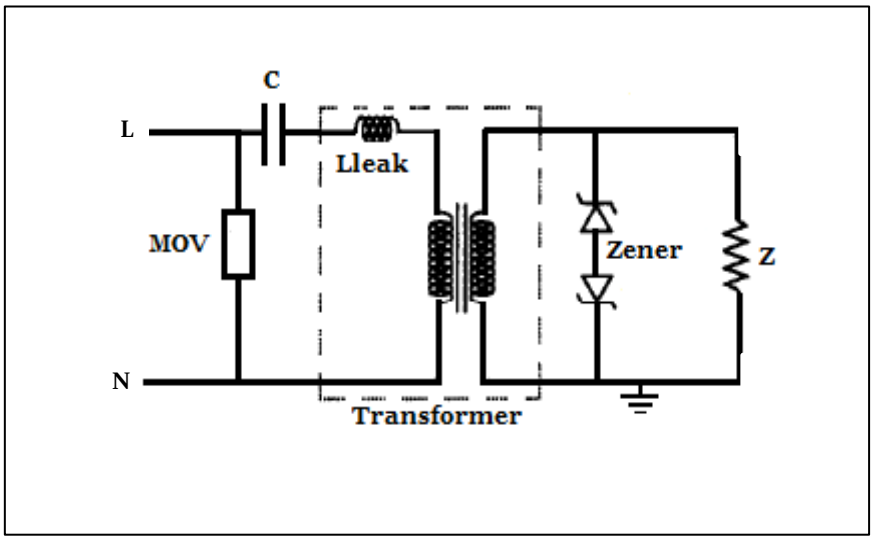

Figure 5.1: Proposed coupling circuit model

A differential mode based passive coupling circuitry has been designed to couple the communication signals onto and from the power line. One terminal was connected to the live conductor (L) and the other to the neutral conductor (N). Single and parallel capacitors are often used due their capacity to block low voltage signals [60][61].This is explained by its frequency varying impedance nature. A high voltage capacitor was used. The capacitor also prevents saturation of the coupling transformer [62].

Between the communication and power line circuitry, the transformer offers galvanic isolation and acts as a limiter [63]. Extra protective circuitry is included to the coupler design; the back to back zener diodes are included to limit the output level as well as grip fast transient disturbances. A metal oxide varistor (MOV) is included for surge protection through its capability to limit overvoltage spikes, therefore avoiding damage to the capacitor.

The network analyser has an input impedance of 50Ω, the value of the capacitor chosen is10nF. The capacitor was chosen so as to set the low frequency -3dB cut-off, which is determined by [64]:

$$f_{LF} = \frac{1}{2\pi RC} \tag{5.1a}$$

Where;
R = the terminating resistance
C = the capacitance.

The transfer function of the coupler is given in Figure 5.2. The -3dB cut off is at 318 kHz as per the design specifications. The transfer function of the couplers back to back is given in Figure 5.3. The LAD4613 transformer used has a limit frequency of operation of 55MHz according to specifications. If the coupler was to be used as a band-pass filter, a series inductor would be added to the leakage inductance of the transformer to determine the high frequency –3dB cut-off point, given by [63]:

$$f_{HF} = \frac{R}{2\pi L} \tag{5.1b}$$

Where;
R = the terminating resistance, 50Ω
L = the inductance in series added to the transformer leakage inductance

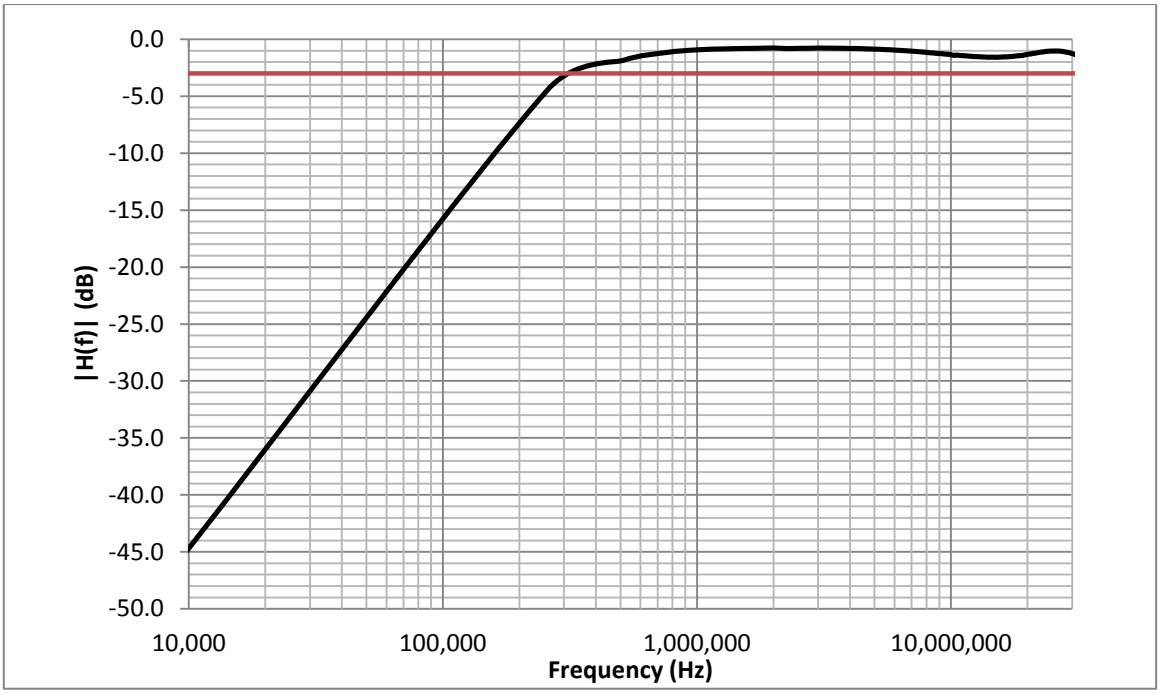

Figure 5.2: The transfer function of the designed coupler

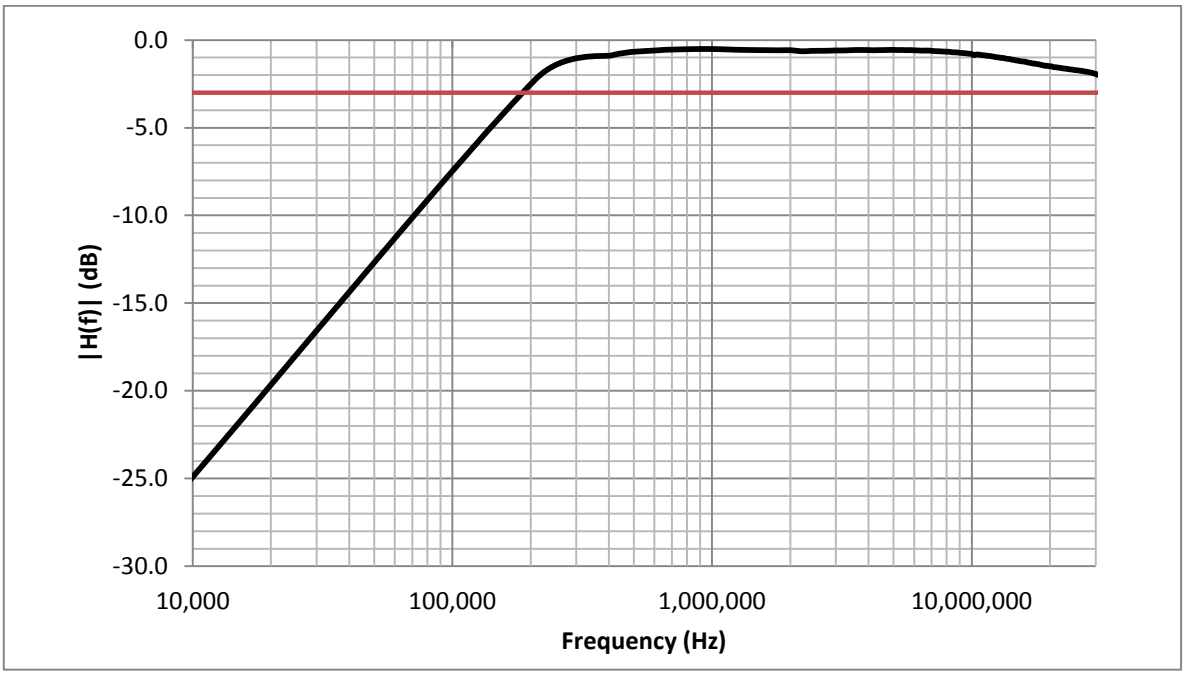

Figure 5.3: The transfer function of the couplers back to back

The cable type and its length used to connect the coupler or any device under test to the network analyzer will affect the results if not properly matched and offset at the output terminals. The capacitance of the cable if not offset will produce a notch at the resulting resonance frequency within the band of interest.

5.2.2 PLC Channel Test Bed Setup

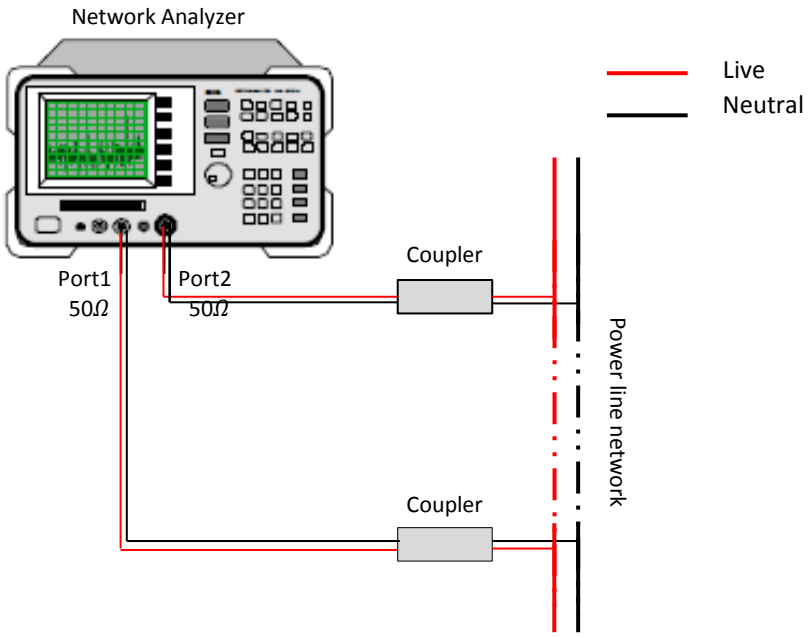

Figure 5.4: Schematic representation of the PLC channel measurement setup

To measure the transfer function of the different networks and topologies, a setup illustrated in Figure 5.4 was used. All measurements were carried out using the use of the Rohde & Shwarz ZVL Network Analyzer. On sending a signal at one port and receiving it on the other port, accurate measurements of S-parameters are obtained. For isolation and protection purposes, the network analyzer is connected to power line network through couplers designed as discussed in the previous section and to obtain the actual transfer functions of the PLC channel, it was ensured that the coupler behaviour was compensated. As opposed to switching off all power supplies and connect the analyser directly, this setup is done to best replicate the actual characteristics of the PLC channel.

Using equation (4.7) where Z_0 denotes the equipment's impedance, the power line's input impedance is attained. Different network configurations are tested in a similar manner.

For the multipath model, a conversion from frequency domain to time domain is required. To achieve this, the Inverse Fast Fourier Transform is applied on measured data.

5.3 Channel Frequency Response Measurement Results

Two test networks were built in order to explore and characterise the PLC channel under different conditions and topology. The networks are constructed using the same cable type. The variations in transmission and receiving points forming the different test configurations are shown in Table 5.1.

5.3.1 Straight Path Channel

The frequency response of a direct connection of two different cable sizes (4mm^2, 2.5mm^2) measured is shown in Figure 5.5. The cables are 99 m in length. The transfer function has significant notches above 5 MHz. This is due to the length of the cable appreciating to multiples of the relative quarter wavelength. The difference in the average path loss of the two cables, shows that a difference in the ratio of the conductor cable core radius to the separation distance will produce a difference in attenuation constant, which in turn determines the attenuation profile of the transfer function.

		Transmit	Receive
Network1	Config_1	(1)	(3)
	Config_2	(2)	(3)
	Config_3	(1)	(2)
Network2	Config_4	(2)	(3)
	Config_5	(1)	(3)
	Config_6	(1)	(4)
	Config_7	(2)	(4)

Table 5.1: The different configuration of the transmission and receiving points for the two networks

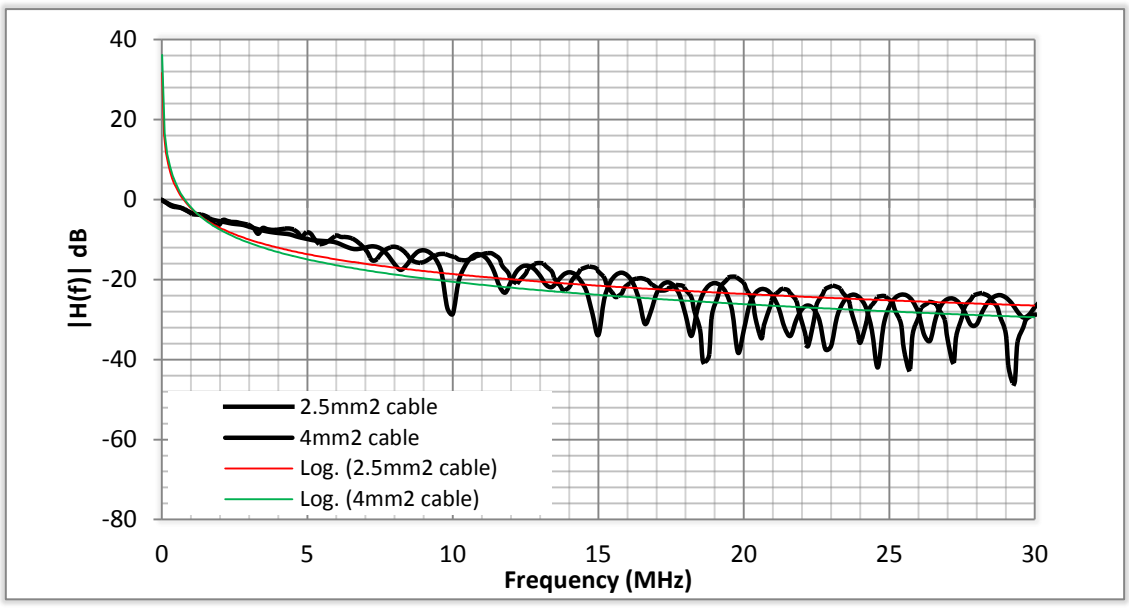

Figure 5.5: The transfer function of different cable cross sectional area sizes

5.3.2 One Branch Network

A live network with a single branch as depicted in Figure 5.6 is tested and the different S-parameters were obtained to get the frequency response for different configurations, that is, for different test points as given in Table 5.1. The utilization of S-parameters for the characterisation of the power lines is discussed in Section 3 of Chapter 2. Shown in Figure 5.7a and 5.7b are the $|S_{11}|$ and $|S_{22}|$ parameters for the different configurations of the single branch network, respectively.

Figure 5.8a shows the channel transfer function and Figure 5.8b shows the phase response for the different configurations of the single branch network. For config. 1 and 2 a positive gain is noted for frequencies less than 5 MHz. As this is a passive channel this can be attributed to the reflection coefficient being non-zero, that is, as the incident and reflected wave pass each other in opposite directions, there are points where the voltages of the two waves add to produce a voltage higher than that of the incident wave because the two are in phase with each other at this points. This is the standing wave pattern which appears in transmission lines which are mismatched or terminated in impedances other than the characteristic impedance[65].

The typical features of the channel transfer functions are notches at different points and the low pass filter characteristic. To determine the average path loss for the different configurations, the least squares method is used and the logarithmic regression estimates are determined. Although there is a marginal difference in the average path loss for the three configurations, the gradient is seen to be slightly larger with the increase in the distance from the transmitting end to the receiving end. The phase responses show distortion at frequencies where notches in the transfer function are found. Unless stated, the branch terminals are open circuit ended.

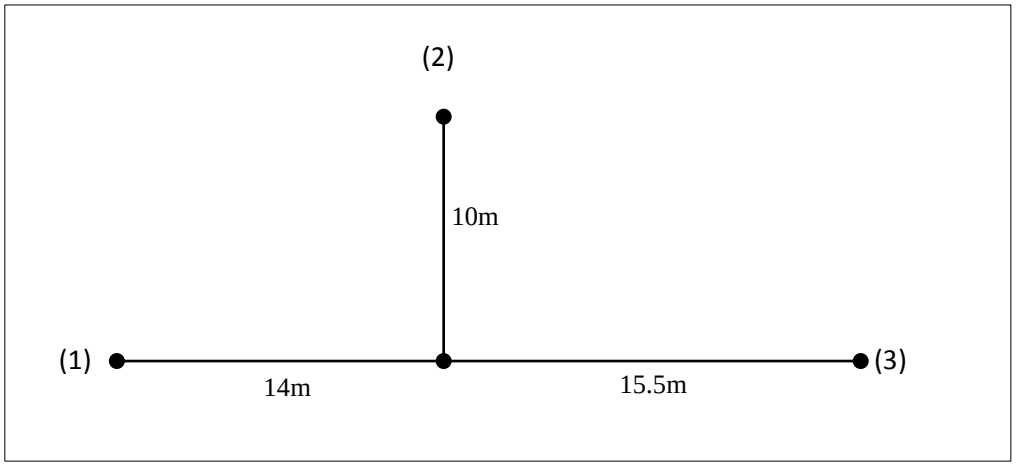

Figure 5.6: The one branch network (Network 1)

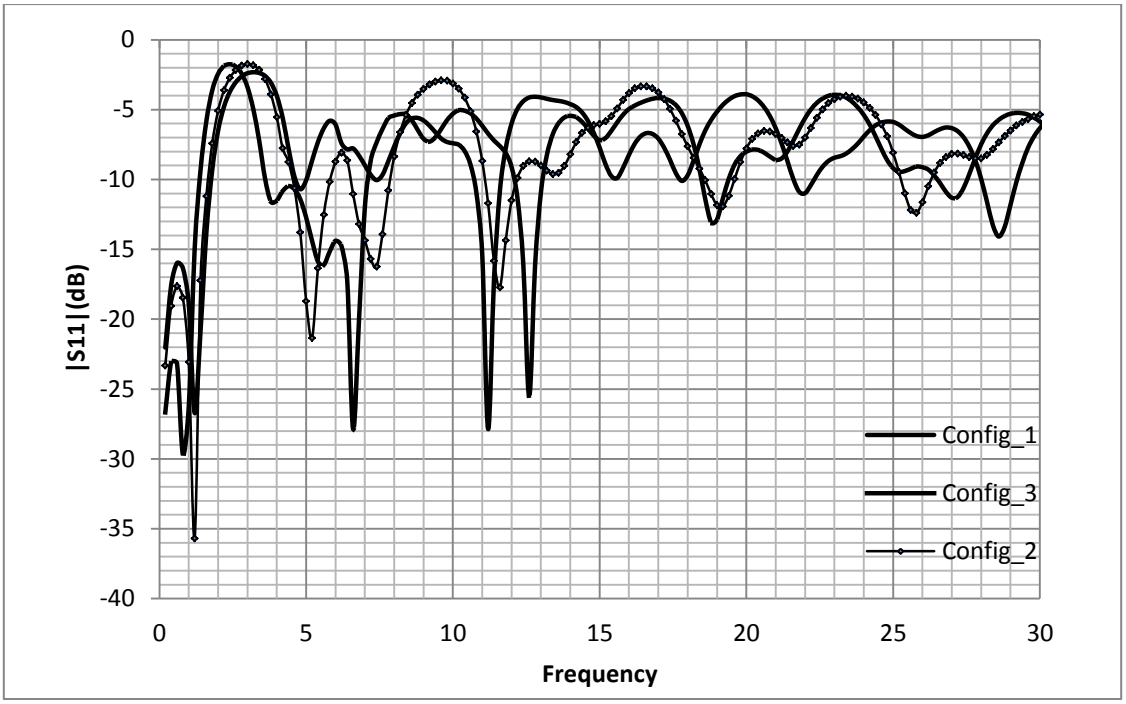

Figure 5.7a: The S_{11} parameters for different configuration of the one branch network

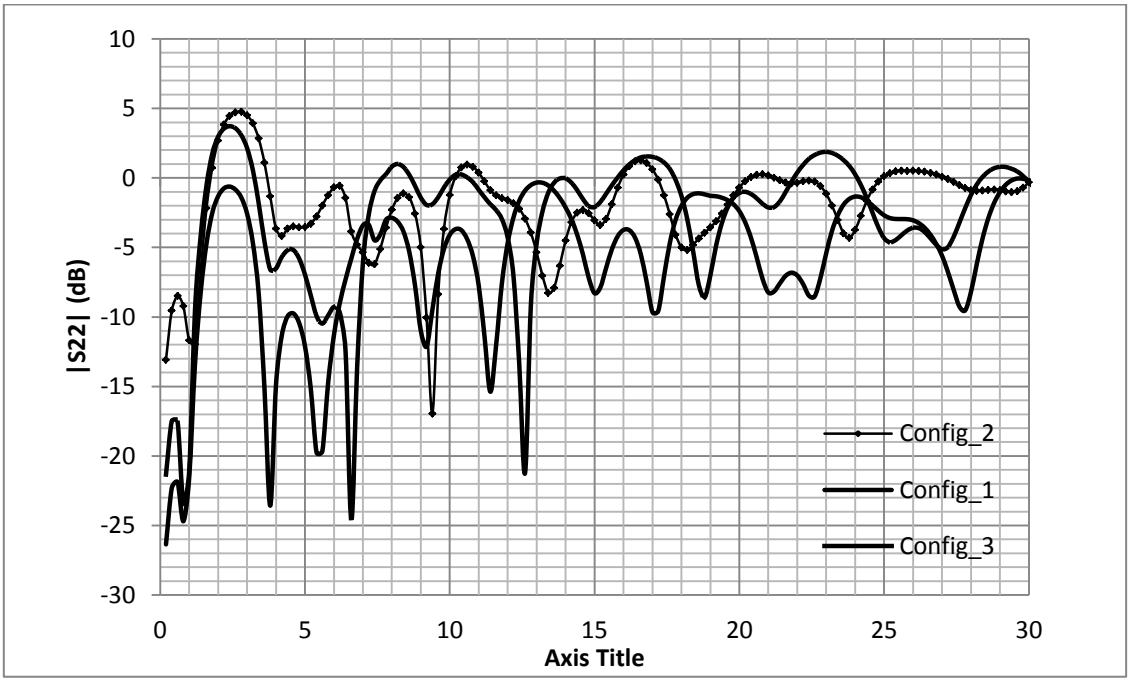

Figure 5.7b: The S_{22} parameters for different configuration of the one branch network

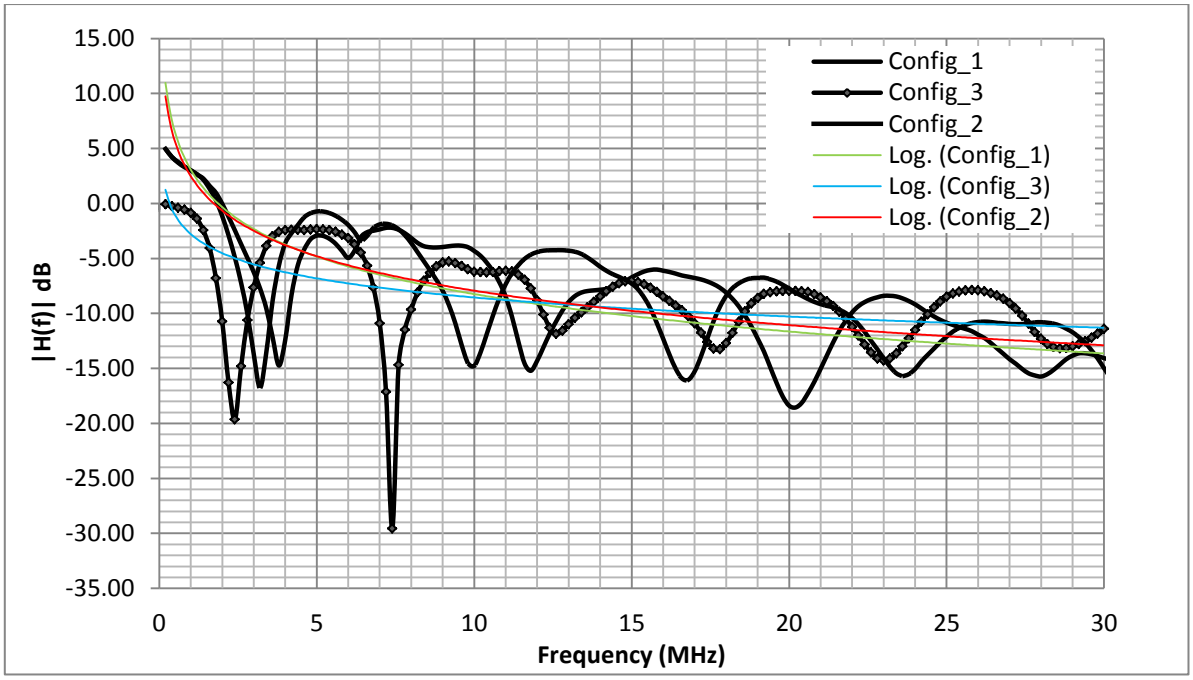

Figure 5.8a: The transfer function for different configurations with one branch and total network length

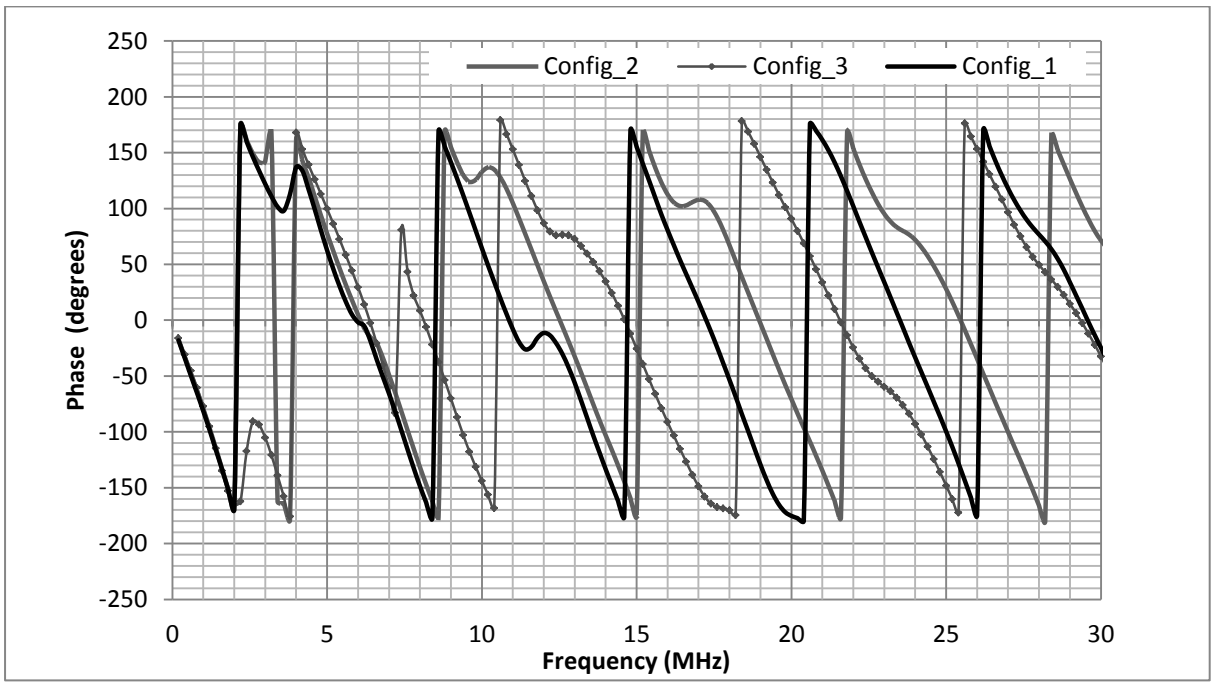

Figure 5.8b: The Phase response for different configurations with one branch and total network length

5.3.3 Two branch network

A similar approach was employed and the frequency response of a two branch network shown in Figure 5.9, for different configurations as given in Table 5.1 is determined by measurements. The transfer functions and phase response for the different configurations are shown below in Figures 5.10a and 5.10b and Figures 5.11a and 5.11b. The transfer functions of the 2 branch network also have deep notches at selected frequencies as well as a low pass filter characteristic. Except where the configuration has equal branch lengths (config_6) the notch separation is none uniform as it is seen with config_1-3 (Figure 5.7). This is as a result of the different branch lengths. There still appears to be a marginal difference in the average path loss obtained from the least squares method for each network configuration.

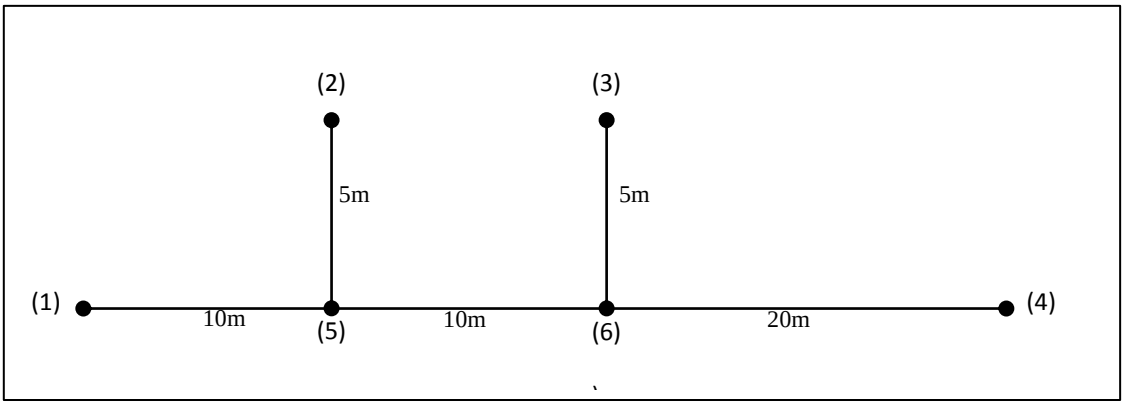

Figure 5.9: The two branched network

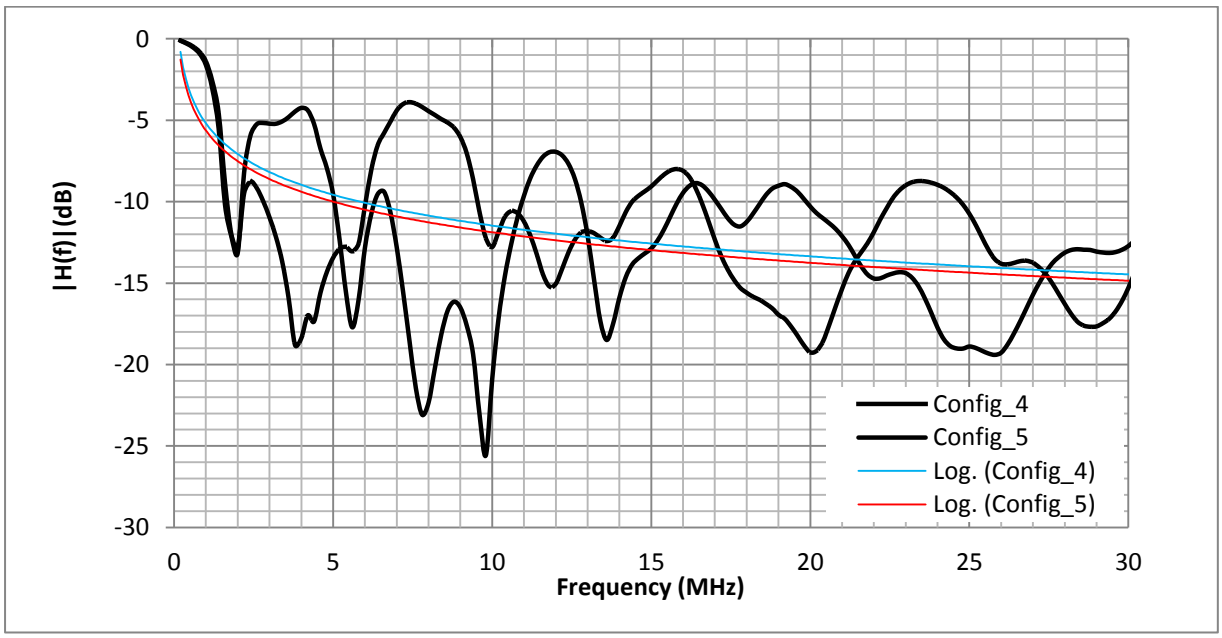

Figure 5.10a: The transfer function for different configurations with 2 branches and one total network length

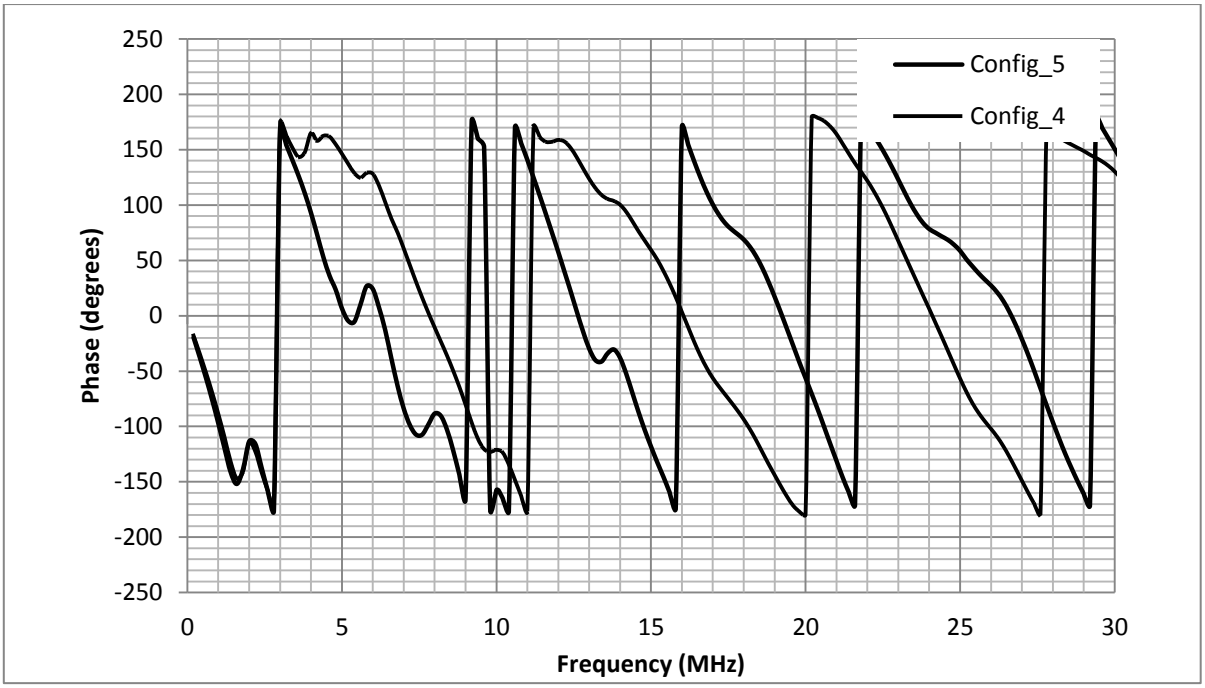

Figure 5.10b: The phase response for different configurations with 2 branches and one total network length

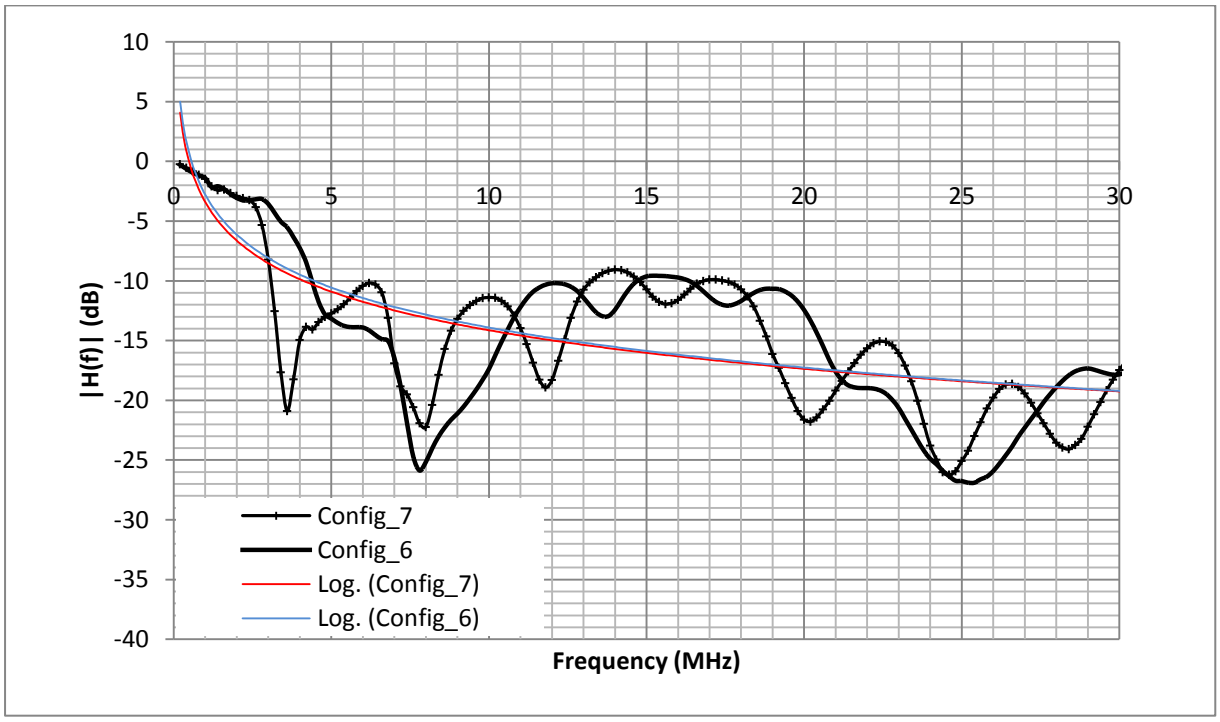

Figure 5.11a: The transfer function for different configurations with 2 branches and one total network length

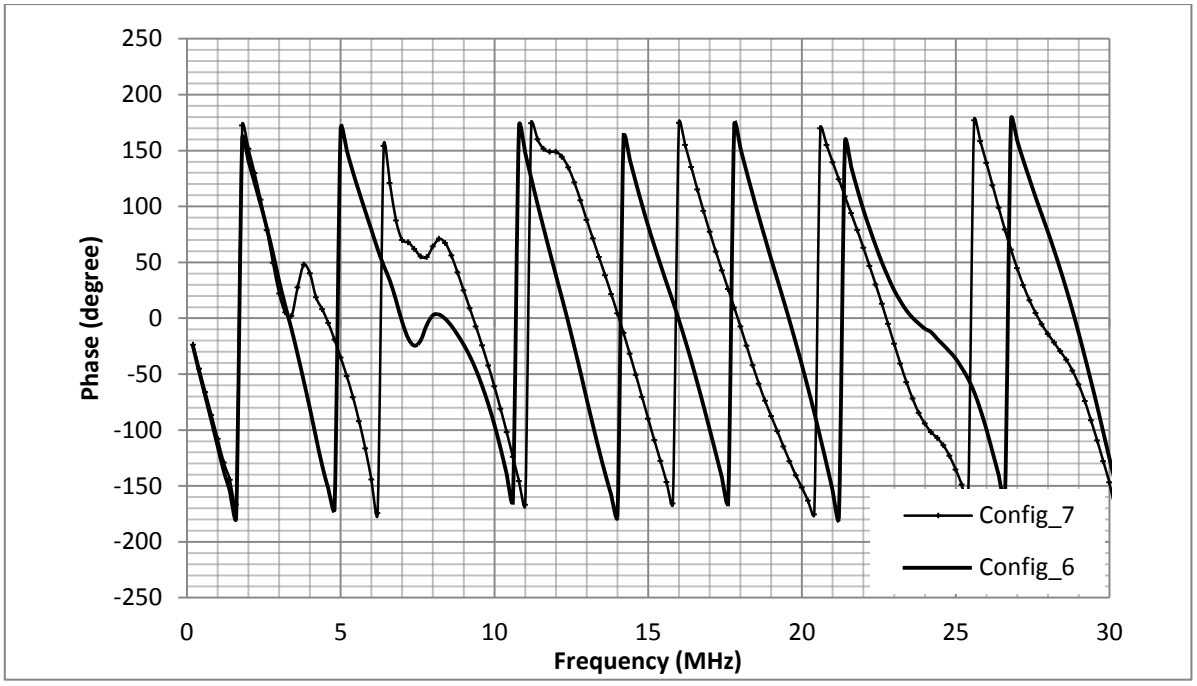

Figure 5.11b: The phase response for different configurations with 2 branches and one total network length

Although there exists the low pass filter (LPF) characteristic of the PLC channel considering channel frequency responses of all the network configurations considered so far, where the cut off frequency is 2.4 MHz for config 1-3, 1.2 MHz for config 4-5 and 2.6MHz for config 6-7, the study of the PLC channel in the entire frequency band is still vital. This is because every channel is generally a LPF and to mitigate this effect, repeaters and regenerators are used. For broadband use, one needs to know the channel response over the entire frequency band and thus a purpose served by this presentation.

5.4 Comparison of models to measurements

5.4.1 One branch network

In Figure 5.12 and 5.13, the channel frequency response of network 1 config_1 obtained from measurements is plotted against the deterministic model by [11] and the parametric model by [34]. The models compare well with the measured frequency response. The notches are consistent with a slight difference in the average attenuation. There is also a slight difference in the phase response of the models to measurements with distortions seen at corresponding notch frequencies.

The normalized impulse response obtained by converting the frequency response from the frequency domain to the time by applying the inverse fast fourier transform is as shown in Figure 5.14. From the normalized impulse response the weighting factor g_i and the delay factor τ_i according to Equation (3.5) are obtained. To model the channel, four paths were considered and the four most significant

peaks in the impulse response considered. The frequency variant input impedance of the channel in this configuration was also measured and is shown in Figure 5.15.

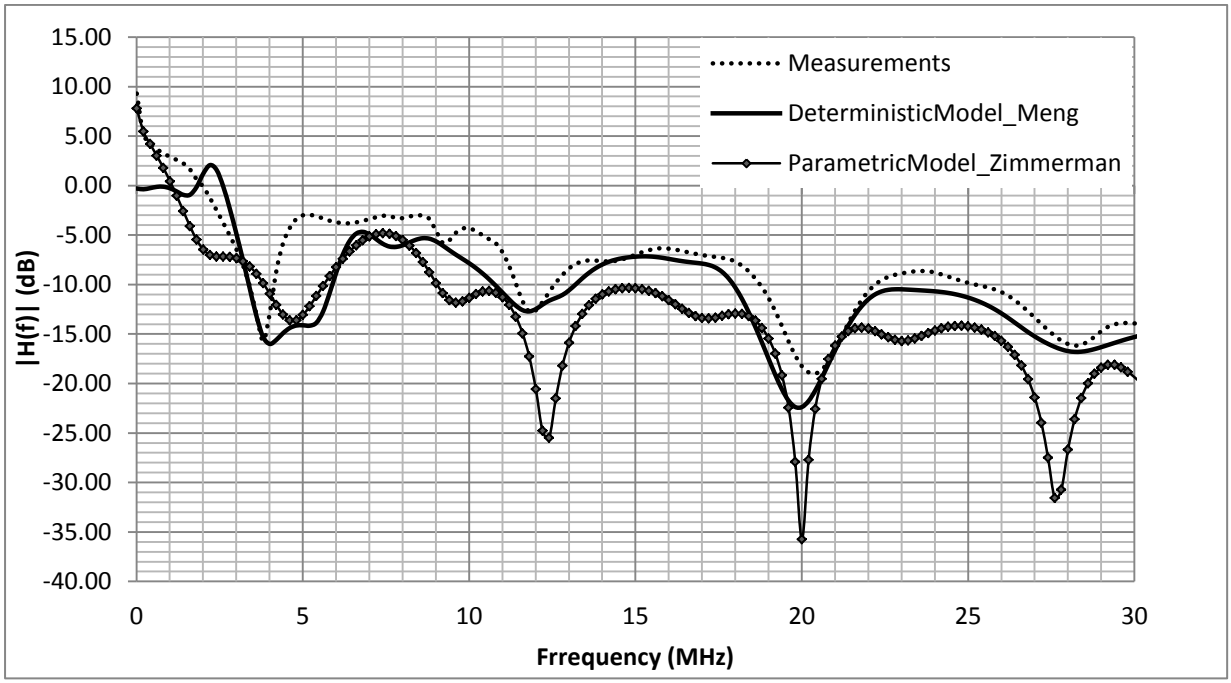

Figure 5.12: Comparison of frequency response of measurements to different PLC models

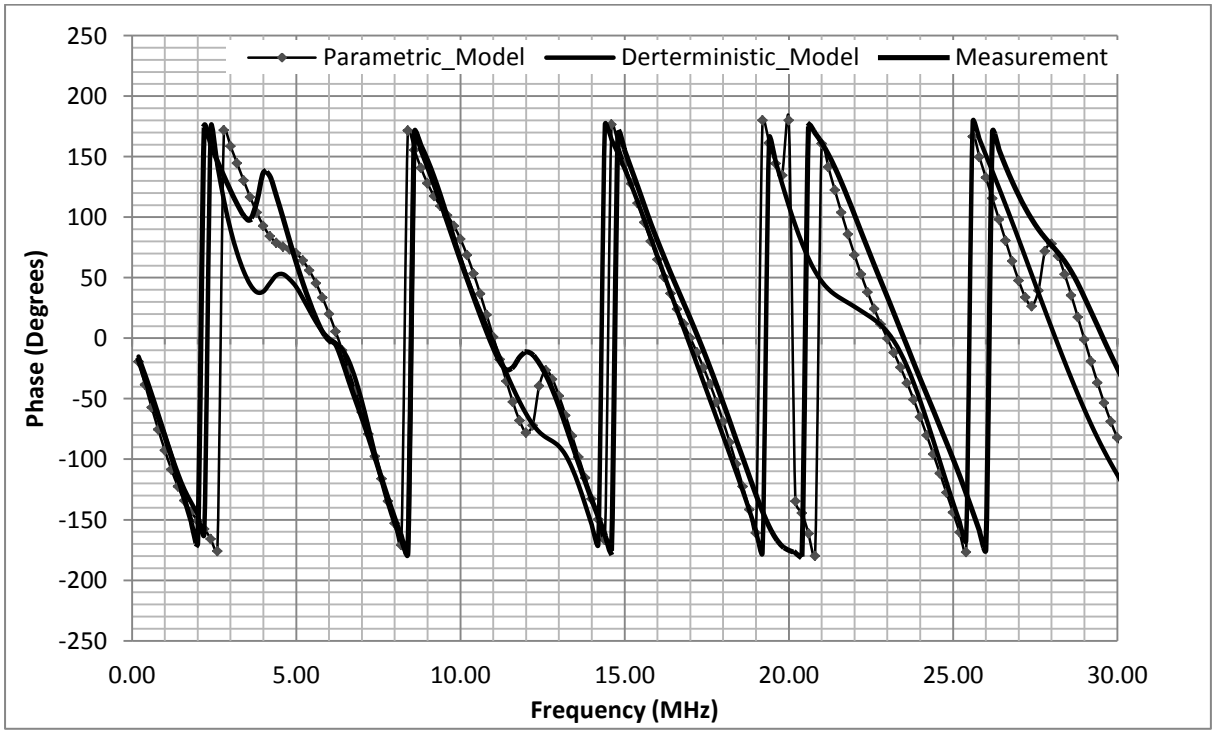

Figure 5.13: Comparison of phase response of measurements to different PLC models

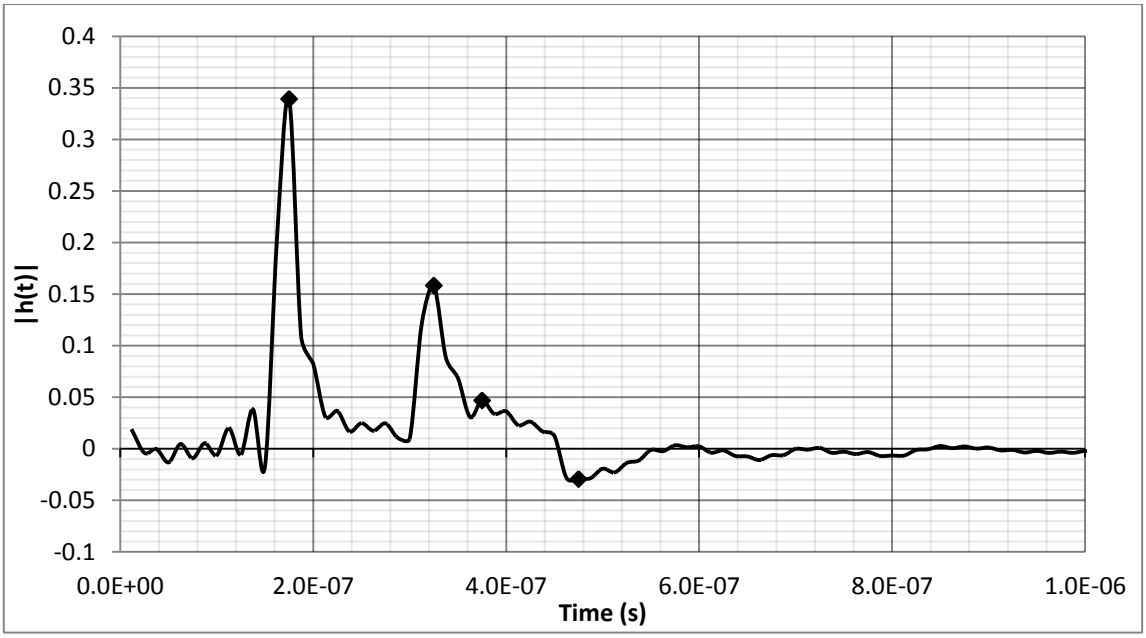

Figure 5.14: The impulse response of the one branch network

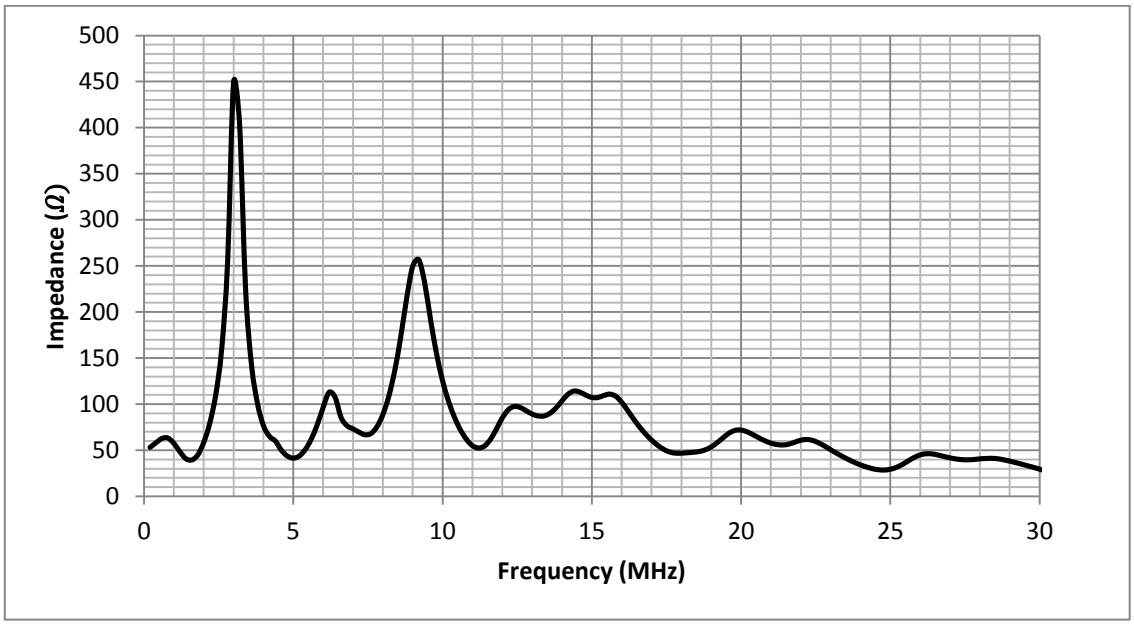

Figure 5.15: The input impedance of the one branch network

5.4.2 Two branch network

For config_6, the channel frequency response for the two branch network is compared to the deterministic model by [11] and the parametric model by [34], as shown in Figure 5.16 and 5.17. Figure 5.18 shows the normalized impulse response of the channel obtained from the conversion from frequency domain to time domain. A selected number of 6 paths was used to obtain the multipath model. The input impedance of the channel measured is shown in Figure 5.19.

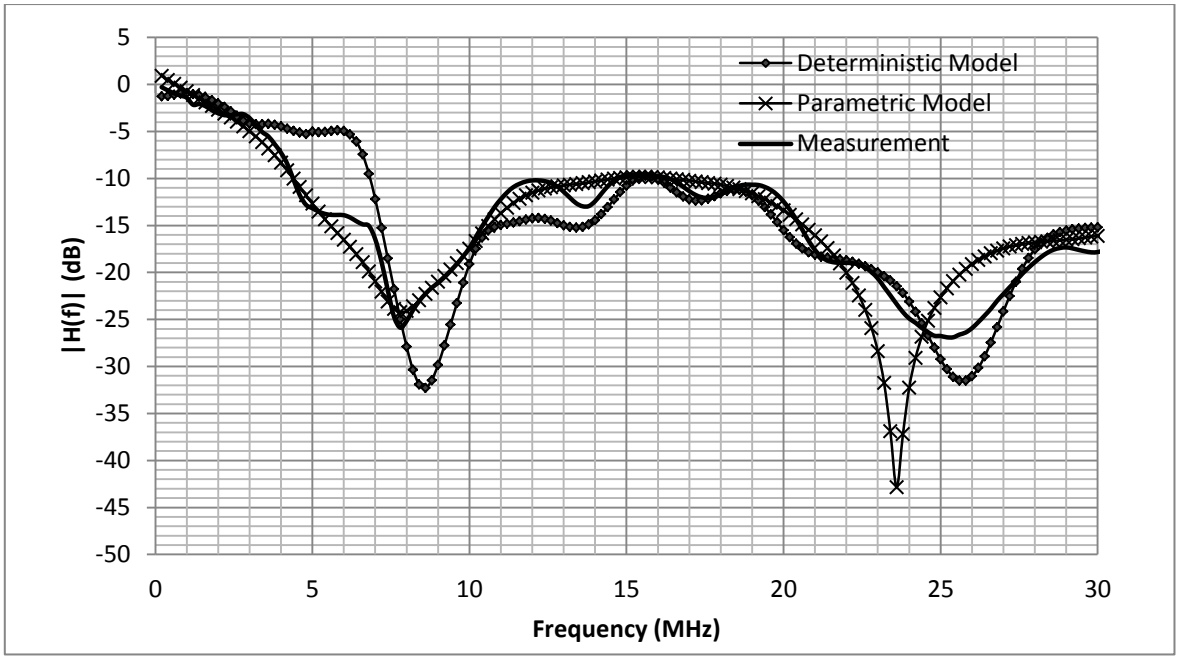

Figure 5.16: Comparison of 2 branch network frequency response of measurements to different PLC models

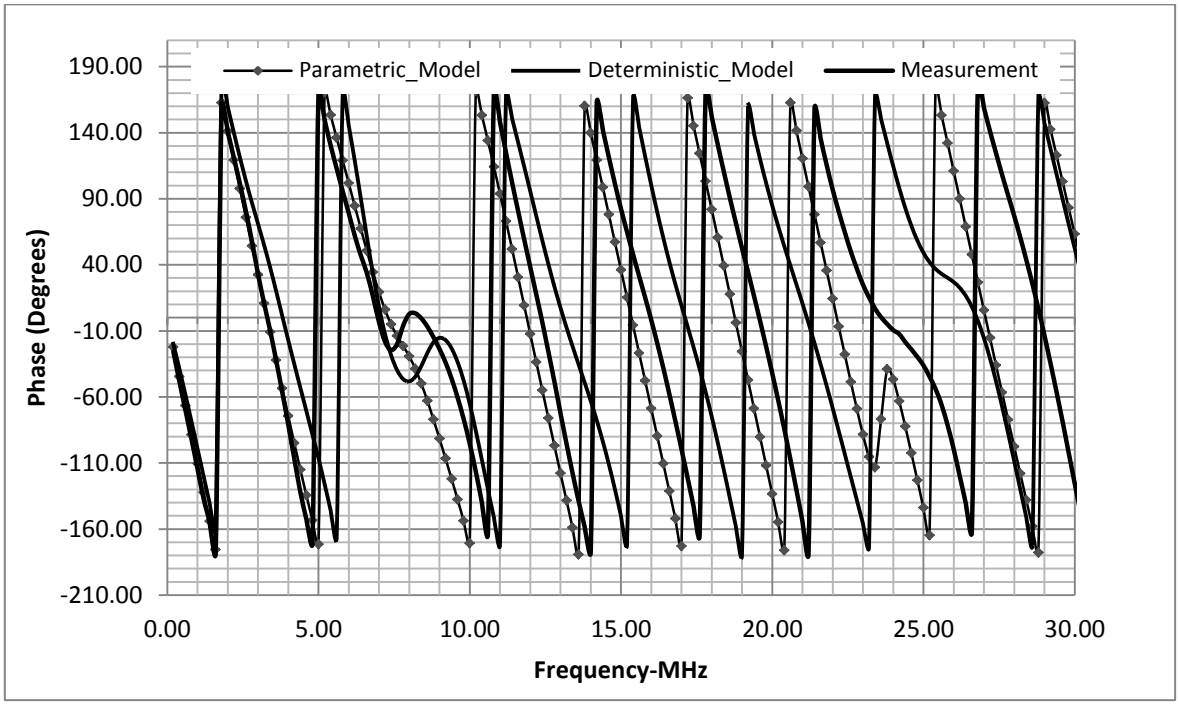

Figure 5.17: Comparison of 2 branch network phase response of measurements to different PLC models

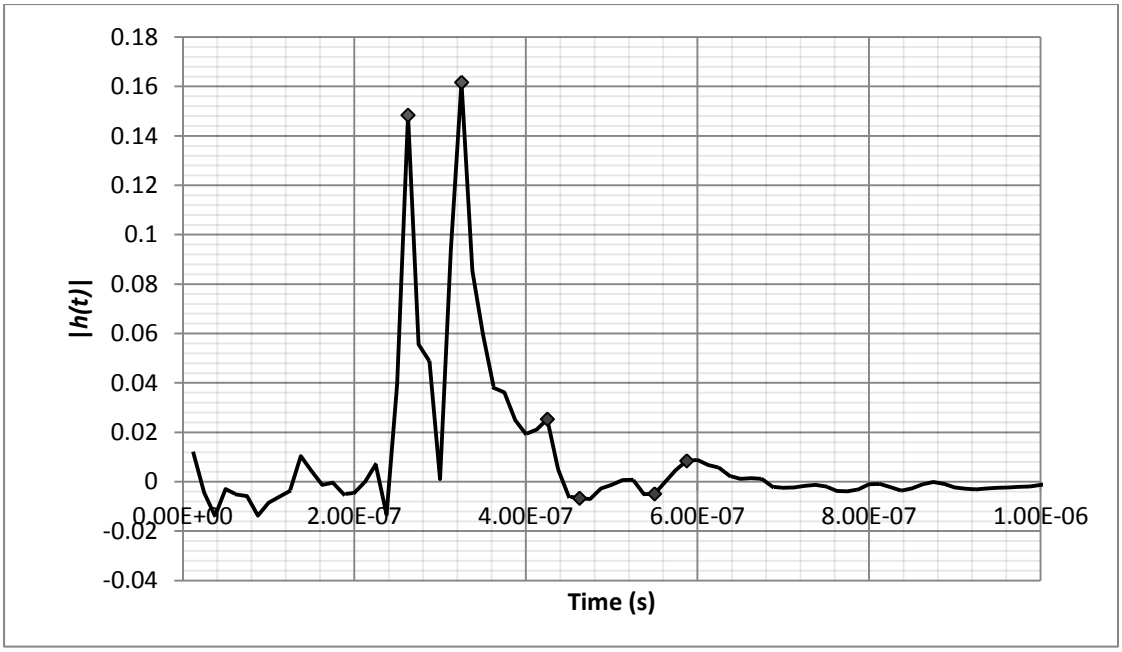

Figure 5.18: The impulse response of the 2 branch network

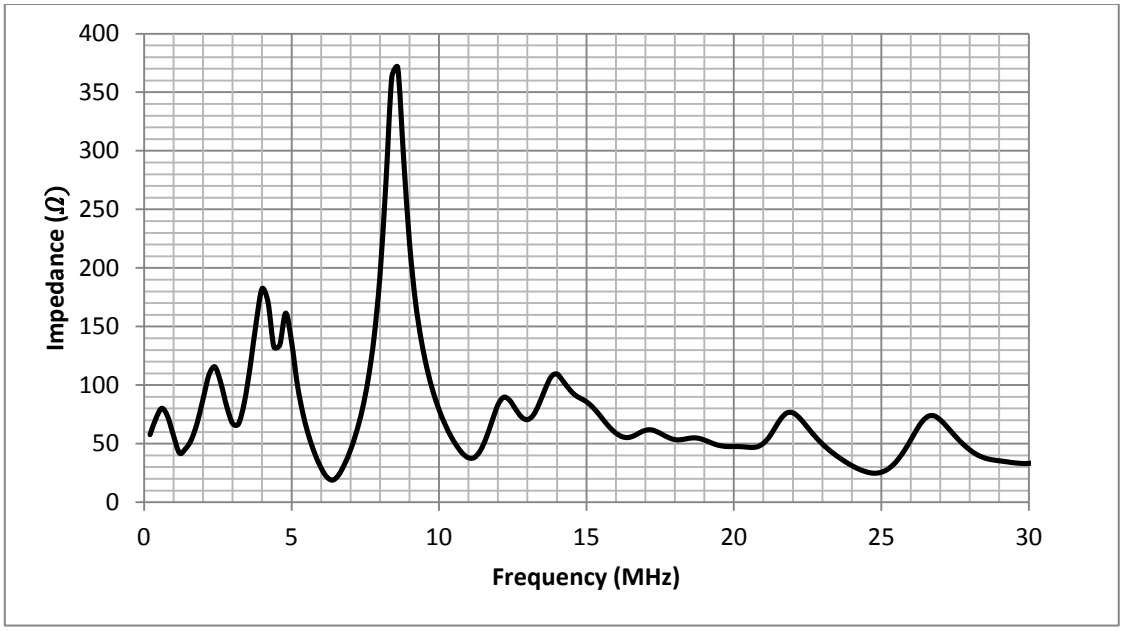

Figure 5.19: The input impedance of a two branch network

5.4.3 Comparison to Proposed Series Resonant Circuit Model

The model proposed in Chapter Three is compared to measurements obtained for Config_3 and Config_6 as shown in Figures 5.20 and 5.21 respectively. The model transfer function follows that of the actual measurements. It shows that an estimate of the transfer function for a channel with an open circuited branch end or high impedance can be produced from the knowledge of the branch length, characteristic impedance and attenuation constant.

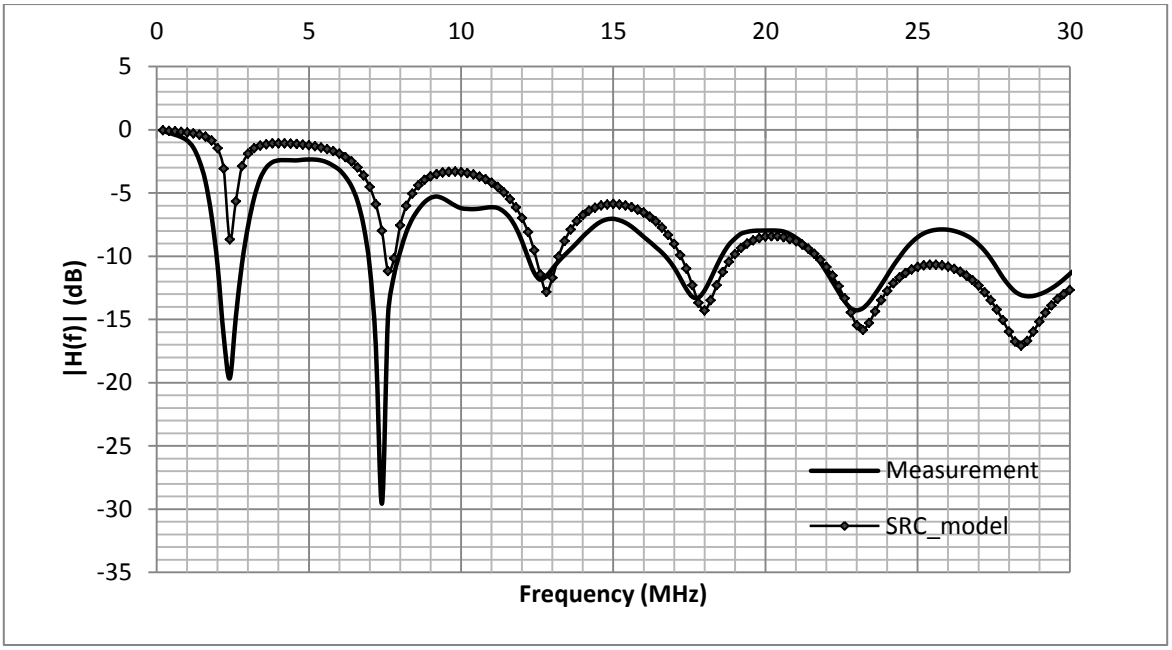

Figure 5.20: Transfer function for Network 1 config_3 compared to the SRC Model

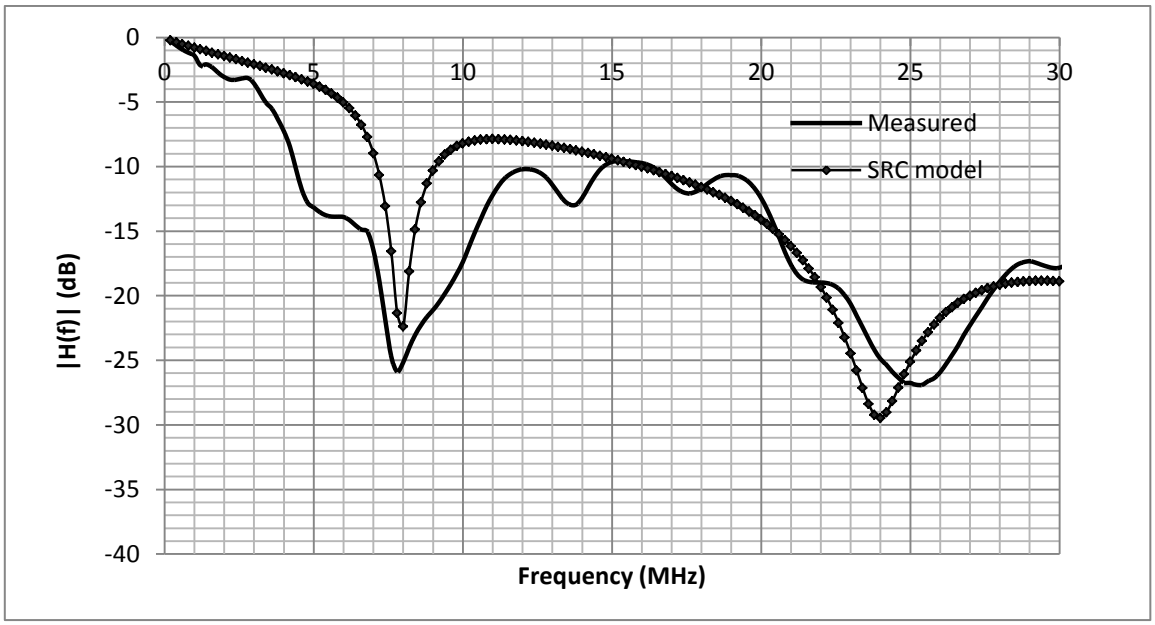

Figure 5.21: Transfer function for Network 2 config_6 compared to the SRC Model

5.5 The effect of Network Topology Variation

5.5.1 Cascading two networks

To analyse the effect of cascading networks so as to verify the cascade approach adopted in some models as discussed in Chapter Three, the one branch network with config_2 was cascaded with the two branched network with config_6, resulting in a three branch network as shown in Figure 5.22a. The resulting measured channel transfer function is shown by the config_8 plot in Figure 5.22b. Also

shown with this result is the addition of the transfer function obtained from config_2 and config_6 independently, that is:

$$Htotal(dB) = Hconfig_1(dB) + Hconfig_2(dB) \quad (5.2)$$

The measured transfer function for the three-branch network follows the same trend as the one obtained from the adding that of config_2 and config_6. The variations are due to the difference in impedance at the cascade point, instead of a receiver termination of 50Ω for network 1 and transmitter input impedance of 50Ω for network 2, the cables are joined to form a straight connection from the same cable type.

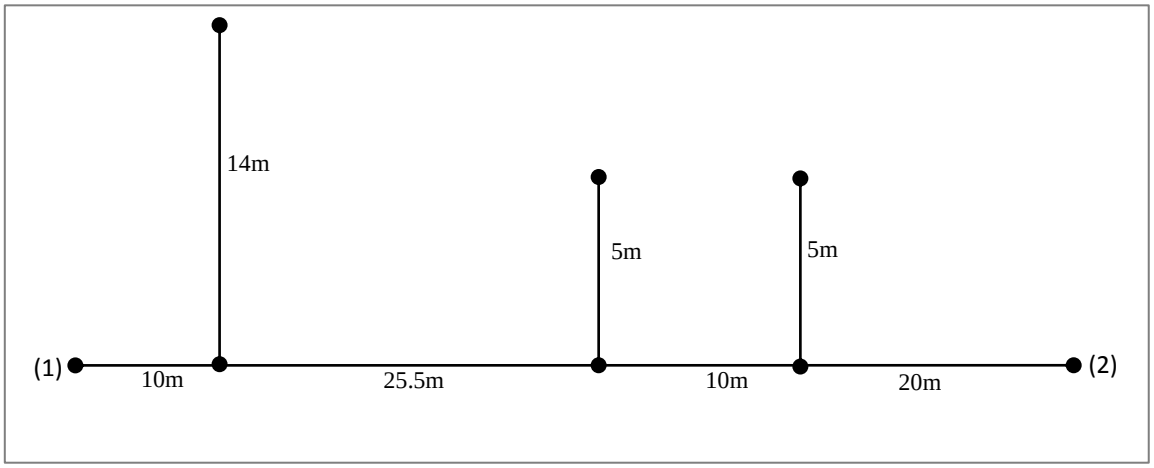

Figure 5.22a: The three branch network

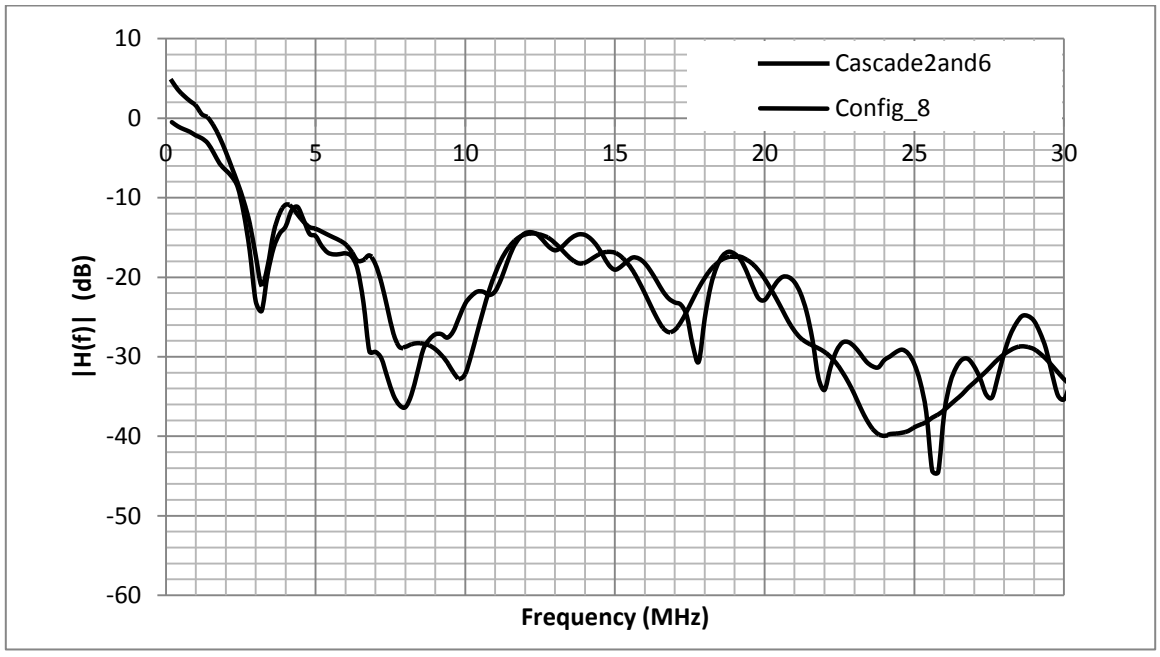

Figure 5.22b: Transfer function of the two networks cascade

5.5.2 Effect of cable length variation

The same network topology for network 1 config_3 was used to take measurements for different branch lengths (15.5 m, 10.5 m, 7.5 m). The channel frequency response acquired from the measurements is as shown in Figure 5.23. From the ability of the deterministic model by [11] to replicate the transfer function of the PLC channel given the channel properties, analysis of the variation in network topology is also done using this model and the transfer function for the different branch lengths shown in Figure 5.24. It should be noted that the average path loss for the channel with the same direct path but different branch length has relatively the same average path loss, bringing us to the conclusion that the branch length has little effect on the attenuation profile where matching the branch termination will see to a less frequency selective channel.

A trend can be seen in the notches occurrence; the separation between the notches is seen to be equal. We consider the electric length of the branch expressed in units of the wavelength λ, related to the propagation velocity v_p and signal frequency *f* by Equation (2.1).

As the impedance of the channel is frequency dependent, for the open circuit end, the first notch will occur at a resonant frequency, relative to the length of the branch, which we shall refer to as *d*, and propagation velocityv_p, related by:

$$f_0 = \frac{v_p}{4d} \tag{5.3}$$

From the measurements the propagation velocity was estimated to be 1.488×10^8. Given the first notch of the open circuit ended branch termination, solving for *d* will give a value of 15.5m.

The subsequent notches will be at frequencies given by:

$$f_{ok} = \frac{v_p}{4d}(2k+1), \quad k = 1,2,\ldots \tag{5.4}$$

For the short circuited branch termination the notch will occur first at zero and then at the frequencies given by:

$$f_{sk} = \frac{v_p}{4d}(2k), \quad k = 1,2,\ldots \tag{5.5}$$

This is directly related to the transmission line theory for an open circuited end line length of (5.6) and (5.7) for a short circuited line end as discussed in Section 3.4, where [53]:

$$l = \frac{(2n-1)\lambda_r}{4} \tag{5.6}$$

$$l = \frac{n\lambda_r}{2} \tag{5.7}$$

Therefore if the branch length is known, we will be able to determine the notch positions and separation for the open circuited and short circuited branch terminations. Moreover having a reference branch length, varying the length by a factor *n* will give a resulting first notch at frequency:

$$f_0' = \frac{1}{n} f_0 \tag{5.8}$$

For a variation in the total length from the transmitter to receiver for a two branch network is explored analytically. Config_6 is taken to be reference length and the transfer function is calculated for twice and five times the reference length. The results are shown in Figure 5.25. The notches are seen to be at the same frequencies for all three cases with a variation in the path loss gradient.

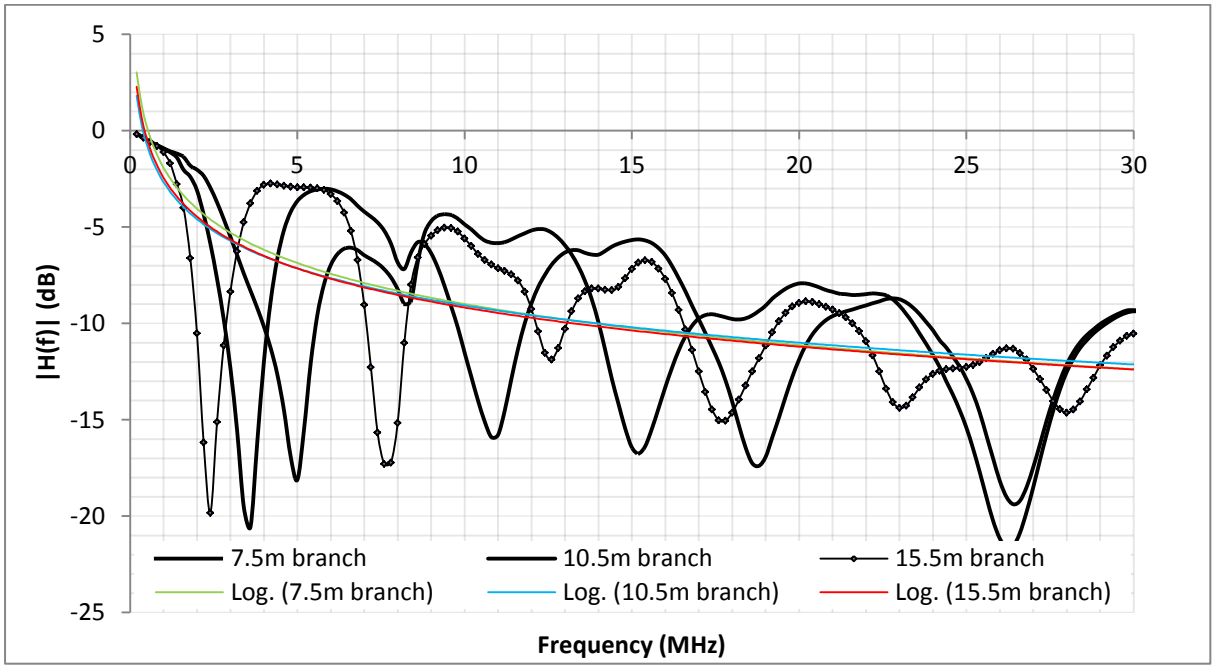

Figure 5.23: Measurement results for variation in branch length of the same network

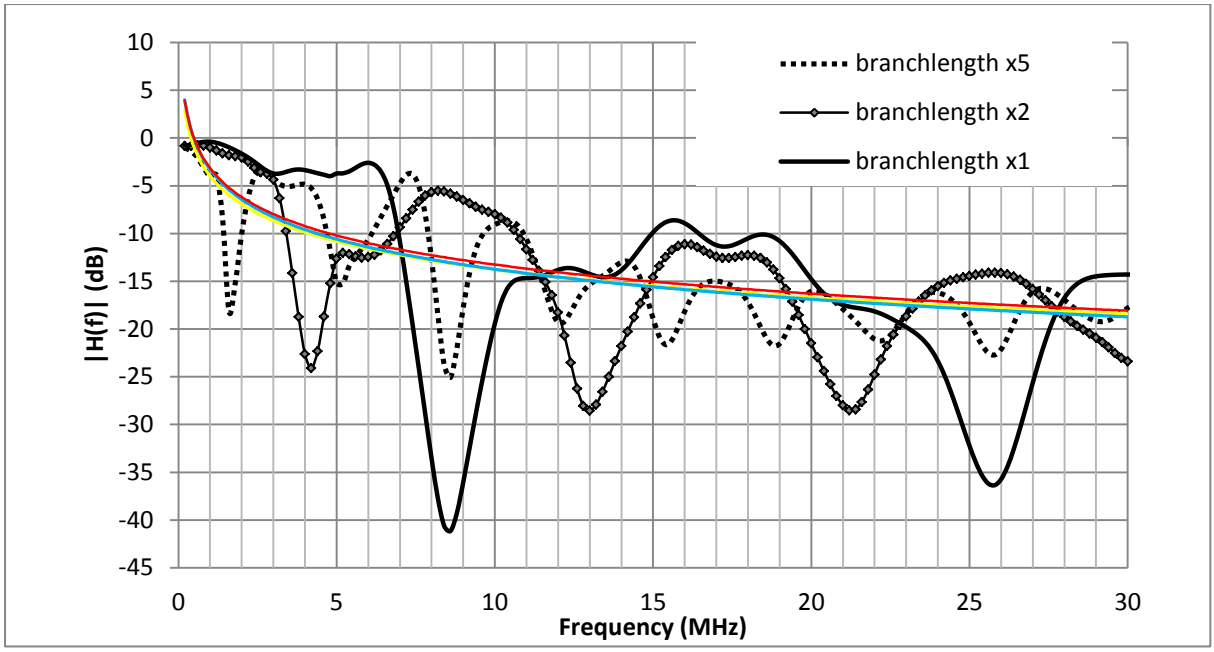

Figure 5.24: Analytical results for variation in branch length of the same network

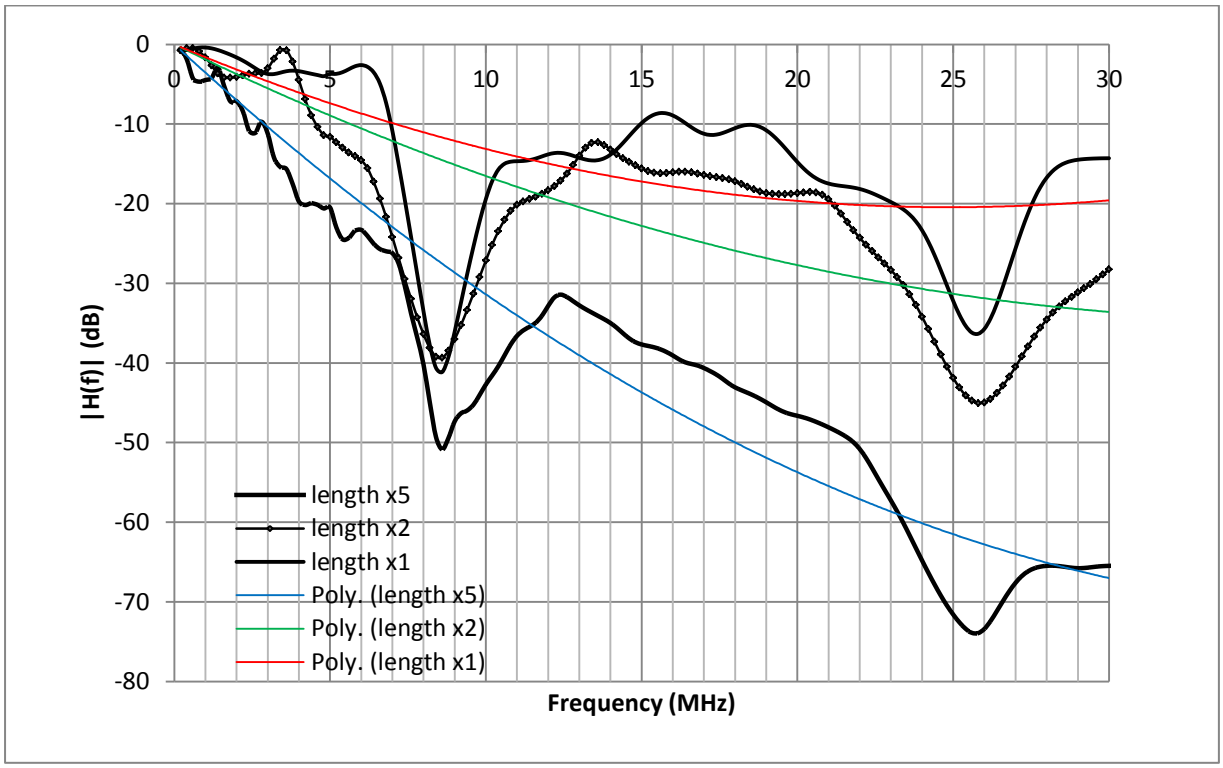

Figure 5.25: Analytical results for variation in total length of the same network, same branch length

5.5.3 Influence of load impedance

The extreme cases for the branch load impedance, that is, short circuited and open circuited branch termination are considered and measurements taken are shown in Figure 5.26. The separation distance between the notches is seen to be equal for both cases. Since the network is made from the same cable with the attenuation constant maximum and minimum bounds given in Table 4.1, the average attenuation bounds were calculated and shown in Figure 5.26. It can be seen that the average attenuation for the channel falls in between the two prediction bounds.

The analysis is also done using the deterministic model by [11] and the transfer function for open circuited, short circuited and matched terminations plotted in Figure 5.27.The matched load branch end gives a transfer function without deep notches and close to that of the regression fit of the transfer functions determining the average path loss.

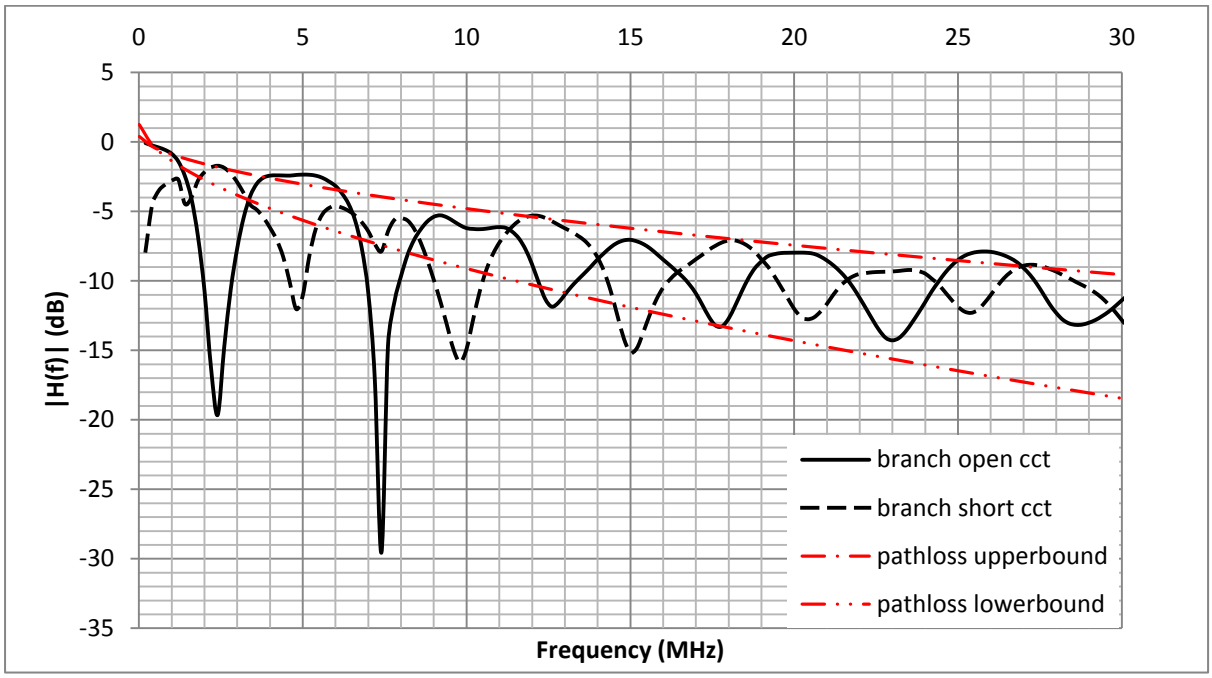

Figure 5.26: Measurement results for variation in branch load impedance of the same network with average path loss prediction bounds

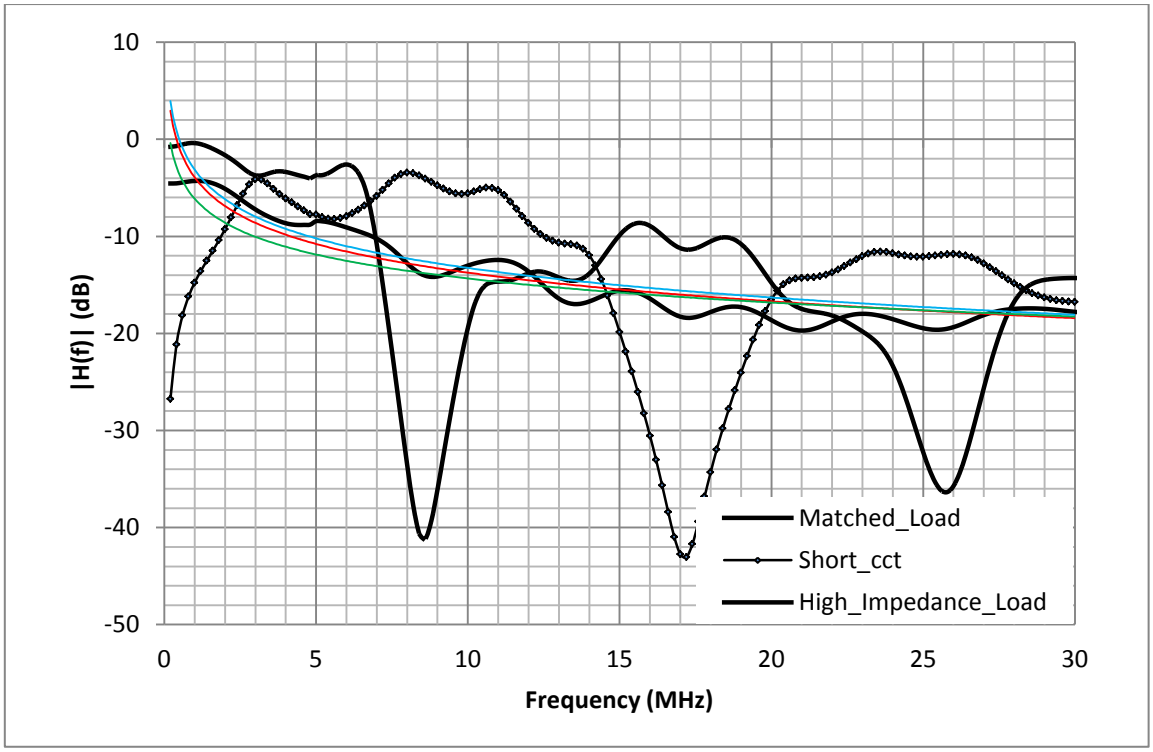

Figure 5.27: Analytical results for variation in branch load impedance of the same network

5.6 Chapter Summary

In this chapter we examined the characteristics of the PLC channel. The measurement methodology is discussed and the channel frequency response results are shown. The frequency response of the channel is seen to be modelled well by the chosen deterministic and empirical models. The proposed SRC model is compared to the transfer function measured for the two networks considered. The channel characteristics are seen to be dependent on length, load and power line characteristics as highlighted in Chapters Two and Three. The typical features of the channel transfer function are notches and low pass filter characteristics relative to the load, length and number of branches as well as the overall channel distance. The notches in the transfer function are seen to be directly dependent on the branch length and a relation to this effect is formed for short circuited and open circuited branch terminations.

CHAPTER SIX

CONCLUSION

6.1 Concluding Remarks

The ever increasing demands in the area of communications call for advances in the Power Line Communications (PLC) technology. This is seen to by proper system design which necessitates accurate channel transfer function models which form the basis for computer simulations. For appropriate models to be formed, the characteristics of the PLC channel have to be well understood. The PLC channel is dependent on multiple factors, resulting in it being referred to as a hostile and unpredictable channel.

In this work we sought to bring a meaningful contribution to the study and application of power line communication modelling through firstly providing a comprehensive summary of transmission properties of typical low voltage power supply networks when used for data transmission. The intrinsic parameters of the power line forming a PLC channel as a transmission line are theoretically derived with respect to the two conductor transmission line theory, the effects of cable composition as well as the dependence of the channel characteristics on the network constituents and topology. This formed the foundation for the analysis of impedance, attenuation and noise as major parameters impeding the communication signal.

Different modelling techniques employing the fundamental line parameter characteristics used to model the PLC channel networks are then studied. A review of the fundamental modelling approaches, that is, the bottom-up and top-down approaches is presented. The formulation of a proposed model following the bottom-up approach is also explained.

A measurement methodology to obtain the parameters of the low voltage cables used in building power network is explained. The theoretical derivations are compared to the measurements where the RMSE between the measured and theoretically derived characteristic impedance and attenuation constant coefficients are found respectively. The close correlation between the measured and theoretical values is confirmed.

Power line couplers are designed and prototypes made to provide an interface between the measuring equipment and the mains. Measurements results were presented, ascertaining the characteristics of the PLC channel and the channel frequency responses compared to models commonly found in literature as well as a proposed model. The dependence of the PLC channel's characteristics on the network constituents and properties is determined. A correlation of channel response characteristic to some different topologies of the power line communication channel is formed. As a result, all research objectives enumerated in the first chapter were attained.

6.2 Future Work

It has been seen that extensive measurements inform the prediction of the channel frequency response, better equipping the modelling process. Essential effects in the simple network configurations for simulation based PLC system performance applications have been covered. Therefore, we propose that further investigations on the variations in network topologies by exploring more complex networks be done, by so doing also confirm the deductions made here.

The much adopted empirical model based on the multipath scenario is seen to replicate the transfer function of a PLC channel fairly well represented by the number of paths less than 10. This therefore is an interest that an optimal number of paths necessary to model a power line channel be found to reduce computation complexity. An optimal number and length of branches given a large network would be explored following this. This would be done by employing scattering theories, especially Mie and Raleigh scattering used in wireless communication where the multipath effect is extensively studied to model the channel.

REFERENCES

[1] Eskom Distribution Code Definitions, Version 5, 2007, last accessed 17 Jan 2014, http://www.eskom.co.za/Whatweredoing/Documents/RSADistributionCodeDefinitionsVer5.1.pdf

[2] M.S. Yousuf and M. El-Shafei, "Power Line Communications: An Overview - Part I," 4th International Conference on Innovations in Information Technology, Dubai, pp.218,222, 18-20 Nov. 2007

[3] K Dostert, "Telecommunications over the Power Distribution Grid- Possibilities and Limitations," Proc 1997 Internat. Symp. on Power Line Comms and its Applications pp.1-9, 1997

[4] H.C. Ferreira, H.M. Grove, O. Hooijen, A.J. Han Vinck, "Power line communications: an overview," AFRICON, 1996., IEEE AFRICON 4th , vol.2, no., pp.558,563 vol.2, 24-27 Sep 1996

[5] K. Honghai; W. Zhengqiu, "Application of AMR based on powerline communication in outage management system," Sustainable Power Generation and Supply, 2009. SUPERGEN '09. International Conference on , vol., no., pp.1,4, 6-7 April 2009

[6] Z. Fan *et al*, "Smart Grid Communications: Overview of Research Challenges, Solutions, and Standardization Activities," Communications Surveys & Tutorials, IEEE , vol.15, no.1, pp.21,38, First Quarter 2013

[7] G. Leen, D. Heffernan, "Expanding automotive electronic systems," *Computer* , vol.35, no.1, pp.88,93, Jan 2002

[8] Mlynek P., Misurec J., Koutny M., Silhavy, P. "Two-port network transfer function for power line topology modeling," Radioengineering, vol. 21, no. 1. 2012.

[9] Power Line Telecommunications (PLT); Coexistence of Access and In-House Powerline Systems", ETSI Technical Specification 101 867, Ver. 1.1.1, Nov. 2000.

[10] R. Róka, S. Dlhá, "Modeling of transmission channels over the low-voltage power distribution network," Journal of Electrical Engineering, Vol. 56, No. 9-10, 2005, pp. 237-245.

[11] H. Meng, S. Chen, Y. L. Guan, C. L. Law, P. L. So, E. Gunawan, and T. T. Lie, "A transmission line model for high-frequency power line communication channel," Proc. 5th Int. Conf. Power System Technology (PowerCon 2002), 2002

[12] H. Philipps, “Modelling of Powerline Communication Channels”, Intl. Symposium on Power-Line Communication and its Applications, Lancaster, UK, 1999.

[13] M. Zimmermann and K. Dostert, “A multipath model for the powerline channel”, IEEE Transactions on Communications, Vol. 50, No. 4, pp. 553-559, Apr. 2002.

[14] T. Esmailian, F. Kschischang, G. Gulak, “An in-building power line channel simulator,” in Proc. Int. Symp. Power Line Communication and its Applic. (ISPLC), Athens, Greece, pp.1-5,29 Mar -9 Apr 2002.

[15] J. Anatory, M.M. Kissaka and N.H. Mvungi, "Channel Model for Broadband Powerline Communication," IEEE Trans. On Power Delivery, Vol.22 No.1, pp. 135-141 January 2007

[16] I. C.Papaleonidopoulos, C. N. Capsalis, C. G. Karagiannopoulos, and N. J. Theodorou, "Statistical analysis and simulation of indoor single-phase low voltage power-line communication channels on the basis of multipath propagation," IEEE Trans. Consumer Electronics, Vol. 49, No. 1, 89-99, February 2003.

[17] H. Hrasnica, A. Haidine, R. Lenhert, Broadband Powerline Communications Networks: Network Design. John Wiley & Sons, 2004

[18] W. Tomasini, Electronic Communications Systems: Fundamentals Through Advanced, 4th edition, Prentice-Hall Inc., Upper Saddle River, New Jersey, USA, 2001.

[19] J..Huloux and L. Hanus, “ST7537 power line modem application,” SGS Thomson Microelectronics, Applicat. Note AN655/0994, 1995

[20] A. Smith, Radio Frequency Principles and Applications: The Generation, Propagation, and Reception of Signals and Noise. Wiley-IEEE Press, 1998

[21] I. C. Papaleonidopoulos, C. G. Karagiannopoulos, N. J. Theodorou, C.N. Capsalis, "Theoretical transmission-line study of symmetrical indoor triple-pole cables for single-phase HF signalling," Power Delivery, IEEE Transactions on , vol.20, no.2, pp. 646- 654, April 2005

[22] H.G Booker , "The elements of wave propagation using the impedance concept," Electrical Engineers - Part III: Radio and Communication Engineering, Journal of the Institution of , vol.94, no.29, pp.171-198, May 1947

[23] D. M. Pozar, Microwave Engineering. 4th Edition New York: Wiley. 2012

[24] S. Ramo, J.R. Whinnery, T. van Duzer, "Fields and Waves in Communications Electronics", New York: Wiley, 1994, pp. 14-155, 180-189, 245-251, 283-287, 331-345

[25] G. Andreou, “Electrical Parameters of Low-Voltage Power Distribution Cables Used for Power-Line Communications,” IEEE Transactions On Power Delivery, Vol. 22, No. 2, April 2007

[26] C. R. Paul, Analysis of Multiconductor Transmission Lines ser. Wiley Series in Microwave and Optical Engineering New York, 2002.

[27] J. Werner, "The HDSL Environment," IEEE Jornal on Selected Areas in Communications, vol. 9, no. 6, Aug. 1991 pp. 784-800

[28] W. Davis, Radio Frequency Circuit Design, Wiley-IEEE Press, 2010

[29] Irwin JD. Basic Engineering Circuit Analysis. MacMillan: New York, 1987.

[30] Mohammadi, M.; Lampe, L.; Lok, M.; Mirabbasi, S.; Mirvakili, M.; Rosales, R.; P. Van Veen, "Measurement study and transmission for in-vehicle power line communication," Power Line Communications and Its Applications, 2009. ISPLC 2009. IEEE International Symposium on , vol., no., pp.73,78, March 29 2009-April 1 2009

[31] Temes GC, Lapatra, JW. Introduction to Circuit Synthesis and Design. McGraw-Hill: New York, 1967.

[32] Korki, M.; Hosseinzadeh, N.; Vu, H.L.; Moazzeni, T.; Chuan Heng Foh, "A channel model for power line communication in the smart grid," Power Systems Conference and Exposition (PSCE), 2011 IEEE/PES , pp.1-7, 20-23 March 2011

[33] H. Philipps, “Performance measurements of power-line channels at high frequencies," in Proc. Int. Symp. on Power Line Comm. and its Applic. (ISPLC), Tokyo, Japan, pp. 229-237,24-26 Mar 1998.

[34] M. Zimmermann and K. Dostert, “A multi-path signal propagation model for the power line channel in the high frequency range,” Proceedings of the International Symposium. Power Line Communications and its Applications (ISPLC 1999), pp. 45-51, Mar. 1999.

[35] Güzelgöz, S.; Celebi, H.B.; Arslan, H., "Statistical Characterization of the Paths in Multipath PLC Channels," Power Delivery, IEEE Transactions on , vol.26, no.1, pp.181,187, Jan 2011

[36] R. Aquilue, "Scattering Parameters-Based Channel Characterization and Modeling for Underground Medium-Voltage Power-Line communications," IEEE Trans. Power Delivery, Vol. 24, No. 3, pp. 1122-1131, July 2009

[37] T. Maenou and M. Katayama, "Study on Signal Attenuation Characteristics in Power Line Communications," IEEE Int. Symp. on Power Line Comm. and Its Applic., Orlando, FL, pp.217-221, 2006.

[38] J. Ahola, Applicability of Power-line Communications to Data Transfer of On-line Condition Monitoring of Electrical Drives, Doctoral Dissertation, Lappeenranta University of Technology, Finland, 2003, ISBN 951-764-783-2.

[39] C.T. Mulangu, T.J.O. Afullo, N.M. Ijumba, "Novel approach for broadband powerline communication channels modeling," Power Engineering Society Conference and Exposition in Africa (PowerAfrica), 2012 IEEE , vol., no., pp.1,4, 9-13 July 2012

[40] C. Lin, J. Curilla, "Temperature-Related Changes in Dielectric Constant and Dissipation Factor of Increase Attenuation in Data Cables Used in Building Plenums", IEEE 16th Conference on Local 121 Computer Networks, Minneapolis, USA, 14-17 October 1991, pp. 74- 79.

[41] S. Tsuzuki, T. Takamatsu, H. Nishio, Y. Yamada, "An estimation method of the transfer function of indoor power-line channels for Japanese houses," in Proc. 6th Int. Symp. Power-Line Communication and its Applications (ISPLC 2002), Athens, 2002, pp.55-59.

[42] M. Zimmermann and K. Dostert, "Analysis and modeling of impulsive noise in broad-band powerline communications," IEEE Transactions on Electromagnetic Compatibility, vol. 44, no. 1, pp. 249-258, February 2002.

[43] P. Langfeld, "The Capacity of typical Power line Channels and Strategies for System Design," Proc. 5th Int. Symp Power-Line Comm., Sweden, pp. 271-78, 2001

[44] S. Galli, A. Banwell, "A novel approach to accurate modeling of the indoor power line channel-Part II: transfer function and channel properties," IEEE Trans. On Power Delivery, vol. 20(3), pp. 1869-78, 2005.

[45] H. Ferreira, L. Lampe, J. Lewbury, "Power Line Communications: Theory and Applications for Narrowband and Broadband Communications over Power Lines," 2010, John Wiley and Sons

[46] H. Philipps, "Development of a statistical model for power line communications channels", IEEE International Symposium on Power Line Communications and Its Applications (ISPLC), Limerick, Ireland, 5-7 Apr 2000.

[47] M. Götz, M. Rapp and K. Dostert, "Power line channel characteristics and their effect on communication systems design", IEEE Commun. Magazine, Vol. 42, No. 4, pp. 78-86, Apr. 2004.

[48] H. Meng, S. Chen, Y.L. Guan, C. Law, P.L. So, E. Gunawan, T.T. Lie, "Modeling of Transfer Characteristics for the Broadband Power Line Communication Channel," IEEE Trans. Power Delivery, Vol. 19, No. 3, , pp1057-1064, July 2004

[49] J. Anatory, N. Theethayi, "Broadband Power Line Communication Systems: Theory and Applications," WitPress 2010

[50] J. Anatory *et. al.* "Broadband power-line communication channel model: Comparison between theory and experiments", Proc. IEEE Int. Symp. Power Line Communications and Its Applications, Jeju city, Jeju Island, pp.322 -324, Apr 2008.

[51] G. Gonzalez, Microwave Transistor Amplifiers. Englewood Cliffs, NJ:Prentice-Hall, 1997

[52] C.T Mulangu, T.J. Afullo, N.M. Ijumba, "Modelling of Broadband Powerline Communication Channels," SAIEE, Vol.102, no.4, December 2011

[53] D. Misra, Radio-Frequency and Microwave Communication Circuits: Analysis and Design. John Wile & sons, 2001

[54] F. Gianaroli, F. Pancaldi, "The Impact of Load Characterization on thr Average Properties of Statistical Models for Powerline Channels," IEEE Trans. On Smart Grid, vol. 4, no.2, pp. 677-685, June 2013.

[55] Gianaroli, F.; Barbieri, A.; Pancaldi, F.; Mazzanti, A.; Vitetta, G.M., "A Novel Approach to Power-Line Channel Modeling," Power Delivery, IEEE Transactions on , vol.25, no.1, pp.132,140, Jan. 2010

[56] C. Hensen , W. Schulz and S. Schwarze "Characterization, measurement and modeling of medium-voltage power line cables for high data rate communication", Proc. IEEE Int. Symp. Power Line Comunications and Its Applications, Lancaster ,UK, pp.37 -44, 1999

[57] Bartolucci Ettore J., Finke Bob H., “Cable Design for PWM Variable-Speed AC Drives, IEEE Transactions on Industry Applications, Vol.37, No 2, March/April, 2001.

[58] Laguna, G.; Barron, R., "Survey on Indoor Power Line Communication Channel Modeling," Electronics, Robotics and Automotive Mechanics Conference, 2008. CERMA '08 , vol., no., pp.163,168, Sept. 30 2008-Oct. 3 2008

[59] IEEE standard for Broadband Over Power Line Hardware," IEEE STD 1675-2008, ppC1,47, Jan. 2009

[60] P.Van Rensburg, H. Ferreira, "Coupling Circuitry: Understanding the Functions of Different Components," ISPLC Proceedings, pp.204-209 March 2003

[61] Bilal, O., Liu, E., Gao, Y., & Korhonen, T. O. "Design of broadband coupling circuits for power line communication." Proc. IS PLC. March 2004.

[62] P. A. Janse van Rensburg and H. C. Ferreira, "Coupling circuitry: understanding the functions of different components", Proc. 7th Int. Symp. Power-Line Comm., Japan, pp.204 -209, 2003

[63] P. A. Janse van Rensburg and H. C. Ferreira "The role of magnetizing and leakage inductance in transformer coupling circuitry", Proc. 8th Int. Symp. Power-Line Comm., Spain, pp.244 - 249, 2004

[64] H. Gassara *et. al.*, "Coupling Interface Circuit Design for Experimental Characterization of the Narrowband Power Line Communication Channel," International Symposium on Electromagnetic Compatibility (EMC), pp.1,6, 6-10 Aug. 2012

[65] B. W. Griffith, Radio-Electronic Transmission Fundamentals, Sci Tech Publishing, 2000